DEFINING THE ROLE OF FOLLICULIN AND ITS INTERACTING PARTNERS

Sara Seifan

2016

Thesis submitted to Cardiff University in fulfilment of the requirements for the degree of Doctor of Philosophy

This work is dedicated to Rienk Doetjes

It is through your presence in our hearts that your absence is felt every day

CONTENTS

Table of contents ……..……..I

Acknowledgments……..……..……...VII

Summary……..…….…….VIII

Declaration……..……..……....IX

Abbreviations……..……...XI

1 CHAPTER 1: GENERAL INTRODUCTION..... 1

1.1 BIRT-HOGG-DUBÉ SYNDROME..... 1

1.2 CLINICAL MANIFESTATION..... 2

1.2.1 Skin..... 2

1.2.2 Lung..... 5

1.2.3 Kidney..... 7

1.2.4 Other clinical manifestations associated with BHD..... 10

1.2.4.1 Colorectal polyps and colorectal cancer..... 10

1.2.4.2 Thyroid nodules and cancer..... 11

1.2.4.3 Parotid tumours..... 12

1.3 FOLLICULIN..... 12

1.3.1 Structure and post-translational modifications..... 15

1.3.2 Mutations..... 17

1.3.3 Interacting partners..... 19

1.3.3.1 FLCN interacting protein 1 (FNIP1)..... 19

1.3.3.2 FLCN interacting protein 2 (FNIP2)..... 20

1.3.3.3 Plakophilin-4..... 21

1.3.3.4 Rpt4..... 21

1.3.3.5 Rag proteins..... 21

1.3.4 Signalling pathways 22
1.3.4.1 Mammalian target of rapamycin (mTOR) signalling 22
1.3.4.2 AMP-activated protein kinase (AMPK) signalling 24
1.3.4.3 Hypoxia Inducible Factor (HIF) signalling 26
1.3.4.4 The Janus kinase/signal transducers and activators of transcription (JAK/STAT) and TGF-β signalling 27
1.3.4.5 Ciliogenesis 29
1.3.4.6 The Ras-Raf-MAPK signalling 29
1.3.4.7 Wnt/Cadherin signalling pathway 30
1.4 AUTOPHAGY 32
1.4.1 Autophagy-related proteins (Atgs) 36
1.4.1.1 Atg8 family of proteins 36
1.4.1.1.1 LIR motif 37
1.4.2 p62 (Sequestosome 1, SQSTM1) 38
1.4.3 unc-51 like autophagy activating kinase 1 (ULK1) 39
1.4.4 AMP-activated protein kinase (AMPK) 41
1.4.5 Mammalian/mechanistic target of rapamycin (mTOR) 43
1.4.6 Rabs 45
1.5 AIMS AND OBJECTIVE OF THIS PROJECT 46
2 CHAPTER 2: MATERIALS AND METHODS 47
2.1 REAGENTS AND CHEMICALS 47
2.2 BUFFERS AND SOLUTIONS 49
2.3 ANTIBODIES 52
2.4 PLASMIDS 53
2.5 METHODOLOGY 54

2.5.1 Cell culture 54
2.5.2 Transfection 55
2.5.3 Bradford protein assay 55
2.5.4 In vivo radiolabelling 56
2.5.5 Immunoprecipitation (IP) 56
2.5.6 GST purification 56
2.5.7 Western blot analysis 56
2.5.8 Site-Directed Mutagenesis 57
2.5.9 Plasmid purification (Miniprep/ Maxiprep) 58
2.5.10 Sequencing 58
2.5.11 Cyquant cell proliferation assay 58
2.5.12 RNA extraction 59
2.5.13 Reverse transcription 59
2.5.14 Quantitative-PCR 60
2.5.15 Modelling of FLCN structure 60
2.5.16 Densitometry 60
2.5.17 Statistical analysis 61

3 CHAPTER 3: INVOLVEMENT OF FLCN IN AUTOPHAGY 62

3.1 INTRODUCTION 62
3.2 METHODS 65
3.3 RESULTS 67
3.3.1 FLCN could possibly be involved in autophagy 67
3.3.2 Autophagy is down-regulated in FLCN-deficient cells 69
3.3.3 FLCN interacts with ULK1 71
3.3.4 FLCN is an ULK1 substrate 73

3.3.5 ULK1 phosphorylates FLCN within a conserved C-terminus 75
3.3.6 ULK1 phosphorylation sites within the C-terminus are shown to be on the surface and are available for phosphorylation 76
3.3.7 WT-FLCN rescues basal autophagy in FLCN deficient cells but not the 3A mutant 78
3.3.8 GABARAP interacts with FLCN 81
3.3.9 FLCN/GABARAP binding is impaired in BHD patient-derived mutants .. 83
3.3.10 FLCN interacts with Rab GTPases associated with autophagy 85
3.3.11 FLCN is not a typical GEF 87
3.4 DISCUSSION 89
4 CHAPTER 4: FAMILIAL MULTIPLE DISCOID FIBROMA (FMDF) 93
4.1 INTRODUCTION 93
4.2 METHODS 95
4.3 RESULTS 98
4.3.1 Families with FMDF have common ancestors and affected members have FNIP1 c.1989delT mutation 98
4.3.2 The c.1989delT mutation predicts the frameshift p.Val663fsX which is a conserved residue in vertebrates 100
4.3.3 FLCN/FNIP1 interaction is impaired by c.1989delT mutation 102
4.3.4 FNIP1/FNIP2 interaction is not modified by c.1989delT mutation 105
4.4 DISCUSSION 107
5 CHAPTER 5: CHARACTERISING FNIP1, FNIP2 AND FLCN INTERACTIONS ……..109
5.1 INTRODUCTION 109

5.2 METHODS 113
5.3 RESULTS 116
5.3.1 Generation of FNIP1 and FNIP2 stable knockdown cell lines 116
5.3.2 Early morphological changes were observed in FNIP1 stable knockdown cell lines 119
5.3.3 When FNIP2 is knocked down, other components of the complex, i.e., FLCN and FNIP1 were observed to be present at higher levels in the cell 122
5.3.4 FNIP1 and FNIP2 both possess conserved LIR motifs 124
5.3.5 Starvation of HK2 cells induces FNIP1 and FNIP2 expression 126
5.3.6 FNIP2 knockdown shows similar molecular defect characteristic to FLCN knockdown cells 128
5.3.7 FNIP knockdown alters expression of selected autophagy proteins 130
5.3.8 GST purification of FLCN, FNIP1 and FNIP2 132
5.3.9 NUP155 IP co-purifies FLCN, and more robustly in the presence of FNIP2 137
5.3.10 FLCN IP also co-purifies NUP155, and more robustly in the presence of FNIP2. 141
5.3.11 HIF1α protein level is significantly higher in old FLCN knockdown cells and new FNIP2 knockdown cells 145
5.4 DISCUSSION 147
6 CHAPTER 6: FINAL DISCUSSION 152
6.1 FLCN IS A POSITIVE DRIVER OF AUTOPHAGY 152
6.2 ROLE OF FNIP1 IN FAMILIAL MULTIPLE DISCOID FIBROMAS (FMDF) 155
6.3 CHARACTERISING FNIP1 AND FNIP2 156
6.4 FLCN, FNIP1 AND FNIP2 AND THE INTERACTING PARTNERS 158

6.5 FUTURE WORK 160

7 REFERENCES..... 161

ACKNOWLEDGMENTS

Firstly I would like to thank my supervisor, Dr Andrew Tee and my co-supervisor, Prof Julian Sampson for all their support and guidance throughout my PhD, and for giving me this opportunity.

I would also like to thank Dr Elaine Dunlop for all the help and guidance in the lab.

Very especial thanks to other members of the Tee lab, Dr Kayleigh Dodd and Dr Ellie Rad for always being there, making me laugh and keeping me sane and above all for being great scientists. Your friendship has carried me through these past few years and I appreciate it.

And last but not least I would like to thank my mother for her never ending love and support; this wouldn't have been possible without you.

SUMMARY

Birt-Hogg-Dubé (BHD) syndrome is a rare autosomal dominant condition caused by mutations in the *FLCN* gene and characterised by benign hair follicle tumours, pneumothorax and renal cancer. Folliculin (FLCN), the protein product of *FLCN*, is a poorly characterised tumour suppressor, currently linked to multiple cellular pathways. Autophagy is an evolutionarily conserved biological process that maintains cellular homeostasis by removing damaged organelles and macromolecules. Although the autophagy kinase, ULK1, is known to initiate autophagy, the underlying mechanisms are still being unravelled and new ULK1 substrates are being identified. In this study, FLCN is identified as a new ULK1 substrate that interacts with the autophagy machinery via GABARAP. FLCN/GABARAP interaction is shown to be modulated by the presence of FNIP1 and FNIP2, as well as ULK1-directed phosphorylation of FLCN. Furthermore, loss of FLCN impairs autophagy while re-expression rescues autophagy. FLCN was found to interact with several Rab small G proteins linked to autophagy, implicating FLCN in vesicular trafficking.

Upon generation of *FNIP1/2* knockdown cell lines it was revealed that FNIP2 is possibly involved in the transcriptional regulation of *FLCN* and is involved in FNIP1's translation and/or stability. Moreover, FNIP1 could be involved in regulation of *FNIP2*'s transcription via a negative feedback mechanism. FNIP proteins were further implicated in autophagy when *FNIP1* and *FNIP2* gene expression were found to be significantly increased upon starvation in HK2 cells. Additionally, p62 and GABARAP protein levels demonstrated a significant increase in *FNIP2* knockdown cell lines suggestive of impaired autophagy.

This work substantially contributes to our understanding of FLCN by linking it directly to autophagy. Furthermore, FLCN and the FNIPs are shown to be involved in multiple protein interactions which could mean that FLCN and its interacting partners might have a more universal housekeeping role, which when lost leads to cancer.

DECLARATION

This work has not previously been accepted in substance for any degree and is not concurrently submitted in candidature for any degree.

Signed……(Candidate) Date ……..

STATEMENT 1

This thesis is being submitted in partial of the requirements for the degree of ……. (Insert MCh, MD, MPhil, PhD etc., as appropriate)

Signed…….(Candidate) Date ……..

STATEMENT 2

This thesis is the result of my own independent work/investigation, except where otherwise stated.

Other sources are acknowledged by explicit references.

Signed…….(Candidate) Date ……..

STATEMENT 3

I hereby give consent for my thesis, if accepted, to be available for photocopying and for inter-library loan, and for the title and summary to be made available to outside organisations.

Signed…….(Candidate) Date ……..

STATEMENT 4: PREVIOUSLY APPROVED BAR ON ACCESS

I hereby give consent for my thesis, if accepted, to be available for photocopying and for inter-library loans after expiry of a bar on access previously approved by the Graduate Development Committee.

Signed……(Candidate) Date …….

ABBREVIATIONS

AICAR	5-aminoimidizole-4-carboxamide riboside
AKT	Protein kinase B
AEC	Alveolar epithelial type II cells
AMBRA1	Activating molecule In BECN1-regulated autophagy protein 1
AMPK	AMP-activated protein kinase
Atg	Autophagy related
Bcl2	B-cell lymphoma 2
BHD	Birt-Hogg-Dubé
BIM	Bcl-2 interacting mediator of cell death
BMP	Bone morphogenetic protein
BNIP3	BCL2/Adenovirus E1B 19kDa interacting protein 3
CaMKK-β	Ca^{2+}/calmodulin-dependent kinase kinase-β
cAMP	Cyclic adenosine 3',5'-monophosphate
CCND1	Cyclin D1
CDKN2B	Cyclin-dependent kinase inhibitor 2B
CMA	Chaperone-mediated autophagy
DENN	Differentially expressed normal versus neoplastic
DNA	Deoxyribonucleic acid

Dpp	Decapentaplegic
ER	Endoplasmic reticulum
ES	Embryonic stem cells
FAK	Focal adhesion kinase
FIP200	FAK family interacting protein of 200 kD
FLCN	Folliculin
FNIP1	Folliculin interacting protein 1
FNIP2	Folliculin interacting protein 2
G protein	GTP-Binding proteins
GABARAP	Gamma-aminobutyric acid receptor-associated protein
GAP	GTPase activating protein
GDP	Guanosine diphosphate
GEF	Guanine nucleotide exchange factor
GLUT1	Glucose transporter type 1
GREM1	Gremlin
GSC	Germline stem cell
GTP	Guanosine-5'-triphosphate
HBE	Human bronchial epithelial cells
HDAC	Histone deacetylase

HEK	Human embryonic kidney cells
HIF-1α	Hypoxia-inducible factor 1-alpha
HIF-2α	Hypoxia-inducible factor 2-alpha
HIF	Hypoxia-inducible factor
HOP	Homotypic fusion and protein sorting
Hsc70	Heat shock cognate 70
IHC	Immunohistochemistry assays
INHBA	Inhibin beta A
JAK	Janus-activated kinase family kinase
LAM	Lymphangioleiomyomatosis
LAMP2A	Lysosome-associated membrane protein 2A
LKB1	Liver kinase B1
MAPK	Mitogen-activated protein kinases
MEF	Mouse embryonic fibroblast
mLST8	Mammalian lethal with SEC13 protein 8
MNU	N-Nitroso-N-methylurea
mRNA	Messenger RNA
mTOR	Mammalian / mechanistic target of rapamycin
mTORC1	Mammalian / mechanistic target of rapamycin complex 1

mTORC2	Mammalian / mechanistic target of rapamycin complex 2
PCP	Planar cell polarity
PDK1	Pyruvate dehydrogenase kinase isoform 1
PE	Phosphatidylethanolamine
PGC-1α	Peroxisome proliferator-activated receptor Gamma, coactivator 1 Alpha
PI3K	Type I phosphatidylinositol 3-kinase
PI4KIIα	Phosphatidylinositol 4-kinase IIα
PKP4	Plakophilin-4 (also known as p0071)
PRAS40	Proline-rich Akt substrate 40 KDa
PSP	Primary spontaneous pneumothorax
PTEN	Phosphatase and tensin homolog
Raptor	Regulatory-associated protein of mTOR
RCC	Renal cell carcinoma
RhoA	Ras homologue family member A
Rpt4	Regulatory particle triple-A ATPase 4
RNA	Ribonucleic acid
rRNA	Ribosomal RNA
ROS	Reactive oxygen species

SAEC	Small airway epithelial cells
Sin-1	Stress-activated MAP kinase-interacting protein 1
SMAD3	Mothers against decapentaplegic homologue 3
SNARE receptor	Soluble N-ethylmaleimide-sensitive factor-attachment protein
STAT	Signal transducer and activator of transcription
TAK1	Transforming growth factor-β-activating kinase 1
TFE3	Transcription factor E3
TGF-β	Transforming growth factor, beta
THBS1	Thrombospondin-1
TNF	Tumour necrosis factor
TP53	Tumor protein P53
TRAIL	TNF related apoptosis-inducing ligand
TSA	Trichostatin A
TSC	Tuberous sclerosis complex
ULK1	Unc-51 like autophagy activating kinase
VEGF	Vascular endothelial growth factor
VHL	Von Hippel-Lindau tumour suppressor protein
Vps34	Vacuolar protein sorting 34

Wnt	Wingless-type MMTV integration site family

1 Chapter 1: General Introduction

1.1 Birt-Hogg-Dubé Syndrome

Birt-Hogg-Dubé (BHD) syndrome (OMIM 135150) is a rare, autosomal dominant, hamartoma disorder which is characterized by benign tumours of the hair follicle (fibrofolliculomas), lung cysts and pneumothorax (collapsed lung), and renal neoplasia. BHD was first described in 1977 by three Canadian doctors – Birt, Hogg and Dubé (Birt et al. 1977). The syndrome had also been identified 1975 by Hornstein and Knickenberg (Hornstein & Knickenberg 1975) and there has been suggestion of renaming the disease to Hornstein-Birt-Hogg-Dubé, however due to confusion this name was never used.

A genome-wide linkage analysis using polymorphic microsatellite markers on a large Swedish family in 2001 mapped the BHD-associated locus to chromosome 17p12-q11.2. (Khoo et al. 2001). Subsequently in 2002 a novel gene BHD, which encodes a 64 KDa protein called folliculin (FLCN), was reported to be inactivated in individuals with BHD syndrome (Nickerson et al. 2002).

1.2 Clinical Manifestation

1.2.1 Skin

Usually after the age of 20, skin lesions start to appear in most of the BHD patients, where these skin lesions are termed Fibrofolliculomas (Menko et al. 2009). Fibrofolliculomas are benign hair follicle tumours appearing on skin as whitish papules. These lesions are mainly developed on the face; they can also be commonly found on the neck, upper torso and ears (Menko et al. 2009). Trichodiscomas (skin-coloured tumours occurring on the upper body), skin tags (acrochordon-like lesions) and fibrofolliculomas were previously considered as distinct hallmarks of BHD syndrome however Fujita *et al*. 1981, De la Torre *et al*. 1999 and Misago *et al.* 2009 showed that these benign tumours were merely a morphological spectrum of the same histological entity (Fujita et al. 1981)(De la Torre et al. 1999)(Misago et al. 2009).

In 2013, Vernooij *et al.* suggested that fibrofolliculomas arise from sebaceous glands rather than hair follicles. They found that most of the epithelial strands making up the lesion are a continuation of the sebaceous glands. This could possibly be as a result of ciliary dysfunction in either the sebaceous gland progenitor or stem cells, which in turn could explain the formation of skin lesions around the areas rich in sebaceous glands such as the nose and perinasal skin (Vernooij et al. 2013).

In 2010, Cocciolone *et al*. suggested a connection between desmoplastic melanoma and BHD in a 58 year old patient as a result of mammalian target of rapamycin (mTOR) up-regulation. There are 6 other cases of melanoma reported in patients with a BHD mutation; although quite possibly the event could be

coincidental and a direct link cannot be confirmed (Cocciolone et al. 2010)(Leter et al. 2008).

The range of skin manifestation in BHD patients varies. Some patients do not develop any skin abnormalities at all whereas the number of fibrofolliculomas in other patients can differ from under 10 to over 100 (Toro et al. 1999).

Some skin abnormalities seen in BHD patients are quite similar to a few other genetic disorders shown in Table 1.1.

Disease	Gene	Lesion	Pathogenesis Mechanism	Inheritance
Birt Hogg Dube Syndrome	FLCN	Fibrofolliculoma	Not fully understood Possibly mTOR dysregulation/ ciliary dysfunction/ autophagic and apoptotic dysregulation	Autosomal dominant/ new mutation
Tuberous Sclerosis Complex	TSC	Angiofibroma	mTORC1 up-regulation/ciliary dysfunction	Autosomal dominant/ new mutation
Cowden Disease	PTEN	Trichilemmoma	PI3K-AKT / mTOR up-regulation	Autosomal dominant
Muir-Torre Syndrome	MLH1/MSH2	Sebaceous adenomas Sebaceous epitheliomas Sebaceous carcinomas	DNA mismatch repair	Autosomal dominant

Table 1.1. Hair follicle tumour syndromes similar to BHD

1.2.2 Lung

The earliest symptoms reported in BHD patients to date are lung problems, where three independent studies have reported early incidents of pneumothoraces in three different patients at the age of seven, fourteen and sixteen (Bessis et al. 2006)(Gunji et al. 2007)(Johannesma et al. 2014). Whereas in 2013 Kunogi Okura *et al.* presented a case of 73 year old woman with her first spontaneous pneumothorax occurring at the age of 73 (Kunogi Okura et al. 2013). These extreme findings can suggest that the age of onset for spontaneous pneumothorax in BHD patients is quite variable.

Toro *et al.* in a study of 152 patients from 49 families first described the presence of pulmonary cysts in BHD patients (Toro et al. 1999). Most of BHD patients are likely to develop pulmonary cysts and are susceptible to recurrent spontaneous pneumothorax. The study of 50 BHD families showed 88% of the families developed pulmonary cysts and 53% of the families had a history of pneumothorax (Toro et al. 2007). In another study, Toro *et al.* reported a 93% pulmonary cyst presence in BHD patients (Toro et al. 2008). The numbers of pulmonary cysts have been postulated by Zbar *et al.* to correlate with episodes of spontaneous pneumothoraces (Zbar et al. 2002). In the Toro *et al*. study of 89 families with BHD, patients with pulmonary cysts were found to have a 24 % risk for spontaneous pneumothorax. They also found that after having one episode of spontaneous pneumothorax, recurrence of the episode becomes more common (Toro et al. 2007). An independent study of 20 BHD families showed 11% of affected BHD patients had a history of pneumothorax however pulmonary CT screening for the presence of pulmonary cysts was not carried in this study (Leter et al. 2008).

According to Toro *et al*. and Tobino *et al.*, although BHD patients usually have multiple pulmonary cysts, lung anatomy and histology mostly appears to be normal and generally lung function is not affected (Toro et al. 2007)(Tobino et al. 2011).

In 2011, Tobino *et al.* carried out a differential study between Lymphangioleiomyomatosis (LAM) and BHD pulmonary cysts in 12 patients and concluded that the distinct characterisation of BHD pulmonary cyst is their predominant distribution towards the medial and lower zone. They also observed that the number of cysts present in different BHD patients varies between 29 to 407, and the shape of the cyst was generally irregular (Tobino et al. 2011). Another study of 17 BHD patients also found that multiple lung cysts are mainly (93%) present in the lower lungs and that the cysts were different in size and shape (Agarwal et al. 2011).

A more recent study used histopathologic examination of the cysts of 11 BHD patients and found that the cysts are lined with epithelial cells or pneumocyte-like cuboidal cells. They also found that some of the cysts had alveolus-like structures within them or as they called it "alveoli within an alveolus" pattern. The cysts were stained for phospho-S6 which proved to be positive, indicating active mTOR pathway in theses cysts (Furuya et al. 2012).

The analysis of 229 lung cysts from 50 BHD patients by Kumasaka *et al.* and comparing them with the analysis of 117 lung cysts from 34 primary spontaneous pneumothorax (PSP) patients, has provided a better characterisation of pulmonary cysts in BHD patients. They found that the BHD cysts are usually surrounded by normal alveolar walls; they could have intracystic septa and are found in both subpleural and intrapulmonary areas. They postulated that BHD cysts grow in size

possibly by expanding at the alveolar-septal junction where the alveolar walls disappear. FLCN loss has also been suggested as the cause of weaker alveoli walls which makes the lungs more vulnerable to mechanical stress which in turn causes cyst formation (Kumasaka et al. 2014).

Overall the common presence of pulmonary cyst in BHD patients could be indicative of important role of FLCN in normal lung physiology.

1.2.3 Kidney

One of the most severe consequences of BHD is the predisposition of the BHD patients to develop renal cell carcinoma (RCC) (Toro et al. 1999).

In a study of 115 BHD patients from 35 families by Houweling *et al.* 12% (14) of the patients developed renal cell carcinoma and 5 out of these 14 individuals had metastatic tumours (Houweling et al. 2011). However in a larger study Pavlovich *et al.* examined 124 individuals with BHD and found 34 (27%) with renal tumours (Pavlovich et al. 2005). Toro *et al.* also studied 89 BHD patients from 50 families and found 30 individuals (34%) had developed renal cell carcinoma (Toro et al. 2008). In a more recent study, Benusiglio *et al.* examined 124 BHD patients from 72 families and found 33 of the patients (27%) with a history of renal tumours (Benusiglio, Giraud, et al. 2014). It is important to take into account that these differences in prevalence of renal cell carcinoma in BHD patient could be due to the number of the population studied and also the way these patients were recruited; for example in Houweling *et al.* study most of the patients were recruited through dermatology clinics whereas in Benusiglio *et al.* study patients were recruited through National Hereditary Kidney Cancer Centre in Paris and the Molecular Genetics Laboratory at

the Edouard Herriot University Hospital in Lyon. Therefore it is difficult to accurately predict the percentage risk of developing kidney cancer in BHD patients.

Interestingly, two independent studies have found somatic mutation of *FLCN* in sporadic renal cell carcinoma (Khoo et al. 2003)(Gad et al. 2007). Khoo *et al.* only found one *FLCN* mutation in 39 studied samples and Gad *et al.* found six *FLCN* mutation in the 92 studied samples. Moreover, a recent case study of a 74 year old man who had no family history of cancer and presented with benign oncocytoma transitioning to regions of high-grade carcinoma; showed that heterozygous loss of *FLCN* was partly the cause of this transition. In the high-grade carcinoma region as well as heterozygous loss of *FLCN* other genes were shown to be dysregulated such as vascular endothelial growth factor A, metalloproteinases matrix metallopeptidase 9 and matrix metallopeptidase 12 which could contribute to angiogenesis and invasiveness (Sirintrapun et al. 2014).

BHD-associated renal tumours have proven to be of diverse histological nature. One of the earliest histological analysis, involving 130 solid renal tumours of 30 BHD patients from 19 families, found most of the tumours to be hybrid oncocytic neoplasms and chromophobe renal cell carcinoma (65 of 130, 50%) or chromophobe renal cell carcinomas (44 of 130, 34%). 12 of the 130 tumours were diagnosed to be clear cell (9%) and 7 of the 130 tumours were diagnosed to be oncocytoma (5%) and only 2% of the tumours (2 of the 130) were papillary (Pavlovich et al. 2002). However the Houweling *et al.* study of 14 BHD patients with renal cell carcinoma from 35 families showed that most of the renal tumours were of chromophobe and clear cell nature, also most of the tumour cells had moderately enlarged nuclei with sharp cell borders and eosinophilic cytoplasm which meant that they could be intermediate between clear cell and chromophobe carcinoma. Five of these patients developed

metastatic disease (Houweling et al. 2011). In a more recent study of 33 BHD patients 23 of them (70%) had tumours with either chromophobe or hybrid chromophobe-oncocytoma characteristics; and only three (9%) had clear cell carcinoma. The rest of them either had carcinoma of papillary or the histology of the renal tumour could not be determined. Four of these BHD patients developed metastatic disease (Benusiglio, Giraud, et al. 2014).

Interestingly there are two independent reports of BHD patients who have developed renal angiomyolipomas. Renal angiomyolipomas are distinct characteristics of TSC and it is not usually seen in BHD patients. However involvement of both TSC and FLCN in mTOR Complex 1 (mTORC1) pathway could be the reason behind the development of renal angiomyolipomas in BHD patients (Byrne et al. 2012)(Tobino & Seyama 2012).

Although originally, because of the high percentage of chromophobe tumours in the Pavlovich *et al.* study, it was thought that the renal tumours in BHD patient arise from the distal nephron (Pavlovich et al. 2002); it was later demonstrated by two independent studies that the site of origin for BHD renal tumours is the proximal tubules (Chen et al. 2008)(Hudon et al. 2010).

1.2.4 Other clinical manifestations associated with BHD

To date the only confirmed manifestations associated with BHD syndrome are: Fibrofolliculomas, pulmonary cysts, spontaneous pneumothorax and renal cell carcinoma, however different studies have reported other clinical manifestations linked to BHD syndrome.

1.2.4.1 Colorectal polyps and colorectal cancer

Hornstein *et al.* and Birt *et al.* were the first groups to describe BHD and they suggested that there is an association between BHD syndrome and colorectal cancer (Hornstein 1976) (Birt et al. 1977). Subsequently two independent studies also proposed that there is a link between BHD syndrome and colorectal cancer (Schachtschabel et al. 1996) (Schulz & Hartschuh 1999). Conversely, in a large study of 33 BHD families with 98 affected members Zbar *et al.* could not find any correlation between polyps or colorectal cancer and BHD (Zbar et al. 2002). Nonetheless, Khoo *et al*. found six affected members of a BHD family presented with colorectal polyps and colorectal cancer, however they discuss that environmental or additional genetic factors could be contributing factors in certain families (Khoo et al. 2002). More recently in a study of 149 BHD patients from 51 families Nahorski *et al.* found 10 of these patients (6.7%) had colorectal polyps or cancer and all of these patients had mutation in exon 11 of FLCN (c.1285dupC), which could be suggestive of a possible genotype-phenotype correlation (Nahorski et al. 2010). However for any study of this nature to reach conclusive and statistical significance, a much larger cohort is needed.

1.2.4.2 Thyroid nodules and cancer

A long term study of 22 BHD patient from 10 families over the course of five years by Kluger *et al.*, found that strikingly 13 of these patients (65%) had developed thyroid nodules or cysts whereas no colorectal carcinoma was detected. Also they could not detect any genotype-phenotype correlation (Kluger et al. 2010). Although this is a great study in characterising the clinical manifestation of the BHD syndrome, since they did not use a control group for comparison the significance of their findings is quite questionable. In a more genetically focused study Benhammou *et al.* also found "6 of 15 patients with thyroid findings". Three of these patients had hypothyroidism, one of them had thyroid nodule and one of them had total thyroidectomy due to thyroid cancer. Although this was not a clinical study it provides further BHD link to thyroid abnormalities (Benhammou et al. 2011). More recently a case study reported a 72 year old man with BHD who was presented with right thyroid nodule. Further investigation revealed that the lesion was thyroid cancer. Interestingly they found loss of heterozygosity of FLCN in the tumour tissue but not the surrounding normal tissue (Benusiglio et al. 2014). Another case study of a 45 year old woman also reported the patient with thyroid cancer. However this patient was diagnosed with BHD after the thyroid cancer and the link between BHD and thyroid cancer was not investigated in this study (Yamada et al. 2015). Interestingly a case study of a 57 year old woman with metastatic anaplastic thyroid cancer demonstrated somatic mutation in *TSC2*, *FLCN* and *TP53* genes. Initially the tumour was successfully treated with everolimus which is an analogue of rapamycin and inhibits mTORC1 activity. However the tumour became insensitive to everolimus treatment after 18 month, which was revealed to be due to mutation in *MTOR* (Wagle et al. 2014).

1.2.4.3 Parotid tumours

Different studies have reported nine individual cases of parotid tumours in BHD patients to date. First case of parotid oncocytoma in a BHD patient was found by Liu *et al.* Then in 2005 Schmidt *et al.* found 4 cases of parotid tumours (three of which were classified as oncocytomas) in a study of 219 BHD-affected individuals (Liu et al. 2000)(Schmidt et al. 2005). Palmirotta *et al.* also reported a case of BHD patient with parotid pleiomorphic adenoma, which was diagnosed before her BHD diagnosis (Palmirotta et al. 2008). Maffé *et al*. has also reported a BHD patient with parotid oncocytoma where they also found loss of heterozygosity of *FLCN* in the tumour tissue (Maffé et al. 2011). In a case study of a 45 year old woman with a Warthin tumour of the parotid gland, Lindor *et al.* diagnosed the patient with BHD (Lindor et al. 2012). Pradella *et al.* also reported a BHD patient with parotid oncocytoma, however they did not observe any loss of the wild-type *FLCN* allele in the neoplastic tissue (Pradella et al. 2013). Although all these studies provide a link between parotid tumour and BHD, there is not enough conclusive statistical evidence to consider parotid tumours as clinical manifestation of BHD.

1.3 Folliculin

The *FLCN* gene encodes a 579 amino acid protein FLCN that is 64kDa. The protein consists of a short hydrophobic N-terminal sequence, one N-glycosylation site, three myristoylation sites and a glutamic acid-rich coiled coil domain centrally located in the protein (Nickerson et al. 2002). Phosphorylation and ubiquinqtion of folliculin has also been observed (Baba et al. 2006)(Dephoure et al. 2008)(Gauci et al. 2009)(Piao et al. 2009)(Wang et al. 2010)(Danielsen et al. 2011)(Wagner et al. 2011).

The protein sequence of FLCN is as follows:

MNAIVALCHFCELHGPRTLFCTEVLHAPLPQGDGNEDSPGQGEQAEEEEGGIQMN
SRMRAHSPAEGASVESSSPGPKKSDMCEGCRSLAAGHPGYISHDKETSIKYVSHQ
HPSHPQLFSIVRQACVRSLSCEVCPGREGPIFFGDEQHGFVFSHTFFIKDSLARGF
QRWYSIITIMMDRIYLINSWPFLLGKVRGIIDELQGKALKVFEAEQFGCPQRAQRMN
TAFTPFLHQRNGNAARSLTSLTSDDNLWACLHTSFAWLLKACGSRLTEKLLEGAPT
EDTLVQMEKLADLEEESESWDNSEAEEEEKAPVLPESTEGRELTQGPAESSSLSG
CGSWQPRKLPVFKSLRHMRQVLGAPSFRMLAWHVLMGNQVIWKSRDVDLVQSAF
EVLRTMLPVGCVRIIPYSSQYEEAYRCNFLGLSPHVQIPPHVLSSEFAVIVEVHAAAR
STLHPVGCEDDQSLSKYEFVVTSGSPVAADRVGPTILNKIEAALTNQNLSVDVVDQ
CLVCLKEEWMNKVKVLFKFTKVDSRPKEDTQKLLSILGASEEDNVKLLKFWMTGLS
KTYKSHLMSTVRSPTASESRN

The protein sequence of FLCN has proven to be highly conserved in vertebrates; however it does not have any significant homology to known proteins. The evolutionary analysis performed on the *FLCN* gene comparing over 5000 mouse and human orthologues by Nahorski *et al.* revealed that at the protein level, FLCN is evolving slower than the average gene. It also revealed that FLCN undergoes stronger purifying selection than the average gene. This was more noticeable between codons 100–230 (Nahorski et al. 2011).

The *FLCN* gene, Folliculin (GENBANK accession #BC015687), was mapped to the BHD locus 17p12-q11.2 by Khoo *et al.* 2001 having done a genome wide linkage analysis in a large Swedish family with BHD Syndrome (Khoo et al. 2001).

BHD is a hereditary syndrome that has an autosomal dominant pattern; however the pathogenesis mechanism through mutation of a single FLCN allele where a complete loss of the gene does not cause BHD is not fully understood.

FLCN can be a tumour suppressor gene according to Knudson's two-hit hypothesis. Knudson suggests that predisposition to cancer in some inherited diseases is as a result of germline mutation in a tumour suppressor gene together with a second somatic mutation in the remaining wild-type copy of the gene. In 2005 Vocke *et al.* observed either somatic mutations or loss of heterozygosity in 54 of 77 (70%) renal tumours in their study (Vocke et al. 2005). Conversely, van Steensel *et al.* studied 5 BHD patients presented with fibrofolliculomas but no kidney tumours and did not find any somatic mutation of *FLCN* or loss of heterozygosity. Subsequently they suggested that haploinsufficiency of FLCN is enough to induce uncontrolled growth in the skin (van Steensel et al. 2007). Furthermore, *in vitro* study of 10 candidate missense and inframe deletion *FLCN* mutations by Nahorski *et al.* revealed that the mutant FLCN proteins produced by these mutations are less stable and degraded (Nahorski et al. 2011). Although these two studies support the haploinsufficiency hypothesis, since deletion of the whole *FLCN* gene, which is observed in Smith-Magenis syndrome (SMS) (OMIM182290) and does not produce any of the BHD symptoms (Bi et al. 2002), makes haploinsufficiency hypothesis less likely to be the mechanism of pathogenesis in BHD.

1.3.1 Structure and post-translational modifications

In 2012, Nookala *et al.* managed to crystallise the C-terminal of FLCN and determined its structure by X-ray crystallography (PDB ID: 3V42). The amino acids at the C-terminal of FLCN form a core β-sheet with helices on one side, which is also followed by an all helical region. This structure is extremely similar to the DENN-domain proteins (Nookala et al. 2012). Proteins containing DENN-domain are known to function as Rab guanine nucleotide exchange factors (GEFs), therefore Nookala *et al.* suggested the Rab GEF role in membrane trafficking for FLCN function (Nookala et al. 2012). Using secondary structure prediction computer programmes, they also analysed the N-terminal of FLCN; which was predicted to form a longin domain. The longin domain is also part of DENN-domain containing proteins that are involved in membrane trafficking (Nookala et al. 2012). It is predicted that FLCN contains a bipartite tryptophan (WD-WQ) motif within the linker region, which consists of 40 amino acids and connects the N-terminal to the C-terminal. The WD-WQ motif is known to be a binding motif for kinesin light chain 1, which is a cargo transporting protein within the cell (Dodding et al. 2011).

Baba *et al.* first identified FLCN phosphorylation which was facilitated by FNIP1 and observed by multiple FLCN bands on their Western blots. They demonstrate that FLCN phosphorylation is partially reduced upon wortmannin treatment (an inhibitor of PI3K), it is drastically reduced upon rapamycin treatment (an inhibitor of mTORC1) and that FLCN phosphorylation was completely abolished upon treatment of compound C, which is an inhibitor of AMPK. Baba *et al*. findings suggest that FLCN is phosphorylated in the cell by a range of different kinases involving in different signalling pathways (Baba et al. 2006). In addition, in a

phosphoproteomic study, FLCN was identified as a phosphorylated peptide, further confirming that FLCN can exist in a phosphorylated form (Gauci et al. 2009).

The first phosphorylation sites identified on FLCN were serine 62 and serine 302, where serine 302 was suggested to be phosphorylated by an unknown kinase downstream of mTORC1 and phosphorylation of serine 62 was shown to be up-regulated by AMPK indirectly (Piao et al. 2009)(Wang et al. 2010). Subsequently Yu *et al.* in a global proteomics experiment, identified mTORC1 as the kinase that phosphorylates serine 62 and serine 73 of FLCN (Yu et al. 2011). More recently Laviolette *et al.* observed that phosphorylation of serine 62 and serine 73 is at its maximum level during the M phase of the cell cycle. Furthermore the FLCN-deficient Mouse embryonic fibroblast (MEF) cells were found to develop much quicker through the cell cycle process. It was also observed that FLCN in its phosphorylated stated (with serine 62 and seine 73 phosphorylated) is a less stable protein suggesting this post-translational modification plays an important role in regulation of cell cycle (Laviolette et al. 2013). Another post-translational modification observed in FLCN by two independent studies is ubiquitination, where Wagner *et al.* found lysine 206 and lysine 559 of FLCN to be ubiquitinated (Danielsen et al. 2011)(Wagner et al. 2011). However these are both proteomic studies on ubiquitination and a FLCN focused study is needed to know more about the relevance of these post-translational modifications.

1.3.2 Mutations

Using positional cloning Nickerson *et al.* mapped FLCN to 700 kb on chromosome 17p11.2., which was made up of 14 exons. They studied 9 BHD families and identified 8 *FLCN* mutations that were producing a truncated protein; five of these mutations were shown to be on exon 11 (Nickerson et al. 2002). Additionally they studied 53 probands from BHD families and found 22 further mutation in exon 11, indicating exon 11 as a mutation hotspot (Nickerson et al. 2002). Khoo *et al.* also identified two mutations in exon 11 in three out of four families screened. Furthermore they found mutation in exon 11 in a sporadic case of BHD (Khoo et al. 2002). Moreover, Schmidt *et al.* studied 30 BHD families and their combined result with the Nickerson *et al.* study further established the mutation hotspot theory. *FLCN* germline mutations were identified in 84% of the patients by sequence analysis and the majority of these mutations were predicted to produce a truncated protein (Schmidt et al. 2005). The first intragenic mutation in BHD patients was reported by Benhammou *et al*. They identified six intragenic deletions and one duplication in individuals clinically diagnosed with BHD whom their initial DNA sequencing had not revealed any mutations (Benhammou et al. 2011). Figure 1.1 illustrates *FLCN* gene with H429X, Y463X and K508R mutatins that were used in this study.

Of all the pathogenic FLCN mutations, approximately 41% are deletion mutations, 36% base substitution, 17% duplication and 5% insert/deletion mutation. An up-to-date database of all BHD mutations is kept on the Myrovlytis Trust website.

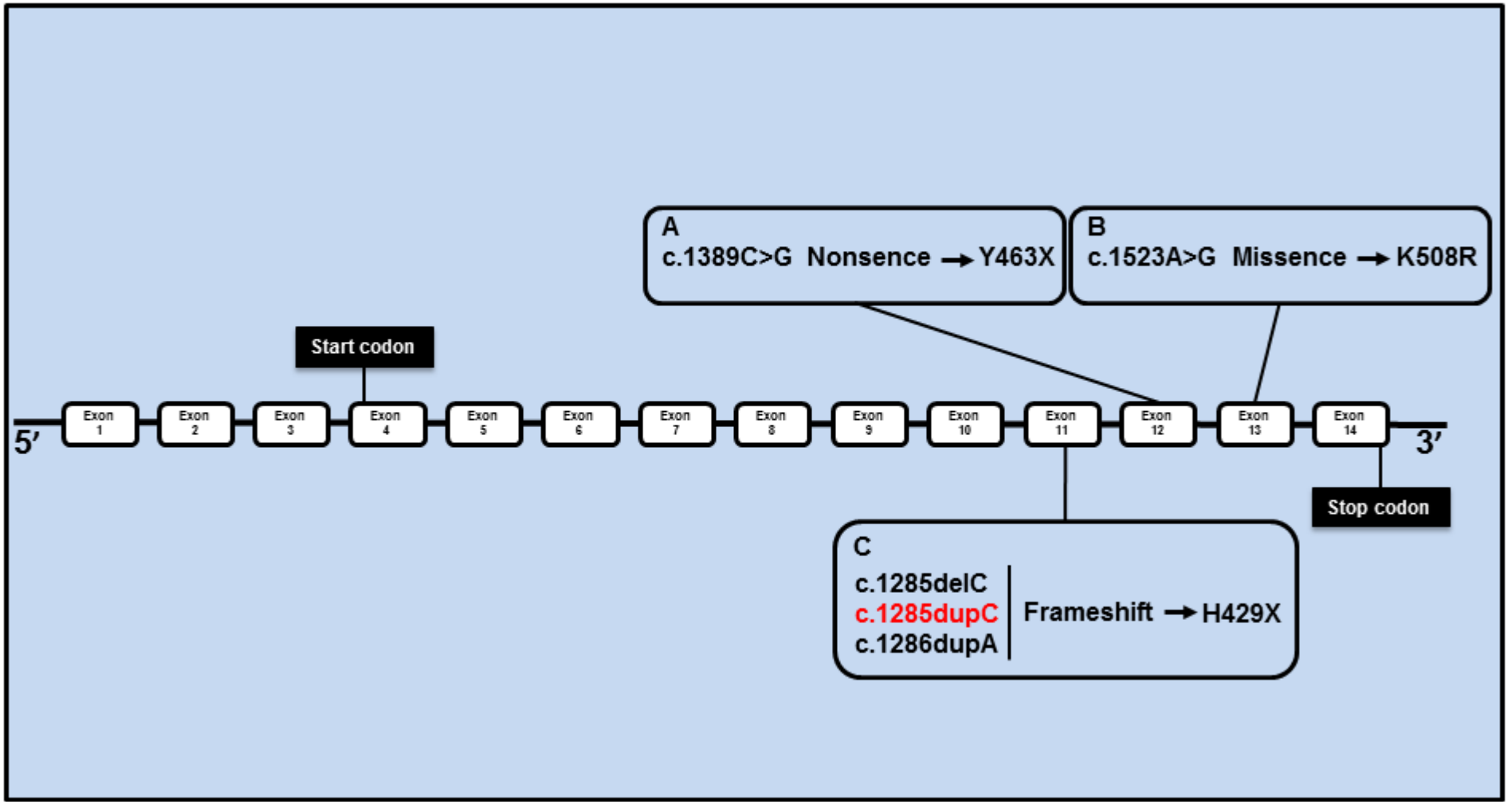

Figure 1.1 Schematic illustration of the *FLCN* gene: the patient mutations used in this study are shown in **A**, **B** and **C**. Three patient mutations can result in H429X, the one in red was used in this study.

1.3.3 Interacting partners

1.3.3.1 FLCN interacting protein 1 (FNIP1)

Baba *et al.* 2006 first identified FLCN interacting protein 1 (FNIP1). They observed that FNIP1 interacts with FLCN and also facilitates phosphorylation of FLCN by AMPK. FNIP1 is an evolutionarily conserved protein that also binds AMPK and is phosphorylated by AMPK (Baba et al. 2006). FLCN/FNIP1 interaction has also been shown to be altered by treatment of AMPK inhibitor (compound C), and also with rapamycin and amino acid starvation (Baba et al. 2006). Moreover Yu *et al.* has demonsterated that FNIP1 is phosphorylated by mTORC1, further placing FNIP1/FLCN in energy sensing pathawys (Yu et al. 2011). FNIP1 has also been shown to be ubiquitinated at lysine 161 (Wagner et al. 2011).

FNIP1 as well as FNIP2 is needed for the recruitment of FLCN to the lysosomes during amino acid starvation. Furthermore, both FNIP1 and FNIP2 have been shown to be essential for interaction between FLCN and the Rag small G proteins and that they facilitate the activation of Rags by FLCN (Petit et al. 2013)(Tsun et al. 2013).

FNIP1 has also been shown to be involved in B cell development in mice by two independent studies published in 2012 (Park et al. 2012)(Baba et al. 2012).

Behrends *et al*. found FNIP1 to interact with GABARAP and therefore is likely involved in human autophagy (Behrends et al. 2010). Zhang *et al.* revealed that FNIP1 contains a DENN domain, further implicating FNIP1 in membrane trafficking during different steps of autophagy (Zhang et al. 2012).

1.3.3.2 FLCN interacting protein 2 (FNIP2)

Nagase *et al.,* in a study of human cDNA library found *FNIP2* gene, which they designated the name KIAA1450 to it then (Nagase et al. 1998). However it was not until 2008 that Hasumi *et al.* identified it as FLCN interacting protein 2 (Hasumi et al. 2008). Subsequently Komori *et al*. found that mouse FNIP2, which they called MAPO1, is necessary for apoptosis induced by O6-methylguanine mispairing in DNA (Komori et al. 2009). More recently two independent studies also confirmed that FNIP2 together with FLCN is required for apoptosis induced by N-Nitroso-N-methylurea (MNU) (Lim et al. 2012)(Sano et al. 2013).

FNIP2 is a homologue of FNIP1 with 49% identity, 74% similarity and is highly conserved across species. FNIP1 and FNIP2 are able to form homodimers and heterodimers. Like FNIP1, it has been shown to bind AMPK and to be phosphorylated by AMPK (Hasumi et al. 2008)(Takagi et al. 2008).

As mentioned before, similar to FNIP1, FNIP2 is required for the recruitment of FLCN to the lysosomes (Petit et al. 2013)(Tsun et al. 2013).

FNIP2 also contains a DENN domain suggesting that it is involved in membrane trafficking (Zhang et al. 2012).

It has been suggested that FNIP2 is required for myelination in the central nervous system (Pemberton et al. 2014). In a study by Pemberton *et al*., a frameshift mutation in *FNIP2* gene in the Weimaraner dog was found to cause hypomyelination of the brain and myelin defect in the spinal cord (Pemberton et al. 2014).

1.3.3.3 Plakophilin-4

Nahorski *et al.* identified Plakophilin-4 (PKP4) that is also known as p0071, as a potential interacting partner for FLCN using yeast-2-hybrid analysis; which was then confirmed by co-immunoprecipitation (Nahorski et al. 2012). They also observed that FLCN partially co-localises with Plakophilin-4 at cell junctions in the interphase; however it is localised at the midbody during cytokinesis (Nahorski et al. 2012). Using the same approach Medvetz *et al.* also found that Plakophilin-4 interacted with FLCN. They demonstrated that cell-cell adhesion and formation of desmosomes were negatively regulated by FLCN. Moreover they observed FLCN-null UOK257 cells had reduced Rho activity and impaired cell migration (Medvetz et al. 2012).

1.3.3.4 Rpt4

Using a Drosophila cDNA library and yeast-2-hybrid, Gaur *et al.* identified Regulatory particle triple-A ATPase 4 (Rpt4) as FLCN interacting partner. This interaction was further confirmed in human HEK293 cells where and endogenous interaction between FLCN and Rpt4 was detected by co-immunoprecipitation. They also suggest a molecular function for FLCN in inhibiting rRNA transcription (Gaur et al. 2013).

1.3.3.5 Rag proteins

FLCN has reportedly been shown to interact with Rag small G proteins. Petit *et al.* demonstrated that FLCN interacts with RagA via its GTPase domain and this

interaction is facilitated by FNIP1. This finding suggests that FLCN could be a guanine nucleotide exchange factor (GEF) towards RagA (Petit et al. 2013). However, FLCN in complex with FNIP2 was shown to function as a GTPase-activating protein (GAP) in a study by Tsun *et al.*. FLCN was found to stimulate GTP hydrolysis by RagC and RagD, but not RagA, RagB. It was also found that FLCN interaction with Rag proteins is required for activation and recruitment of mTOR to the lysosomal membrane during amino acid starvation (Tsun et al. 2013). FLCN was demonstrated to interact with inactive Rag heterodimers in Martina *et al.* study whereas TFE3 was shown to interact with active Rags. TFE3 was also shown to be phosphorylated at serine 311 upon mTOR activation by FLCN (Martina et al. 2014).

1.3.4 Signalling pathways

1.3.4.1 Mammalian target of rapamycin (mTOR) signalling

FLCN was first implicated in mTOR signalling through interaction with AMPK which was facilitated by FNIP1 and FNIP2 (Baba et al. 2006)(Hasumi et al. 2008). mTOR is a serine/threonine kinase that is highly conserved and has been shown to regulate cell growth, proliferation and metabolism in response to environmental changes (Wullschleger et al. 2006). There is compiling evidence suggesting that mTOR dysregulation is involved in human disease such as cancer and diabetes (Sarbassov et al. 2005)(Landau et al. 2009).

The exact role of FLCN in mTOR signalling is not quite clear and there are contradictory studies regarding FLCN function in this pathway. Three independent studies have observed down-regulation of mTOR activity through loss of phosphorylation on ribosomal protein S6 (p-rpS6), in FLCN-deficient cells (Takagi et

al. 2008)(Hartman et al. 2009)(Bastola et al. 2013). Additionally Hartman *et al.* observed low levels of p-rpS6 (Ser 235/236) in renal oncocytic cysts and tumors from the *Bhd*$^{+/-}$ mice (Hartman et al. 2009).

Conversely other studies have observed up-regulation of mTORC1 upon loss of FLCN expression. When *Flcn* was knocked out specifically in mouse kidneys by Baba *et al.*, although mTOR expression levels were found to be unchanged, phosphorylation of rpS6 on Serine 240/244 was shown to be elevated; indicating an up-regulation of mTORC1 activity (Baba et al. 2008). Similarly Chen *et al*. showed mTORC1 pathway was activated upon complete loss of *Flcn* in mouse kidney cysts and tumours through phosphorylation of both mTOR and rpS6 (Chen et al. 2008). Furthermore, heterozygous loss of *Flcn* in *Flcn*$^{d/+}$ mice, also resulted in higher levels of phosphorylated rpS6 protein (Ser240/244) in kidney tumour tissue (Hasumi et al. 2009). More recently, Hasumi *et al.* also observed that *Flcn* knockout mice developed cardiac hypertrophy due to increased mTORC1 activity (Hasumi et al. 2014). Two other clinical studies have also observed increased phospho-mTOR and phospho-rpS6 expression in epithelial cells of the pulmonary cysts from BHD patients. They postulate that heterozygous loss of *Flcn* causes dysregulation of mTORC1 signalling which leads to formation of the cysts (Furuya et al. 2012)(Nishii et al. 2013).

Remarkably Hudon *et al.* revealed that depending on the cellular context of the *Flcn* knockout mouse, both elevation and reduction of phosphorylated rpS6 protein levels could be observed (Hudon et al. 2010). In concordance Khabibullin *et al.* observed a highly cell type dependence modification of mTORC1 signalling upon loss of *FLCN*. Knock down of *FLCN* in small airway epithelial (SAEC) cells resulted in increased mTORC1 activity which was observed by two fold increase in phospho-

rpS6; whereas *FLCN* knock down in human bronchial epithelial (HBE) cells did not modify mTORC1 signalling (Khabibullin et al. 2014).

Therefore, this inconsistency observed in mTORC1 signalling in FLCN-deficient cells and mouse models could be multifactorial. Differences in sample preparation, different gene targeting strategies used for making mouse models as well as cellular context and cell types, all play a role in different outcome of mTORC1 signalling upon loss of FLCN.

1.3.4.2 AMP-activated protein kinase (AMPK) signalling

AMP-activated protein kinase (AMPK) is one of the key regulators of energy in eukaryotic cells that restores energy homeostasis through inhibiting anabolic growth by repression of the mTORC1 pathway. AMPK also promotes catabolism through induction of autophagy and enhances cell survival during periods of starvation when energy is in short supply (Alers et al. 2012)(Hardie et al. 2015). FLCN has been shown to interact with AMPK and to be phosphorylated by AMPK. Both interaction of FLCN with AMPK and its phosphorylation by AMPK is facilitated by FNIP1 and FNIP2 (Baba et al. 2006)(Hasumi et al. 2008)(Takagi et al. 2008). Phosphorylation of FLCN at serine 62 was shown to increase the affinity of the FLCN/FNIP complex towards AMPK, whereas serine 302 phosphorylation decreased the affinity of the complex for AMPK (Piao et al. 2009)(Wang et al. 2010). Mouse embryonic fibroblasts (MEFs) generated from *Flcn*$^{-/-}$ (KO) mouse in the Yan et al. study displayed increased AMPK activity. Consequently this AMPK activation upon loss of Flcn resulted in upregulation of PGC-1α, increased mitochondrial biogenesis, ROS production, and HIF activation. When serine 62 within FLCN was mutated to alanine,

interaction of the FLCN/FNIP complex with AMPK was reduced and this reduction significantly enhanced the phosphorylation of AMPK (Yan et al. 2014). Yan *et al.* data suggests that when the FLCN/FNIP complex is bound to AMPK it can block activation of AMPK; since AMPK has been shown to phosphorylate FLCN via FNIPs this could indicate a feedback mechanism for the AMPK/FLCN pathway.

Study on *Caenorhabditis elegans* (*C. elegans*) by Possik et al. revealed that when *flcn-1* was mutated (flcn-1(ok975) mutation), to produce a loss-of-function allele, phospho-AAK-2 levels were increased (AAK-2 is an AMPK orthologue). Phospho-AMPK levels in MEFs were also observed to be increased upon loss of *Flcn*, which could be rescued back to normal levels when wild type FLCN was re-expressed in these MEFs (Possik et al. 2014).

Conversely, isolated primary mouse alveolar epithelial type II cells (AECs) from lungs of *Flcn*$^{f/f}$*:SP-C-Cre* mice exhibited significant reduction of AMPK(Thr172) phosphorylation (Goncharova et al. 2014). Subsequently, FLCN-deficient cell survival was shown to be increased by 5-aminoimidizole-4-carboxamide riboside (AICAR) treatment, and by expressing the constitutively active AMPK (AdAMPK-CA) in FLCN-deficient cells (Goncharova et al. 2014). In concordance, Khabibullin *et al*. also showed that FLCN knockdown in HBE cells resulted in reduction of AMPK activity; however, AMPK activity was not affected upon loss of FLCN in SAEC cells (Khabibullin et al. 2014). Hasumi *et al.* also observed reduction in phospho-AMPKα (Thr172), indicating a decreased AMPK activity in *Flcn* knockout hearts. *Flcn*-deficient hearts had a cardiac hypertrophy phenotype which could be as a result of AMPK dysregulation; however, treatment with AICAR or metformin that are both AMPK activators did not improve the cardiac phenotype (Hasumi et al. 2014).

FLCN together with FNIP2 have been shown to activate AMPK when DNA is damaged by alkylating agents, *i.e.*, treatment with N-methyl-N-nitrosourea (MNU), to initiate apoptosis (Lim et al. 2012)(Sano et al. 2013).

Over all, these findings suggest that similar to the effects on the mTORC1 pathway by FLCN, the effect of FLCN on AMPK signalling pathway is probably highly dependent on the cell type.

1.3.4.3 Hypoxia Inducible Factor (HIF) signalling

In 2011, Preston *et al.* observed that HIF-induced gene expression during hypoxia is negatively regulated by FLCN in hypoxic conditions. In this study, the UOK257 cell line was analysed, which is derived from a BHD patients's renal tumour. These UOK257 cells had high levels of HIF activity compared to the cell line stably expressing wild type FLCN. Both mRNA and protein levels of HIF-1α and HIF-2α downstream transcriptional targets, *i.e.,* VEGF-A, BNIP3, CCND1 and GLUT1, were shown to be elevated in hypoxia and to a lesser extent under normoxia in FLCN deficient cells. However, loss of FLCN did not affect mRNA or protein levels of HIF-1α in either hypoxic or normoxic condition; indicating that FLCN regulates the transcriptional activity of HIF-1α rather than its expression (Preston et al. 2011). Additionally, immunohistochemical staining of HIF-1α, BNIP3, GLUT1 and VEGF-A in chromophobe renal carcinoma tumour from a BHD patient, demonstrated nuclear localisation of HIF-1α and elevated levels of BNIP3, GLUT1 and VEGF-A compared to unaffected tissue to further support this theory (Preston et al. 2011).

Moreover, histopathological study of the resected lung of a 33 year old woman by Nishii *et al.*, revealed that HIF-1α was localised to the nucleus in the cyst-

lining cells, indicating the activation of HIF-1α transcription target genes. Immunohistochemical staining demonstrated elevated levels of VEGF in the cyst-lining cells and endothelial cells of the wall compared to the normal lung tissue, indicative of high HIF-1α activity. In slight contrast to the Preston *et al.* study, western blot analysis revealed HIF-1α protein to be present at higher levels in cystic lung tissue compared to the normal lung tissue (Nishii et al. 2013).

Using a HIF reporter assay, Yan *et al.* showed that *FLCN* null MEF cells exhibited a two fold increase in HIF activity compared to normal cells in hypoxia. In concordance with the Preston *et al.'s* study they also did not observe any change in the expression levels of HIF-1α or HIF-2α protein upon loss of FLCN in MEFs. AMPK was observed to be constitutively active in these *FLCN* null MEFS, which in turn resulted in increased PGC1α and mitochondrial biogenesis which led to increased production of reactive oxygen species (ROS), which is thought to drive HIF activity in this context (Yan et al. 2014). Overall loss of FLCN has been shown to cause an elevation in HIF activity; however its mechanism seems to be cell type dependent.

1.3.4.4 The Janus kinase/signal transducers and activators of transcription (JAK/STAT) and TGF-β signalling

The JAK/STAT signalling pathway facilitates cellular responses to the chemical signals from outside the cell such as cytokines and growth factors (Mohr et al.). Decreased expression of the *Drosophila FLCN* homologue (*dBHD*) in the Singh *et al.* study revealed that *dBHD* was essential for maintenance of male germline stem cell (GSC) in the fly testis. Further experiment suggested that *dBHD* probably regulates GSC maintenance downstream of the Decapentaplegic (Dpp) signalling

pathway which functions downstream of JAK/STAT signalling pathway. They postulated that the dBHD and the Dpp signals synergise on downstream targets (Singh et al. 2006).

Dpp is homologue of the vertebrate bone morphogenetic proteins (BMPs). BMPs are members of the TGF-β superfamily, which has been shown to be essential for regulation of different cellular functions including stem cell renewal (Ying et al. 2003)(Tossidou & Schiffer 2012).

FLCN has been observed to regulate TGF-β signalling by several independent studies. Using microarray analysis, Hong *et al.* observed that *TGF-β2* (*TGFB2*), *Inhibin β A* (*INHBA*, a subunit of activin A), *SMAD3* (*SMAD3*) and *thrombospondin-1* (*THBS1*) were down-regulated, and *Gremlin* (*GREM1*) was upregulated in FLCN-deficient UOK257 cells as well as mutant *FLCN-H255R* UOK257 cells compared to the UOK257 cells expressing wild type FLCN. Furthermore, RT-PCR and immunohistochemical staining revealed that genes involved in TGF-β signalling (*TGFB2, INHBA, SMAD3, THBS1, GREM1*) and the encoded proteins were dysregulated in renal tumours from BHD patients (Hong et al. 2010). Cash *et al.* found that *Bhd*$^{-/-}$ ES cells display defective TGF-β mediated transcriptions such as Bcl-2 Interacting Mediator of Cell Death (BIM). Since Trichostatin A (TSA) treatment which is a histone deacetylase (HDAC) inhibitor could reverse the biological and molecular defects of *Bhd*$^{-/-}$ cells; Cash *et al.* suggest that this defect is probably due to HDAC-mediated effects on chromatin at Smad-dependent promoters (Cash et al. 2011). More recently, using RT PCR, Khabibullin *et al.* found loss of FLCN in in HBE cells resulted in decreased INHBA that is a TGF-β pathway component. Conversely in FLCN-deficient SAEC cells increased levels of

INHBA was observed while SMAD3 and CDKN2B were decreased (Khabibullin et al. 2014).

1.3.4.5 Ciliogenesis

A study carried out by Luijten *et al.* provided evidence that FLCN has the ability to localize in the primary cilia and the motile cilia in HK2 and primary HNE cells, respectively. In the same study FLCN was both knocked down and over expressed in HK2 cell lines; results demonstrated that after 72 hours fewer cells had normal and functional cilia. Of interest after 96 hours the cilia of these cells started to function normally similar to the wild type in both experiments. This observation suggests that FLCN could be controlling the onset of ciliogenesis. Knowing that the existence of cystic lesions are indeed a hallmark of ciliopathies, these cystic lesions could be an indication that BHD is also a ciliopathy (Luijten et al. 2013).

1.3.4.6 The Ras-Raf-MAPK signalling

The Raf-MAPK pathway is one of the most important downstream signalling pathways of Ras, a small GTPase protein, known to be frequently mutated and dysregulated in various cancers. It has been shown that this pathway is involved in cancer progression via cell proliferation, migration, survival, angiogenesis etc. (Dhillon et al. 2007). Several studies have indicated that within FLCN-null kidneys the Ras-Raf-MAPK pathway seem to be activated due to the loss of FLCN, which resulted in abnormal cell growth and proliferation in these cells (Baba et al. 2008)(Hudon et al. 2010).

Of interest, heterozygous loss of *Drosophila dBHD* in flies with a constitutively expressed Ras1 that is involved in MAPK signalling pathway during eye development, caused over proliferation and hyperplastic growth of the eye, resulting in death (Gaur et al. 2013). Moreover, Gaur *et al.* also demonstrated that FLCN has the ability to interact with Rpt4, causing inhibition of rRNA synthesis within the nucleolus in both human and *Drosophila* cells. Since an increase in rRNA synthesis is essential for the activation of the Ras-Raf-MAPK pathway in *Drosophila*, it could be concluded that FLCN acts as an inhibitor towards the Ras pathway (Gaur et al. 2013). According to the Gaur *et al.* study the hyperplastic growth seen in BHD patients could be partly as a result of increased activation and stimulation of the Ras-Raf-MAPK pathway and upregulation of rRNA synthesis (Gaur et al. 2013).

1.3.4.7 Wnt/Cadherin signalling pathway

In order to better understand the targets of FLCN and its role in cell signalling pathways, microarray studies were carried out by Reiman *et al.*. Wnt and cadherin signalling genes were shown to be the most differentially expressed genes in FTC-133 *FLCN* null cells compared to the wild type (Reiman et al. 2012). The Cadherin pathway is known to regulate the formation of cell-cell junctions. Loss of FLCN has been shown to cause a reduction in the E-cadherin located at the adherence junctions (Nahorski et al. 2012). Additionally, Medvetz *et al.* demonstrated that FLCN null UOK257 cells had increased desmosome formation compared to FLCN expressing UOK257 cells and formed both normal and abnormal desmosomes (Medvetz et al. 2012).

B-catenin is one of the essential components of the Wnt signalling pathway. Luijten *et al*. found that FLCN also played a role in planar cell polarity (PCP) regulation via isolating B-catenin in cilia (Luijten et al. 2013). Both pathways have been associated with cancer (Jeanes et al. 2008)(Hsu et al. 2012) and could possibly contribute to tumourigenesis in BHD patients.

1.4 Autophagy

Autophagy is a biological process that is evolutionarily conserved in eukaryotic cells and is vital for cell survival during nutrient starvation where intracellular lipid and protein components are broken down to replenish cellular energy and amino acid supplies. Basal autophagy also plays an important role in maintaining the cellular homeostasis when unwanted or damaged proteins and cytoplasmic organelles are degraded (Choi et al. 2013)(Ávalos et al. 2014). Christian De Duve first suggested the term autophagy, meaning “self-eating” in Greek, for the process in Ciba Foundation Symposium on Lysosomes in 1963 (Klionsky 2008).

Three different types of autophagy are known; macroautophagy, microautophagy, and chaperone-mediated autophagy (CMA). Different types of autophagy vary in their function and the manner in which the cargo is delivered to the lysosomes. Chaperone-mediated autophagy is the selective type of autophagy. In this process cytosolic proteins that contain a pentapeptide motif (which is recognised by the chaperone heat shock cognate 70 (Hsc70)), are transferred directly to the lysosomes through binding to the receptor lysosome-associated membrane protein 2A (LAMP2A). Microautophagy is the process in which cytoplasmic materials are engulfed directly by lysosomes that usually involves small molecules (Ravikumar et al. 2009) (Ávalos et al. 2014).

Macroautophagy (referred to as autophagy hereafter) is a cellular process in which unwanted cytoplasmic material are sequestered in a double-membrane vesicle called the autophagosome. After maturation autophagosomes fuse with lysosomes to form autolysosomes, where lysosomal hydrolases digest the autophagosome’s material. When degradation is complete, permeases transport

amino acids and lipids back into the cytoplasm for recycling (Figure 1.2) (He & Klionsky 2009)(Tanida 2011).

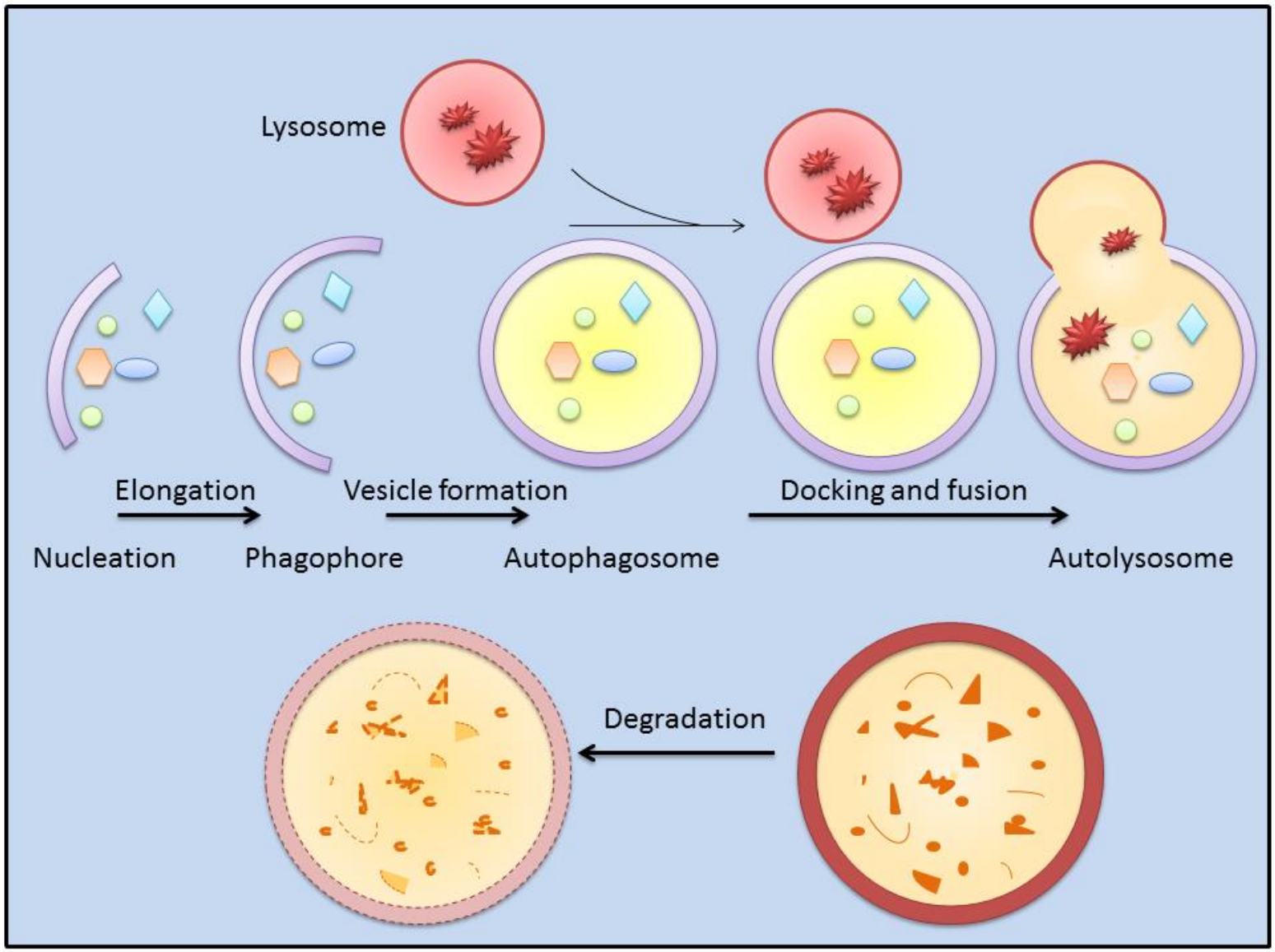

Figure 1.2 Schematic illustration of the main autophagic events

Formation of autophagosomes starts at the phagophore which is the assembly sites or precursor for autophagy. Phagophore double membrane assembly was postulated to be a *de novo* process in the cytosol, however quite a few laboratories found conflicting data in regard to the presence of ER and golgi markers in the phagophore and autophagosome suggesting that the phagophore arises from the ER or the golgi complex (Tsukada & Ohsumi 1993)(Strømhaug et al. 1998)(Orsi et al. 2010). Activation of the class-III phosphoinositide 3-kinase (PI3K) Vps34, is necessary for the formation of phagophores. Vps34 acts in a larger complex with Atg14, beclin 1 and AMBRA1. Phosphorylation of Beclin-1 by ULK1 (the mammalian orthologue of Atg1) activates the Vps34 complex which in turn initiates autophagy (Ravikumar et al. 2009)(Russell et al. 2013). Recruitment of Atg12, Atg5, Atg16 and Atg8–PE (phosphatidylethanolamine) are known to be essential for elongation of the phagophore membrane (He & Klionsky 2009).

When the phagophore is sealed, the autophagosome is formed and the cargo is delivered to the lysosomes for degradation. Atg8 family of proteins have been shown to be vital for the maturation of the autophagosomes. Additionally the autophagy initiating complexes such as Atg16 and ULK1 need to dissociate from the autophagosome for the lysosomal fusion to occur (Nair et al. 2012)(Ganley 2013).

In mammalian cells lysosomal membrane protein LAMP-2 and the small GTPase Rab7 are known to be required for the fusion of lysosomes and autophagosomes (Jäger et al. 2004). Other proteins involved in lysosomal fusion are homotypic fusion and protein sorting (HOPs) membrane-tethering complexes and soluble N-ethylmaleimide-sensitive factor-attachment protein receptor (SNAREs) (Ganley 2013). More recently it was stablished that GABARAP, a sub family of Atg8 proteins, is needed for the fusion of lysosomes and autophagosomes. It was shown

that GABARAP interacts with Phosphatidylinositol 4-kinase IIα (PI4KIIα) and recruits it to the lysosomes which facilitates the lysosome/autophagosome fusion (Wang et al. 2015).

The engulfed materials within autolysosome are then degraded by the lysosomal acid hydrolases. Vacuolar permeases transport the small molecule products of this degradation back to the cytosol to be used in protein synthesis and cell maintenance (He & Klionsky 2009).

1.4.1 Autophagy-related proteins (Atgs)

Studies on *Saccharomyces cerevisiae* have revealed numerous autophagy-related (Atg) proteins that are involved in autophagy. Many of these Atg proteins are recruited to the phagophore assembly site for the initiation of autophagy (Klionsky et al. 2011).

1.4.1.1 Atg8 family of proteins

Microtubule-associated protein 1A/1B-light chain 3 (LC3) is encoded by the *MAP1LC3* gene in humans and is one of the Atg8 family members. LC3 has a molecular mass of 17 kDa and is a soluble protein which is spread universally in mammalian tissues (Tanida et al. 2008).

LC3 is present in two forms within the cell the un-conjugated form or LC3I and the phosphatidylethanolamine (PE) conjugated or LC3II. LC3I has a cytosolic location whereas LC3II is membrane-bound. It has been shown that LC3II localises to the autophagosome and is degraded by lysosomal hydrolases after the fusion.

Therefore turnover of LC3 can be used as an autophagy marker (Kabeya et al. 2004)(Klionsky 2005).

The γ-aminobutyric acid receptor-associated protein (GABARAP) is another Atg8 family member that is encoded by the *GABARAP* gene. It is a 27 kDa protein and unlike the first basic alpha-helix amino acid structure of LC3, GABARAP has an acidic nature. However GABARAP, similar to LC3 gets conjugated in the cells during autophagy and it has been suggested that it functions downstream of LC3 (Slobodkin & Elazar 2013). GABARAP was first identified as a membrane trafficking protein; it has also been linked to SNARE proteins that facilitate intracellular trafficking events (Wang et al. 1999)(Elazar et al. 2003). Furthermore, independent studies have observed up-regulation of Atg8 family members under different stress conditions from yeast to human cell lines (Egami et al. 2005)(van Zutphen et al. 2010).

1.4.1.1.1 LIR motif

Using detailed deletion mapping analyses and X-ray crystallography, LC3-interacting region (LIR) motifs of p62 and of the Cvt cargo receptor Atg19 were the first to be identified. It revealed a short hydrophobic common W-X-X-L motif where X can be any amino acid (Pankiv et al. 2007)(Ichimura et al. 2008). Further studies have revealed that a LIR motif may also have the sequence of W/F/Y-X-X-L/I/V. It has been shown that the F-type LIR motifs evolutionary have a higher affinity for GABARAP family of Atg8s (Johansen & Lamark 2011)(Alemu et al. 2012). Serine and threonine are used in the X position of the motif dominantly in some LIR containing proteins which could be an indication of phosphorylation regulation of the region. Additionally the presence of an acidic charge (E, D, S or T) on either N- or C-

terminal of the motif has been shown to be evolutionary conserved and it has been postulated to play a role in the affinity of the interaction (Birgisdottir et al. 2013).

1.4.2 p62 (Sequestosome 1, SQSTM1)

p62 is a protein encoded by the *SQSTM1* gene in humans. It was the first autophagy protein to be implicated in selective autophagy (Pankiv et al. 2007). It is also known that p62 functions as a scaffold protein in the NF-kB pathway (Moscat et al. 2007). Mice knockout studies of p62 by Komatsu *et al.* has shown that p62 can bind to LC3 and ubiquitin to regulate the formation of protein aggregates (Komatsu et al. 2007). Furthermore p62 is known to regulate apoptosis through activation of polyubiquitinated caspase-8 by promoting aggregation of CUL3-modified caspase-8 which leads to the full activation of apoptotic process (Jin et al. 2009).

p62 contains few well known domains, such as a zinc finger(ZZ), a tumour necrosis factor receptor associated factor 6 (TRAF6) and a LIR; the presence of these multiple domains indicates multifunctional activity of the protein. P62 is dominantly a cytoplasmic protein however, its presence in the nucleus has been observed as well ((Kabeya et al. 2004).

The removal of p62 from the cytoplasm is predominantly done via autophagy therefore the amount of p62 is generally used as readout of autophagic activity. p62 accumulation in immunocytochemistry or increased levels of p62 via western blots are usually an indication of autophagy impairment (Pircs et al. 2012)(Lippai & Lőw 2014).

1.4.3 unc-51 like autophagy activating kinase 1 (ULK1)

ULK1 is the mammalian orthologue of Atg1 which is a serine/threonine kinase. It functions at the initiating step of autophagy and its kinase activity is necessary for assembly and formation of autophagosomes (Itakura & Mizushima 2010). Yeast studies have revealed that upon starvation Atg1 in a complex with four other Atg proteins Atg13, Atg17, Atg29, and Atg31 recruits Atg9 and the autophagy-specific PI3K complex to the phagophore which results in recruitment of the Atg2-Atg18 complex and the Atg conjugation systems (Suzuki et al. 2007). When Atg1 complex is formed the kinase activity of Atg1 becomes elevated which is required for cycling of the Atg protein within the phagophore and autophagy progression (Reggiori et al. 2004)(Noda & Inagaki 2015).

There are two orthologues of the yeast Atg1 in mammals ULK1 and ULK2. ULK1 in a complex with ATG13, FIP200 and ATG101 drives autophagosome formation and the complex is positively regulated by many internal ULK1-mediated phosphorylation events, including ULK1 autophosphorylation (Jung et al. 2009)(Ganley et al. 2009). It has been shown that ULK1 can be phosphorylated at multiple sites however not all the kinases responsible for ULK1 phosphorylation have been identified. Similar to yeast Atg1, ULK1 autophosphorylation is demonstrated to be crucial for elevated activity and stability of the complex (Dorsey et al. 2009).

Downstream ULK1 substrates are gradually being identified. AMBRA1 was the first ULK1 substrate identified that is integral to the autophagy machinery but is not a component of the ULK1-ATG13-FIP200 complex (Löffler et al. 2011). More recently, ULK1 phosphorylation of ATG9 was identified as an important step during expansion of the isolation membrane (Papinski et al. 2014). Additionally, a further molecular link has been identified, whereby active ULK1 can directly phosphorylate

Beclin1, allowing pro-autophagy Vps34 complexes to promote autophagy induction and autophagosome maturation (Jung et al. 2011). ULK1 is known to indirectly impact autophagy via phosphorylation of both AMPK and Raptor within mTORC1 (Löffler et al. 2011)(Jung et al. 2011). It was revealed that ULK1 phosphorylates Raptor at multiple serine and a threonine sites (Ser696, Ser792, Ser855, Ser859, Ser863, Ser877 and Thr706). Raptor phosphorylation by ULK1 and also their direct interaction was shown to impair the interaction between mTORC1 and Raptor (Dunlop et al. 2011).

It has been established that the phosphorylation status of the ULK1 complex drastically changes with the nutrient status of the cell and the complex is regulated by both mTORC1 and AMPK (Alers et al. 2012).

When growth conditions are optimal, mTORC1 phosphorylates Atg13 and Ulk1/2 via their interaction with raptor which in turn disables the kinase activity of ULK1/2 (Ganley et al. 2009). Upon starvation, the inhibitory mTORC1 phosphorylation sites become dephosphorylated and the pre-activated ULK1 becomes autophosphorylated to further enhance ULK1. ULK1 also phosphorylates FIP200 and Atg13 within the complex which causes the complex to translocate to the phagophore (Hosokawa et al. 2009).

ULK1 has been shown to directly interact with AMPK and to be phosphorylated by AMPK. AMPK positively regulates ULK1 activity via phosphorylation (Kim et al. 2011)(Bach et al. 2011).

1.4.4 AMP-activated protein kinase (AMPK)

AMPK is a serine/threonine kinase that was originally found to phosphorylate and inactivate several lipogenesis enzymes. AMPK is known as an evolutionarily conserved protein that plays an important role in energy-sensing in the cell which is activated by metabolic stress (Hardie 2007). Studies on *Saccharomyces cerevisiae* revealed that SNF1, the yeast orthologue of AMPK, positively regulates autophagy (Wang et al. 2001). Using HT-29 cells and HeLa cells it was demonstrated that autophagy was inhibited when the cells were treated with compound C which is an inhibitor of AMPK. This evidence suggests an essential role for AMPK in the regulation of autophagy in mammals (Meley et al. 2006). Under starvation, AMPK is activated via LKB1 and increased AMP concentration in the cell which leads to activation of Tuberous Sclerosis Complex 1 and 2 (TSC1/2), which inhibits signal transduction through Rheb/mTORC1. However, it has been suggested that other conditions apart from starvation also regulate autophagy through activation of AMPK. Activation of Ca^{2+}/calmodulin-dependent kinase kinase-β (CaMKK-β) by Ca^{2+} mobilizing agents such as vitamin D compounds, thapsigargin, ATP and ionomycin, activate AMPK when free cytosolic Ca^{2+} is increased; which has been shown to drive autophagy in human breast cancer and cervix carcinoma cells (Høyer-Hansen et al. 2007). Tumour necrosis factor (TNF)-related apoptosis-inducing ligand (TRAIL) has also been shown to induce autophagy through transforming growth factor-β-activating kinase 1 (TAK1)-mediated activation of AMPK in MCF10A cells (Herrero-Martín et al. 2009).

When cells are deprived of energy, AMPK directly binds to and phosphorylates ULK1, inducing autophagy. Multiple ULK1 residues have so far been identified to be phosphorylated by AMPK. Egan *et al.* found Ser467, Ser555, Thr574

and Ser637 on ULK1 as potential AMPK phosphorylation sites of which three sites (Ser555, Thr574 and Ser637) were confirmed as direct AMPK phosphorylation sites by tandem mass spectrometry and *in vitro* kinase assays (Egan et al. 2011). Two further AMPK phosphorylation sites were uncovered subsequently on ULK1 as Ser317 and Ser777. It was demonstrated that phosphorylation of Ser317 and Ser777 by AMPK is required for efficient autophagy induction (Kim et al. 2011). Bach *et al.* also identified Ser555 as the AMPK phosphorylation site on ULK1. It was shown that ULK1/14-3-3 binding is mediated through AMPK phosphorylation of Ser555 (Bach et al. 2011).

1.4.5 Mammalian/mechanistic target of rapamycin (mTOR)

TOR1 and TOR2 genes were first identified in *Saccharomyces cerevisiae* when the yeast was being screened for resistance to the drug rapamycin (Heitman et al. 1991). mTOR is a serine/threonine protein kinase that has been shown to be involved in cellular process including cell growth, cell proliferation, cell motility, cell survival, protein synthesis, transcription and autophagy (Huang & Fingar 2014). mTOR interacts with other proteins and forms two different kinase complexes in the cell called mTOR complex 1 (mTORC1) and mTOR complex 2 (mTORC2) that have distinct functions. However, it's only mTORC1 that is affected by rapamycin treatment; at least with short term, treatment (Wullschleger et al. 2006). mTORC1 consists of mTOR, mLST8 (or GβL), and the regulatory-associated protein of TOR (raptor); and mTORC2 consists of mTOR, mLST8, Rictor, Sin-1 and Protor-1/2 (Kim et al. 2002). Although rapamycin has been shown to strongly induce autophagy in yeast, in mammalian cells rapamycin has proven to be less effective at autophagy induction and appears to be cell line dependent. It has been suggested that this partial induction of autophagy is as a result of rapamycin only inhibiting phosphorylation of S6K1 and not other mTORC1 substrates. Moreover, treatment with Torin1 (a member of the pyridinonequinoline class of kinase inhibitors) as an ATP-competitive mTOR inhibitor potently induced autophagy in in both MEFs and HeLa cells (Thoreen & Sabatini 2009)(Thoreen et al. 2009).

When Akt is activated by growth factors, it is relocated to the plasma membrane and is phosphorylated by PDK1. Subsequently Akt phosphorylates tuberous sclerosis complex 2 (TSC2), which inactivates the TSC1/TSC2 complex. As TSC1/2 acts as a GAP towards Rheb, this in turn promotes formation of GTP-Rheb which results in direct activation of mTORC1 (Long et al. 2005)(Huang & Manning

2009). Additionally, one of mTORC1 components PRAS40, was shown to be a direct substrate to Akt and its phosphorylation upon insulin induction was observed to activate mTORC1(Vander Haar et al. 2007). It can be concluded that removal of growth factors and amino acid starvation can result in mTORC1 inactivation which leads to autophagy induction.

The presence of amino acids and nutrient availability has also been shown to be a positive regulator of the mTORC1 activity through the Rag small G proteins. Rags are a group of small G proteins that can form heterodimers and bind directly to mTORC1 to localise it to the lysosomes where GTP-Rheb is located. Expression of an active Rag mutant ($RagB^{GTP}$-D^{GDP}) in human embryonic kidney (HEK)-293T cells increased the binding of mTORC1 to these Rags and made the mTORC1 pathway insensitive to amino acid starvation. In the presence of amino acids, RagA and RagB are GTP-bound and recruit mTORC1 to lysosomal membranes (Sancak et al. 2008)(Sancak et al. 2010). More recently, Demetriades *et al.* demonstrated that Rag GTPases also bind TSC2 which is dependent on the amino acid levels of the cells. It was also shown that TSC2 is recruited to the lysosomes upon amino acid starvation which was observed to be necessary for inactivation of mTORC1 (Demetriades et al. 2014).

As mentioned before, mTORC1 interacts with ULK1 and can directly phosphorylate ATG13 and ULK1. Phosphorylation of ULK1 Ser757 by mTORC1 has been demonstrated to be of importance for ULK1 inhibition. By repressing the kinase activity of the ULK1 complex, mTORC1 acts as one of the fundamental inhibitors of the autophagy (Dorsey et al. 2009)(Kim et al. 2011)(Kang et al. 2013).

1.4.6 Rabs

Other than the main autophagy proteins, additional regulators such as the Rab small G proteins are also involved in autophagy. Rab GTPase proteins are part of the Ras-like GTPase superfamily which regulate vesicular trafficking (Chua et al. 2011). All Rab small G proteins (like other GTPases) are either GDP-bound, which is the inactive form, or GTP-bound which is the active form. It has been shown that Rab-GDP has a cytoplasmic location while Rab-GTP has a membrane location (Bento et al. 2013). Rabs switch between active GTP-bound and inactive GDP-bound states, and are regulated by guanine nucleotide exchange factors (GEFs) and GTPase activating proteins (GAPs) (Barr & Lambright 2010).

A number of Rab small G proteins have been found to be involved in the different stages of autophagy including Rab1, Rab5, Rab7, Rab8A and B, Rab9A, Rab11, Rab23, Rab24, Rab25, Rab32, and Rab33; however the exact function of these Rabs has not been fully characterised (Ao et al. 2014). Rab7 has been shown to be involved in autophagosome maturation and lysosomal fusion during autophagy (Gutierrez et al. 2004)(Mizushima & Komatsu 2011). Ypt7 (the yeast orthologue of Rab7) was first implicated in the fusion of autophagosomes with the vacuole in *Saccharomyces cerevisiae*, where yeasts lacking the Ypt7 displayed accumulation of autophagosomes (Kirisako et al. 1999). Rab24 has also been shown to localise to endoplasmic reticulum (ER) and was found to be involved in autophagosome maturation (Ao et al. 2014). The involvement of Rab24 in autophagy was confirmed when immunohistochemistry studies in neuronal PC12 cells revealed co-localisation of Rab24 with LC3 (Egami et al. 2005). Hirota & Tanaka have demonstrated that Rab32 localises to the ER in HeLa cells and COS cells and is necessary for autophagic vacuole formation. Furthermore, knockdown of Rab32 was shown to

impair basal autophagy which was demonstrated by accumulation of p62 and LC3II (Hirota & Tanaka 2009).

1.5 Aims and objective of this project

Although advances have been made recently in regards to BHD, it still remains a poorly understood disease. To better understand BHD, the main aims of this study were:

I) To examine the role of FLCN in the context of autophagy.

II) To characterise and better understand the role of FLCN interacting partners FNIP1 and FNIP2 and to further investigate FLCN's cellular function.

2 Chapter 2: Materials and methods

2.1 Reagents and chemicals

3-[(3-Cholamidopropyl)dimethylammonio]-1-Propanesulfonate (CHAPS), Thermo scientific, cat no: 28300

Agar, Sigma, cat no: A1296

Ampicilin sodium salt, Sigma, cat no: A0166-5G

Calcium chloride, 1mol/l, BDH/VWR, cat no: 190464K

Calcium chloride, dihydrate, Sigma, cat no: C3306

Chloroquine diphosphate, Sigma, cat no: C6628

Dimethyl Sulphoxide (DMSO), Sigma, cat no: D8418

Dithiothreitol (DTT), Sigma, cat no: 43816/646563

Dulbecco's Modified Eagle Medium (DMEM), Gibco, Invitrogen, cat no: 41966-029

Ethanol, Fisher Scientific, cat no: E/06500F/17

Foetal Bovine Serum (FBS), Gibco, Life Technologies, cat no: 10270-106

Glucose, Sigma, cat no: G7528

Glycerol, Sigma, cat no: G6279

Glycine, Sigma, cat no: G8898, G8790

HEPES, Sigma, cat no: H3375

Hydrochloric acid, Sigma, cat no: 320331

Kanamycin Sulfate, Roche, cat no: 90522923

Magnesium chloride, anhydrate, Sigma, cat no: M8266

Magnesium chloride, hexahydrate, Sigma, cat no: M2670

Mercaptoethanol, Sigma, cat no: M3148

Methanol, Fisher Scientific, cat no: M/3900/17

N,N,N,N-tetramethylethylene diamine (TEMED), Sigma, cat no: T9281

Penicillin-Streptomycin (5,000 U/mL), Gibco, Life Technologies, cat no: 15070-063

Penicillin G sodium salt, Sigma, cat no: P3032

Potassium chloride, Sigma, cat no: P9333

Powdered Milk, Marvel, cat no: 92964

Protogel 30%-acrylamide, National diagnostics, cat no: EC-890

Protogel-resolving buffer, National diagnostics, cat no: EC-892

Protogel-stacking buffer, National diagnostics, cat no: EC-893

Puromycin, Invitrogen, cat no: A11138-03

Recovery cell culture freezing medium, Gibco, Invitrogen, cat no: 12648-010

Sodium bicarbonate, Sigma, cat no: S5761

Sodium chloride, Sigma, cat no: S7653

Sodium Dodecyl Sulfate (SDS), Sigma, cat no: L6026 + L4390

Sodium fluoride, Sigma, cat no: S7920

Sodium hydroxide, Sigma, cat no: S8045

Sodium orthovanadate, Sigma, cat no: 450243

Streptomycin sulphate, Invitrogen, cat no: 15140-122

Tris, Sigma, cat no: 15,456,3

Triton X-100, Sigma, cat no: T8787

Trypsin-EDTA solution, Invitrogen, cat no: R-001-100

Tryptone, Bacto, Becton Dickinson, cat no: 211705

Tween 20, Sigma, cat no: P1379

Yeast extract, Bacto, Becton Dickinson, cat no: 212750

2.2 Buffers and solutions

BHD lysis buffer

20 mM Tris, 135 mM NaCl, 5 % (v/v) glycerol, 50 mM NaF and 0.1 % (v/v) Triton X-100, pH 7.5

Buffer B

40 mM HEPES, 120 mM NaCl, 1 mM EDTA, 10 mM pyrophosphate, 10 mM β-glycerophosphate, 50 mM NaF, 1.5 mM Na3VO4, 0.3% (w/v) CHAPS, pH 7.5

Krebs Ringer buffer (KRB)

20 mM HEPES, 115 mM NaCl, 5 mM KCl, 10 mM NaHCO3, 2.5 mM MgCl2, 2.5 mM CaCl2, pH 7.4

Luria Broth (LB)

15g Tryptone, 7.5g Yeast Extract, 15g NaCl, 1.5g Glucose, 1.5g Anhydrous MgCl

Combine with 1.5l of dH20 and adjust to pH 7.0 before autoclaving.

Luria Agar

10g Tryptone, 5g Yeast Extract, 10g NaCl, 1g Glucose, 1g Anhydrous MgCl

Add 1l of dH20 and adjust pH to 7.0 before adding 15 g Agar, 2ml of 1M NaOH Autoclave for 12 min before pouring.

Phosphate-Buffered Saline (PBS) (1X)

One tablet dissolved in 200 mL of deionized water (Sigma, cat no: P4417)

TBS

Add 2.42g Tris-base and 8g NaCl to 1l of dH20. Adjust pH to 7.6

TBS-T

Add 2.42g Tris-base and 8g NaCl to 1l of dH20. Adjust pH to 7.6 and add 1ml Tween-20 to give 0.1% (w/v)

Low Salt Wash Buffer

40mM HEPES, 2mM EDTA, 10mM β-Glycerophosphate, 150mM NaCl, 0.3% (w/v) CHAPs, pH 7.4

High Salt Wash Buffer

40mM HEPES, 2mM EDTA, 10mM β-Glycerophosphate, 400nM NaCl, pH7.4

Western Transfer Buffer x 10

144.07g Glycine, 30.285g Tris-Base, 2g SDS

Make up to 1l with dH20

Running Buffer x 10

144.07g Glycine, 30.285g Tris-Base, 10g SDS

Make up to 1l with dH20

Running buffer

3-8% gels: NuPAGE® Tris-Acetate SDS Running Buffer (Life technologies, cat no: LA0041)

4-12% gels: NuPAGE® MES SDS Running Buffer (Life technologies, cat no: NP0002)

2.3 Antibodies

β-actin, Polyclonal, Rabbit, Cell Signalling, cat no: 4967

Flag, Monoclonal, Mouse, Sigma, cat no: A8592

FLCN, Polyclonal, Rabbit, A kind gift from Prof. Arnim Pause (McGill University, Canada)

FNIP1, Monoclonal, Rabbit, abcam, cat no: ab134969

GABARAP, Polyclonal, Rabbit, ABGENT, cat no: AP1821a

Goat HRP conjugated, Sigma, cat no: A9452

GST, Monoclonal, mouse, Merck Millipore, cat no: 05-782

Guinea pig HRP conjugated, Sigma, cat no: A5545

HA, Monoclonal, Rat, Roche, cat no: 11 867 431 001

HIF1α, Monoclonal, Mouse, BD Biosciences, cat no: 610959

LC3, Polyclonal, Rabbit, NovusBiologicals, cat no: NB100-2220

Mouse HRP conjugated, Sigma, cat no: RABHRP1

Myc, 9E10, Monoclonal, Mouse, Sigma, cat no: M5546

NUP155, Polyclonal, Rabbit, abcam, cat no: ab157104

p62, Polyclonal, Guinea pig, Progen Biotechnik, cat no: GP62-C

Rab35, Polyclonal, Rabbit, Proteintech, cat no: 11329-2-AP

Rabbit HRP conjugated, Sigma, cat no: RABHRP2

Rat HRP conjugated, Sigma, cat no: A5795

SUZ12, Monoclonal, Rabbit, Cell Signalling, cat no: 3737

ULK1, Polyclonal, Rabbit, Cell Signalling, cat no: 4773

V5, Monoclonal, Mouse, Invitrogen, cat no: R960-25, R961-25

2.4 Plasmids

Flag-NUP155, was a kind gift from Dr Qing Kenneth Wang, Ph.D., M.B.A. Director of Centre for Cardiovascular Genetics Cleveland Clinic Professor of Molecular Medicine Professor of Genetics, Case Western Reserve University.

GST-FLCN, was generated in pDEST27, using the Gateway system (Life Technologies).

HA-FLCN, was generated in the pN3HA backbone (a kind gift from Dr. Sylvia Neumann, The Scripps Research Institute, San Diego, USA). This plasmid was used to generate all the mutant constructs of FLCN in this study, using site-directed mutagenesis (Agilent technologies).

HA-FNIP1, was a kind gift from Dr. Laura Schmidt (National Institutes of Health, Bethesda, USA).

HA-GABARAP, from pDONR35 was cloned into pcDNA-HA, using the Gateway system (Life Technologies).

HA-LC3B, was cloned into pDEST15, using the Gateway system (Life Technologies)

HA-p62, from Addgene, Plasmid #28027.

Myc-FNIP2, was a kind gift from Dr. O. Hino (Juntendo University School of Medicine, Tokyo, Japan).

ptfLC3, from Addgene Plasmid #21074.

Untagged-FLCN, was generated in the pcDNA3.1 vector, using the Gateway system (Life Technologies).

V5-FNIP1, was generated in pcDNA3.1/nV5-DEST, using the Gateway system (Life Technologies).

V5-ULK1, wild type was subcloned from IMAGE clone 3526749 (Source Bioscience LifeSciences), into pcDNA3.1 using the Gateway system (Life Technologies). The kinase dead ULK1 mutant, K46I, was made using site-directed mutagenesis (Agilent Technologies, 200521).

2.5 Methodology

2.5.1 Cell culture

All cell lines were cultured in DMEM supplemented with 10 % (v/v) foetal calf serum, 100 U/ml penicillin and 100 µg/ml streptomycin, unless otherwise stated.

Once confluent, cells were passaged as follows, cell lines were washed twice in trypsin, this was removed via aspiration before a 5 min incubation at 37 ºC. Cells were then resuspended in DMEM and transferred to a new flask.

For long term storage, cells were frozen down in recovery cell culture freezing medium (Gibco, Invitrogen) using cryogenic freezing container and stored in cryogenic vials in liquid nitrogen.

For complete starvation, cells were washed twice in phosphate buffered saline (PBS) and incubated in Krebs Ringer buffer (KRB) for 4 h.

To harvest the cells, plates were washed once in PBS before being resuspended in lysis buffer supplemented with protease inhibitors (1mM Na3VO4, 2µM antipain, 10µM leupeptin, 1µg/ml pepstatin, 0.1mM PMSF, 1mM DTT and 1mM benzamidine) Cells were incubated on ice for 20 min to aid lysis then centrifuged for 8 min at 4 ºC, 13.000rpm.

2.5.2 Transfection

Cells were transfected using Lipofectamine® 2000 Reagent (Life Technologies) according to the manufacturer's protocol. Cells were 70-90 % confluent at the time of transfection. Cells were harvested 24–36 h post-transfection in BHD lysis buffer (unless otherwise stated) and cell lysate was centrifuged and protein quantified using Bradford reagent (Sigma-Aldrich). The experiments were either performed immediately or cell lysates were stored at –80 ºC for further analysis.

For large scale transfections, $CaCl_2$ transfection was used. DNA complexes were prepared by combining the DNA with ddH_2O, $CaCl_2$ was then added and the solution was vortexed. BES solution was then slowly added dropwise whilst aerating the sample with a drawn glass pasteur pipette. Mixtures were left to stand at room temperature for 15-20 min (until precipitate becomes visible) then added dropwise to the cells. Media was changed on day two and cells were harvested on day three.

2.5.3 Bradford protein assay

A standard curve was set using BSA dissolved in dH20. To analyse total protein, 12.5µl of sample was diluted into 750µl of Bradford reagent and absorbance measured at 595nm using the Jenway Genova Spectrophotometer.

2.5.4 In vivo radiolabelling

Transfected HEK293 cells were incubated in phosphate-free medium containing 0.2 mCi [32P]-orthophosphate (PerkinElmer) for 4 h. These cells were harvested using BHD lysis buffer. HA-FLCN was immunoprecipitated with anti-HA antibody bound to protein G-Dynabeads (Life Technologies) and washed in lysis buffer.

2.5.5 Immunoprecipitation (IP)

Cell lysates were diluted in 500 µL BHD lysis buffer (plus protease inhibitors) and rotated with 1 µL of the appropriate antibody at 4 °C for 2h. 20 µL of a 50:50 slurry of protein-G Sepharose beads(GE Healthcare Life Sciences) were then added and samples were rotated for another hour at 4 °C. Beads were then washed three times in BHD lysis buffer (plus protease inhibitors) before elution in 40 µL of 1x sample buffer (from 4xNuPAGE LDS sample buffer, Life Technologies).

2.5.6 GST purification

Samples for GST-pulldown were lysed in Buffer B plus protease inhibitors (without the addition of DTT) and incubated with glutathione-Sepharose beads (GE Healthcare Life Sciences). Beads were washed three times in lysis buffer, and GST-tagged proteins were eluted using 10 mM glutathione.

2.5.7 Western blot analysis

The Invitrogen NuPage Novex gel system was used for electrophoresis. 3-8 % Tris-acetate gels or 4-12 % Bis-Tris gels were used depending on the molecular size of the protein of interest. Samples were prepared in 4x sample buffer and incubated at 70 ºC for 10 min prior to loading. Gels were run at 150 V for 1 h and proteins were transferred to a polyvinylidene fluoride membrane (PVDF) at 25 V for 2

h in transfer buffer using the wet transfer system. After transfer, the membrane was blocked in 5% (w/v) dry milk powder in TBS-T for a minimum of 2 h. The membrane was then incubated overnight in primary antibody in 2% BSA/TBS-T. The following day membranes were washed three times in TBS-T and then incubated in 1:10000 dilution of the appropriate HRP-conjugated secondary antibody for a minimum of 30 min. Following three further TBS-T washes, membranes were incubated in Enhanced Chemiluminesence (ECL) solution (Amersham) for 1 min. Autoradiography films were then used to visualise the signal.

2.5.8 Site-Directed Mutagenesis

The QuikChange II XL Site-Directed Mutagenesis Kit, 10 Rxn (Agilent Technologies) was used to make the mutation constructs. PCR reactions were performed according to the manufacturer's protocol and cycling conditions.

Following PCR, 1 µL of the Dpn I restriction enzyme (10 U/µL) was added directly to each PCR reaction. Reactions were incubated at 37 °C for 1 h to digest the parental DNA.

XL1-Blue supercompetent cells were thawed on ice. For each reaction to be transformed, 50 µL of the supercompetent cells was added to a prechilled 14-ml BD Falcon polypropylene round-bottom tube. 1 µL of the Dpn I-treated DNA from each reaction was transferred to separate aliquots of the supercompetent cells. The transformation reactions were incubated on ice for 30 min, heat shocked for 45 s at 42 °C and then placed on ice for a further 2 min. 0.5 mL of NZY broth or SOC medium, preheated to 42 °C, was added per tube and the transformation reactions were incubated at 37 °C for 1 h with shaking at 225–250 rpm. The appropriate volume of each transformation reaction was spread on agar plates containing the

appropriate antibiotic for the plasmid vector. The transformation plates were incubated at 37 °C for >16 h. Resulting colonies were purified and sequenced to check for the presence of desired mutation.

2.5.9 Plasmid purification (Miniprep/ Maxiprep)

Three colonies from each plate of site-directed mutagenesis was picked and grown over night in 5 mL LB broth containing the appropriate antibiotic (in order to have at least one correct and in frame desired mutated sequence). Bacterial cells were pelleted and the plasmid DNA was extracted using QIAprep® Miniprep kit (QIAGEN) according to the manufacturer's protocol.

Once the sequence was verified, for large scale plasmid purification, each colony was grown in a starter culture of 5 mL LB medium containing the appropriate selective antibiotic. It was incubated for 4-5 h at 37°C with vigorous shaking (250 rpm). The starter culture was then diluted in 500mL of LB medium containing the appropriate selective antibiotic and incubated overnight (12-16h) at 37°C with vigorous shaking (250 rpm). The bacterial cells were harvested by centrifugation at 6000 x g for 15 min at 4°C. The plasmid DNA was extracted using QIAprep® Maxiprep kit (QIAGEN) according to the manufacturer's protocol.

2.5.10 Sequencing

The purified plasmids were sent to Eurofins MWG Operon for sequencing.

2.5.11 Cyquant cell proliferation assay

Cells were seeded at 4000 per well of a 96 well plate. Cells were treated with appropriate drug for 24 h or 48 h, the media was then removed and the plate was frozen at –80 ºC. Cell proliferation rate was determined using the CyQuant® Cell Proliferation Assay Kit (Life Technologies) following the manufacturer's protocol.

Essentially, lysis buffer containing CyQUANT GR dye was added to each well and gently pipette to allow lysis of the cells and incorporation of the dye to the DNA. Fluorescence was detected by excitation at ~485 nm and emission detection at ~530 nm using a plate reader. Cell number was calculated using a standard curve generated from 250 to 50000 cells.

2.5.12 RNA extraction

For the extraction of mRNA, cells were harvested in RNA protect Cell Reagent and centrifuged at 5,000 rpm for 5 min to produce a pellet, the supernatant was discarded and the pellet was saved for mRNA extraction. mRNA was extracted using the Qiagen mRNA extraction kit in accordance with manufacturer's protocol, QIA shredders (QIAGEN) were utilised to homogenise the pellet. Resulting mRNA concentration was determined using the nanodrop spectrophotometer.

2.5.13 Reverse transcription

To prepare the complementary DNA (cDNA), first the genomic DNA (gDNA) is eliminated using gDNA Wipeout Buffer, 7x (QIAGEN) and total RNA from each sample (up to 1 µg) in a 14 µl volume reaction which is incubated at 42°C for 2min. The reverse transcription reaction is prepared as follows:

Quantiscript Reverse Transcriptase	1 µl
Quantiscript RT Buffer, 5x	4 µl
RT Primer Mix	1 µl
gDNA eliminated reaction	14 µl

This reaction was incubated in a thermal cycler (Applied Biosystems) with the following cycle:

42 °C for 30min

95 °C for 3min

The product was stored on ice for real-time PCR.

2.5.14 Quantitative-PCR

Quantitative real-time PCR reactions were conducted in 96-well plates using appropriate primer assays and Sybr Green PCR Master mix (QIAGEN). Amplification was performed as follows:

1. Initial denaturation step (95 °C, 15 min)

2. 40 cycles of denaturation (94 °C, 15 s)

3. Annealing step (55 °C, 30 s)

4. Extension step (72 °C, 40 s).

The amplification products were quantified during the extension step in the fortieth cycle. The results were then determined using the ddCT (delta-delta-Ct) method, and standardised to β-actin. A dissociation step was performed, which verified that only one PCR product was produced with each primer set to show the specificity of each primer.

2.5.15 Modelling of FLCN structure

Crystal structure coordinates used in this study are as deposited in the protein data bank (PDB Id: 3V42). The model was generated using PyMOL v.1.3.

2.5.16 Densitometry

The density of the visualised bands in western blotting was measured and analysed using the Image J. program version 1.46.

2.5.17 Statistical analysis

One way ANOVA followed by LSD post-hoc testing (as appropriate) was used for statistical analysis, with $p < 0.05$ taken to be significant.

3 Chapter 3: Involvement of FLCN in autophagy

3.1 Introduction

Autophagy is an evolutionarily conserved process where intracellular lipid and protein components are broken down to replenish cellular energy and amino acid supplies. Autophagy also removes protein aggregates, redundant macromolecules and dysfunctional organelles that, if not efficiently recycled, contribute to cell stress and consequently disease. Autophagy can play both pro- and anti-oncogenic roles in cancer development (Choi et al. 2013). Autophagy involves sequestering cytoplasmic material in double-membrane vesicles known as autophagosomes, which subsequently fuse with lysosomes to form autolysosomes. Once fusion occurs, lysosomal hydrolases degrade sequestered material allowing permeases to transport amino acids and lipids into the cytoplasm for use in either biosynthesis or the generation of energy (He & Klionsky 2009).

Yeast screens uncovered over 30 autophagy-related (*ATG*) genes, many of which are recruited to the phagophore assembly site, a pre-autophagosomal membrane structure (Klionsky et al. 2011). Atg8 is conjugated to phosphatidylethanolamine (PE) and selectively incorporated into autophagosomes, making it a commonly used autophagy marker. Mammals have two ATG8 subfamilies, the microtubule-associated protein 1 light chain 3 (MAP1LC3, commonly called LC3) subgroup and the γ-aminobutyric acid receptor-associated protein (GABARAP)/Golgi-associated ATPase enhancer of 16 kDa (GATE-16) subfamily (Shpilka et al. 2011). Both mammalian ATG8 subfamilies are modified by PE conjugation, localise to autophagosomes and are essential for autophagy (Kabeya et

al. 2004). Current evidence indicates that LC3 and GABARAP act at different stages of autophagosome formation (Weidberg et al. 2010).

ULK1 (the mammalian equivalent of Atg1) acts at the most upstream step of autophagy (Itakura & Mizushima 2010). ULK1 is a serine/threonine protein kinase that forms a complex with ATG13, FIP200 and ATG101, which drives formation of autophagosome (Hosokawa et al. 2009)(Mercer et al. 2009). This kinase complex is positively regulated by many internal ULK1-mediated phosphorylation events, including ULK1 autophosphorylation (Jung et al. 2009)(Ganley et al. 2009). Additionally, when there is enough energy and nutrient for the cell, mTORC1 promotes cell growth in part by inhibiting autophagy via phosphorylation of ULK1 (Hosokawa et al. 2009)(Jung et al. 2009). Conversely, during energy and nutrient deprivation when it is not viable for the cells to grow, AMPK interacts with and phosphorylates ULK1 to enhance autophagy (Kim et al. 2011).

As mentioned in Chapter 1, mutations in *FLCN* are responsible for Birt-Hogg-Dubé (BHD) syndrome which is characterised by benign hair follicle tumours, pneumothorax, pulmonary cysts and renal cancer (Nickerson et al. 2002).

FLCN was recently shown to be a Rab GEF towards Rab35 (Nookala et al. 2012). FLCN is a known downstream substrate of AMPK, where AMPK phosphorylates FLCN and FLCN interacting protein FNIP1 (Baba et al. 2006). FNIP1 has recently been identified as an interactor of GABARAP (Behrends et al. 2010). BHD is also a ciliopathy and FLCN is localised at primary cilia (Luijten et al. 2013). Interestingly, a compromised ability to activate autophagy has been hypothesised to underlie some ciliopathies (Pampliega et al. 2013). Furthermore, FLCN was recently shown to localise to lysosomes and modulate nutrient sensing through the Rag small G proteins (Petit et al. 2013)(Tsun et al. 2013)(Martina et al. 2014). Given these

different possible links to autophagy, it was speculated that FLCN might play a fundamental role in autophagy. Hence the main aim of this result chapter was to determine whether FLCN might be involved in the regulation of autophagy.

3.2 Methods

Cell Culture - It has been reported that kidney tumour in *Flcn* $^{+/-}$ mice initiated from renal proximal tubule cells (Hudon et al. 2010). Therefore, human renal proximal tubule (HK2) cells were utilised with stable FLCN knockdown as a model of BHD to explore renal pathology in this study. Stable FLCN knockdown in human kidney cells (HK2) was made by Dr. Tijs Claessens (Dr Andrew Tee's laboratory, Cardiff University, UK). *Flcn*$^{+/+}$ and -/- MEF cells were gifted by Prof. Arnim Pause (McGill University, Canada). All cell lines were cultured in DMEM supplemented with 10 % (v/v) foetal calf serum, 100 U/ml penicillin and 100 µg/ml streptomycin (Life Technologies). Lipofectamine® 2000 Reagent (Life Technologies) was used for transfection according to the manufacturer's protocol. Cells were 70-90 % confluent at the time of transfection. Cells were harvested 24–36 h post-transfection. Experiments were performed under normal growth conditions, unless otherwise stated. For complete starvation, cells were washed twice in phosphate buffered saline (PBS) and incubated in Krebs Ringer buffer (KRB) (20 mM HEPES (pH 7.4), 115 mM NaCl, 5 mM KCl, 10 mM $NaHCO_3$, 2.5 mM $MgCl_2$, 2.5 mM $CaCl_2$) for 4 h.

Immunoprecipitation, GST-pulldown and western blotting - Cells were lysed in BHD lysis buffer (20 mM Tris, 135 mM NaCl, 5 % (v/v) glycerol, 50 mM NaF and 0.1 % (v/v) Triton X-100, pH 7.5 plus protease inhibitors), centrifuged and protein quantified using Bradford reagent (Sigma-Aldrich). Anti-HA and anti-V5 coupled to Protein G-Sepharose beads (GE Healthcare Life Sciences) were used to immunoprecipitate HA and V5-tagged proteins as appropriate. Immunoprecipitates were washed three times in lysis buffer and resuspended in NuPAGE LDS sample buffer (Life Technologies). Samples for GST-pulldown were lysed in Buffer B (40 mM

HEPES (pH 7.5), 120 mM NaCl, 1 mM EDTA, 10 mM pyrophosphate, 10 mM β-glycerophosphate, 50 mM NaF, 1.5 mM Na_3VO_4, 0.3% (w/v) CHAPS plus protease inhibitors and incubated with glutathione-Sepharose beads (GE Healthcare Life Sciences). Beads were washed three times in lysis buffer, and GST-tagged proteins were eluted using 10 mM glutathione. Western blotting was performed as previously described. Blots shown are representative of at least three independent experiments.

In vivo phosphate radiolabelling - Transfected HEK293 cells were incubated in phosphate-free medium containing 0.2 mCi [32P]-orthophosphate (PerkinElmer) for 4 h. These cells were harvested using BHD lysis buffer. HA-FLCN was immunoprecipitated with anti-HA antibody bound to protein G-Dynabeads (Life Technologies) and washed in lysis buffer x3, prior to being suspended in x1 sample buffer and SDS-PAGE.

Structural modelling - Crystal structure coordinates used in the current manuscript are as deposited in the protein data bank (PDB Id: 3V42). The model was generated using Pymol.

Densitometry and statistical analysis - Densitometry was performed using ImageJ. v1.43 software. One way ANOVA followed by LSD post-hoc testing (as appropriate) was used for statistical analysis, with $p < 0.05$ taken to be significant.

Protein alignment - Clustal Omega provided by The European Bioinformatics Institute (EMBL-EBI) was used for all multiple alignments.

3.3 Results

3.3.1 FLCN could possibly be involved in autophagy

p62 (also known as Sequestome1, SQSTM1) is a well-known marker of autophagy. As discussed in chapter 1, p62 is integrated to autophagosomes and gets degraded during autophagy (Pankiv et al. 2007). Of interest, p62 was shown to be over-expressed in renal cell carcinoma (Creighton et al. 2013). Over-expression of p62 could also be present in BHD patient RCC, since BHD syndrome predisposes patients to renal cell carcinoma. It was, therefore, important to analyse whether FLCN loss could enhance p62 protein levels. As expected, immunohistochemistry done by our collaborators in Maastricht revealed elevated p62 protein levels in a BHD patient renal tumour (with a c.499C>T mutation encoding a truncated FLCN mutant, pGln167X) when compared to unaffected tissue (Figure 3.1.A).

Also when autophagy was induced in normal HK2 cells via starvation after 4 h, FLCN mRNA level showed a significant increase (Figure 3.1.B). Similar up-regulation of FLCN mRNA has been reported in starved *Drosophila* larvae (Erdi et al. 2012), raising the possibility that FLCN might be involved in autophagy.

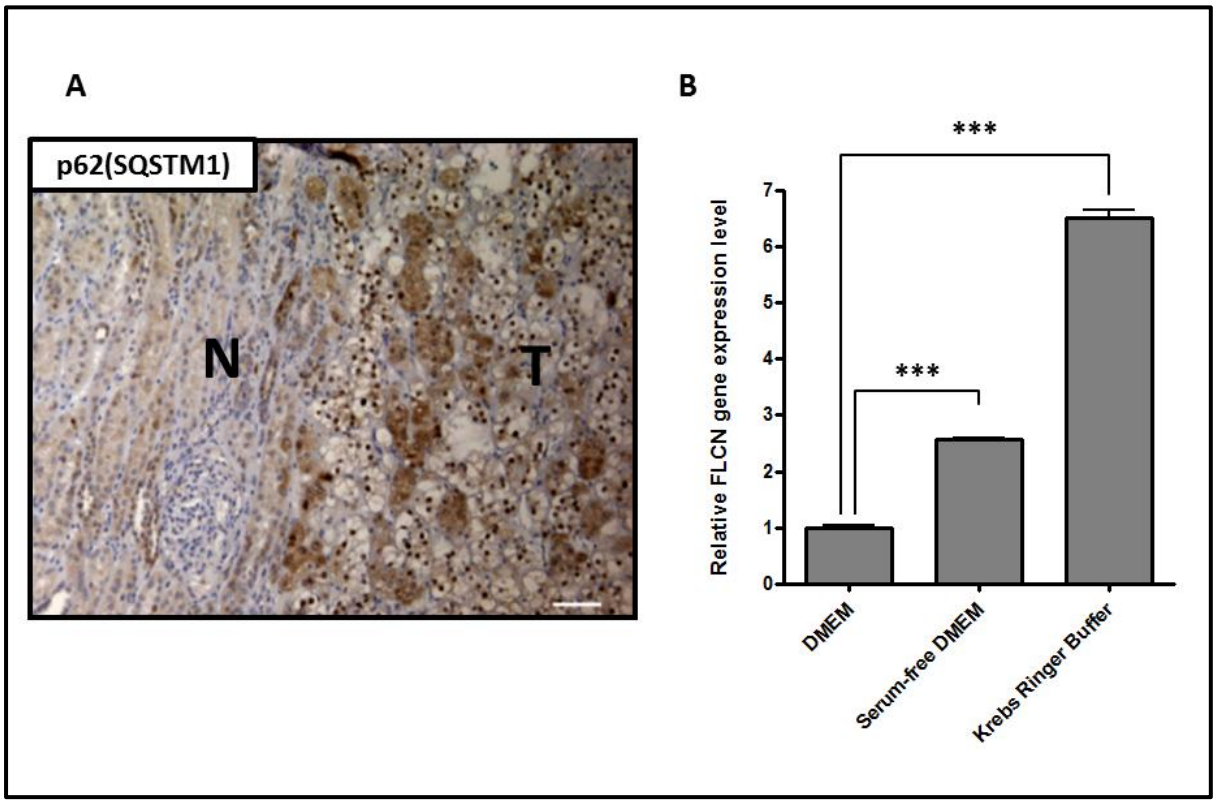

Figure 3.1 FLCN is likely involved in autophagy: (**A**) Immunohistochemistry of p62 (SQSTM1) indicates that p62 (SQSTM1) expression is higher in the renal tumour (T) from a BHD patient when compared to surrounding unaffected normal (N) renal tissue (IHC carried out by our collaborators (M.VanSteensel, Maastricht University)). (**B**) Relative levels of FLCN mRNA was determined from HK2 cells after 4 h of growth in DMEM with and without serum, as well as Krebs Ringer Buffer (lacking amino acids and glucose). Levels were standardised to β-actin. N=3, *** $P < 0.001$.

3.3.2 Autophagy is down-regulated in FLCN-deficient cells

For reasons mentioned in the methods section HK2 cells were used in this study. p62 protein levels were shown to be elevated in FLCN-deficient HK2 cells when compared to control HK2 cells, which was significant in normal growth conditions. However under starvation condition where the cells were incubated in Krebs Ringer buffer for 4 h, although p62 protein level was still higher in FLCN-deficient HK2 cells this elevation was not significant (Figure 3.2 A). This result could imply that FLCN may play a role in basal autophagy; however it could be expendable for more severe conditions such as starvation-induced autophagy. A similar pattern was also observed in *Flcn*$^{-/-}$ mouse embryonic fibroblasts (MEFs) (Figure 3.2 B).

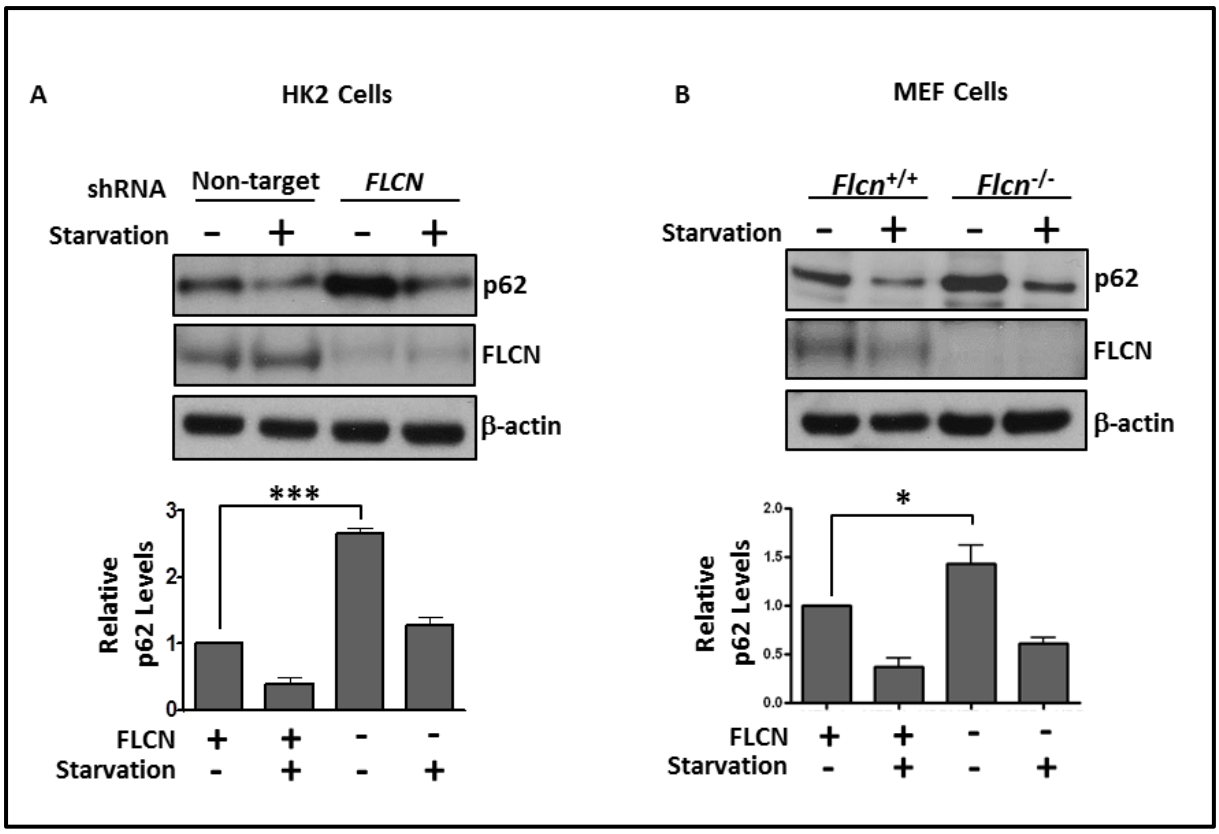

Figure 3.2 Autophagy is down-regulated in FLCN-deficient cells: In both (**A**) HK2 cells and (**B**) MEF cells with and without loss of FLCN, p62 (SQSTM1) protein expression levels were determined in the presence or absence or starvation media (Krebs Ringer Buffer, lacking both amino acids and glucose). FLCN expression was determined to validate FLCN deficiency, and β-actin serves as a loading control. The relative levels of p62 (SQSTM1) was determined by densitometry and is graphed, N=3, * $P < 0.05$, *** $P < 0.001$.

3.3.3 FLCN interacts with ULK1

Since AMPK and mTOR have both been shown to regulate autophagy through direct phosphorylation of ULK1 and, have also been linked to FLCN (Kim et al. 2011)(Baba et al. 2006), several experiments were designed to explore the relationship that FLCN might have in the regulation of autophagy and whether AMPK and/or mTOR was involved. Initially, interaction of ULK1 with FLCN was assessed. It was observed that immunoprecipitated V5-tagged ULK1 co-purified with FLCN (Figure 3.3A). In the same experiment a kinase dead mutant of ULK1 was also immunoprecipitated and FLCN-ULK1 interaction was shown to be more robust in the presence of inactive ULK1. To further characterise this novel interaction of FLCN with ULK1 with respect to BHD, a panel of BHD patient derived mutations were used. The C-terminal truncating mutations (Y463X and H429X) interacted more avidly with ULK1 than either wild-type FLCN or a BHD patient-derived point mutation, K508R (Figure 3.3B). This could suggest that the C-terminus of FLCN does not bind directly to ULK1 and may play a role in dissociation from ULK1.

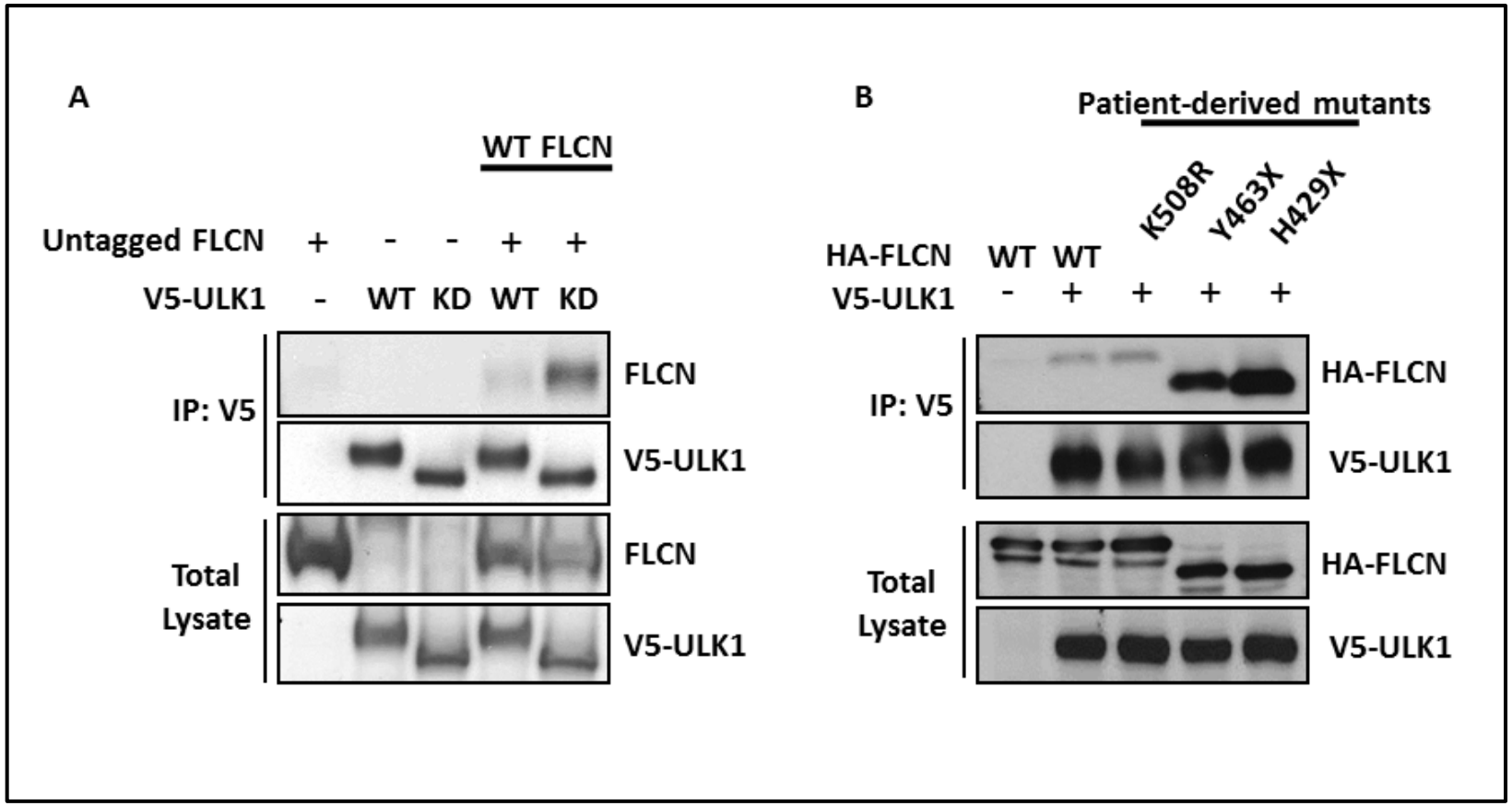

Figure 3.3 FLCN interacts with ULK1: (**A**) Untagged FLCN was co-expressed with or without either V5-tagged ULK1 wild-type or kinase dead (KD) in HEK293 cells. From generated cell lysates, V5 antibodies were used to immunoprecipitate V5-ULK1 and associated FLCN was determined by western blotting. Total lysates were analysed for total expression of both FLCN and V5-ULK1. (**B**) Similar to (**A**), but comparing interaction with HA-FLCN wildtype and 3 patient-derived mutations (K508R, Y463X and H429X).

3.3.4 FLCN is an ULK1 substrate

Given that the kinase-dead form of ULK1 bound more strongly to FLCN, it is possible that FLCN could be a downstream substrate of ULK1. To explore whether FLCN was an ULK1 substrate, ULK1 kinase assays were carried out. HEK293 cells expressing HA-FLCN were radiolabelled by [^{32}P] *in vivo* and the [^{32}P] incorporation into HA-FLCN was determined in the presence or the absence of ULK1. The result shows that FLCN is phosphorylated by ULK1 *in vivo* (Figure 3.4A). This result combined with the FLCN-ULK1 interaction data above suggest that ULK1 is likely to bind to and phosphorylate FLCN in a transient manner rather than having a stable association. (The radioactive experiments were carried out by Dr. Andrew Tee, Cardiff University, UK)

The cold samples were sent for mass spectrometry in Prof John Blenis Lab (Boston, Harvard Medical School), where three phosphorylation events were identified within the C-terminus of FLCN. These three sites (Ser406, Ser537 and Ser542), were unique to FLCN when co-expressed with wild-type ULK1 but not kinase dead ULK1 (Figure 3.4B and C).

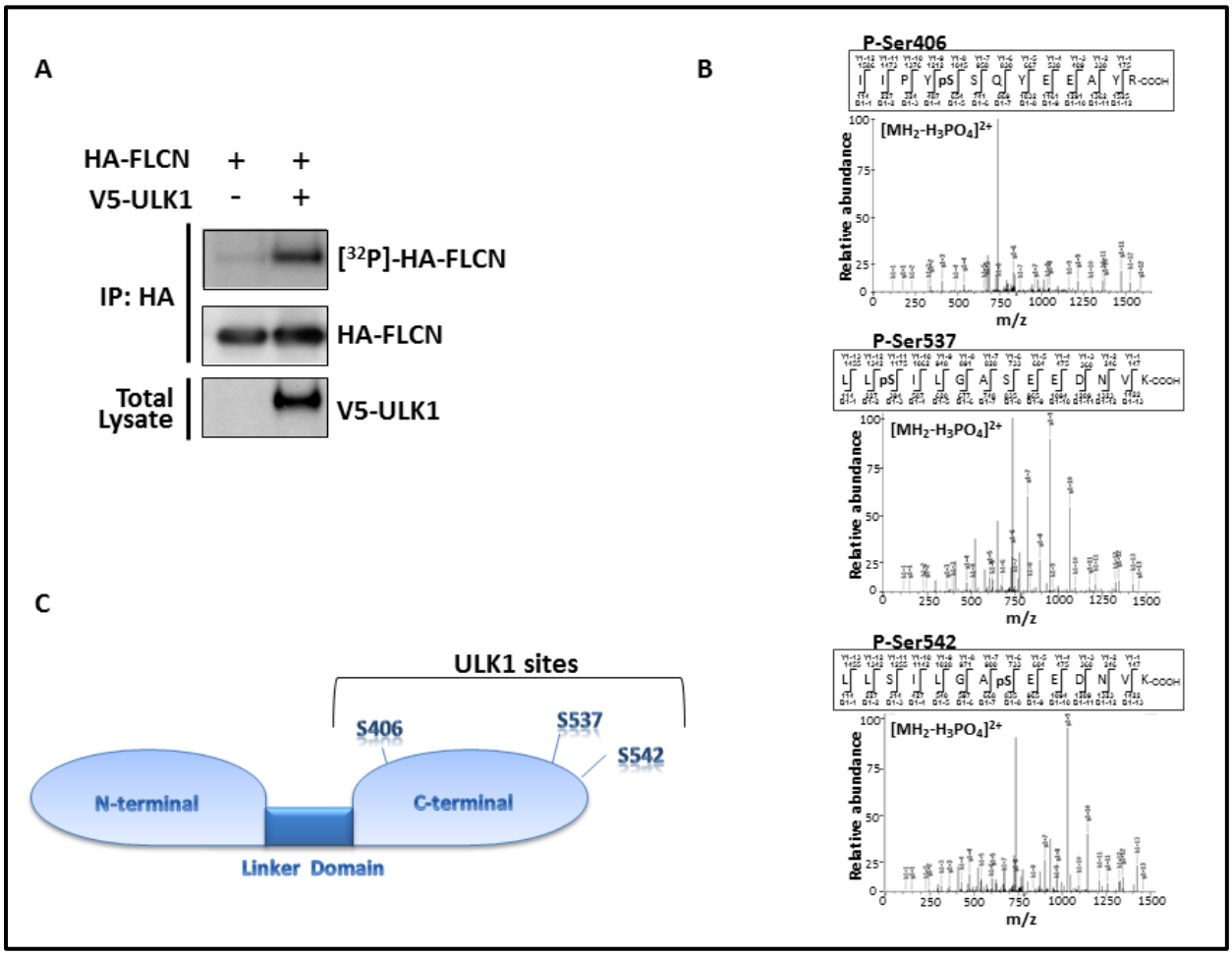

Figure 3.4 FLCN is an ULK1 substrate: (**A**) HA-FLCN was immunoprecipitated from radiolabeled [^{32}P]-orthophosphate labelled HEK293 cells with and without V5-ULK1. Levels of HA-FLCN and radiolabeled [^{32}P]-HA-FLCN are shown as well as expression levels of V5-ULK1. (**B**) Purified HA-FLCN from HEK293 cells expressing ULK1 or kinase dead ULK1, was analysed by MS-MS MALDI-TOF to identify protein phosphorylation events that were dependent on ULK1. Three unique ULK1-dependent phosphorylation sites are shown (S406, S537 and S542) and are also represented in a cartoon representative of FLCN (**C**).

3.3.5 ULK1 phosphorylates FLCN within a conserved C-terminus

A FLCN protein alignment between species was performed in clustal omega which showed that the identified phosphorylation sites on FLCN (Ser406, Ser537 and Ser542) are quite conserved in vertebrates, particularly in mammals (Figure 3.5).

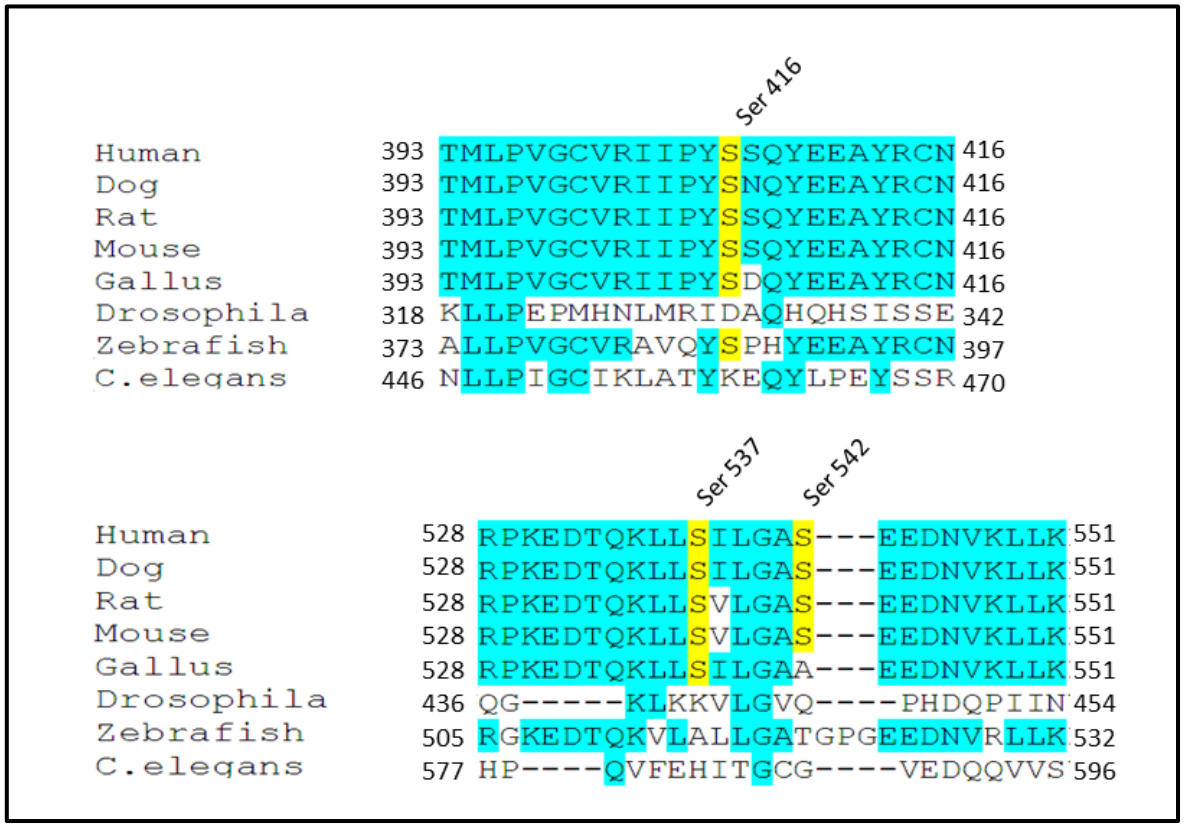

Figure 3.5 ULK1 phosphorylates FLCN at a conserved C-terminus: C-terminal amino acid alignments spanning the regions where the three ULK1 phosphoryation sites are shown.

3.3.6 ULK1 phosphorylation sites within the C-terminus are shown to be on the surface and are available for phosphorylation

A structural model of FLCN showing the three best conserved ULK1-mediated phosphorylation sites of FLCN was generated from the recently determined C-terminal structure of FLCN using PyMol (Figure 3.6), from the crystal structure [PDB Id: 3V42]. All three identified ULK1 phosphorylation sites are solvent exposed to the surrounding environment, making them accessible for phosphorylation.

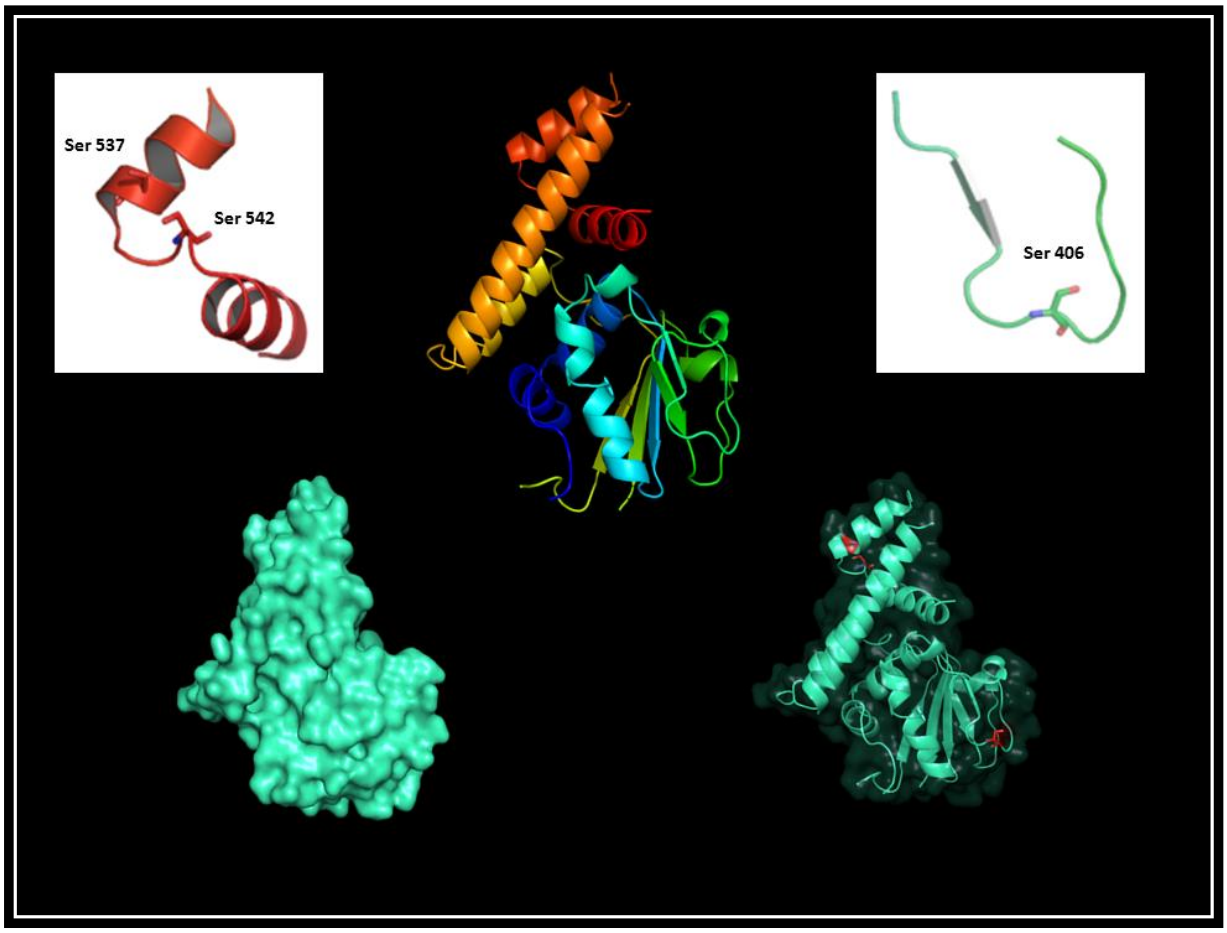

Figure 3.6 Model structure of FLCN: The top middle figure shows the alpha helices and beta sheets structure of FLCN. Bottom left demonstrates the surface structure of the FLCN and bottom right the three ULK1 phosphorylation sites, in red, are shown to be on the surface, which are magnified at the top.

3.3.7 WT-FLCN rescues basal autophagy in FLCN deficient cells but not the 3A mutant

To determine if it is actually the lack of FLCN that effects p62 protein level elevation, WT-FLCN was re-expressed in these FLCN-deficient HK2 cells together with HA- p62 to specifically measure autophagy in the transfected cells. As indicated by the marked reduction in p62, FLCN restored a higher level of autophagy in these cells (Figure 3.7).

To test if the phosphorylation of FLCN by ULK1 plays a role in this rescue effect upon re-expression, a triple serine to alanine mutation of the ULK1 phosphorylation sites on FLCN was made which from now on will be referred to as 3A-FLCN (Figure 3.8.A). Both WT-FLCN and 3A-FLCN were over expressed in FLCN deficient HK2 cells together with HA-p62. It was observed that WT-FLCN over expression in FLCN-deficient HK2 cells reduces the expression levels of p62 protein, hence restores autophagy. Of interest, overexpression of 3A-FLCN did not rescue autophagy but rather impaired autophagy even further (Figure 3.8.B). Therefore, FLCN phosphorylation by ULK1 likely plays a positive role in autophagy.

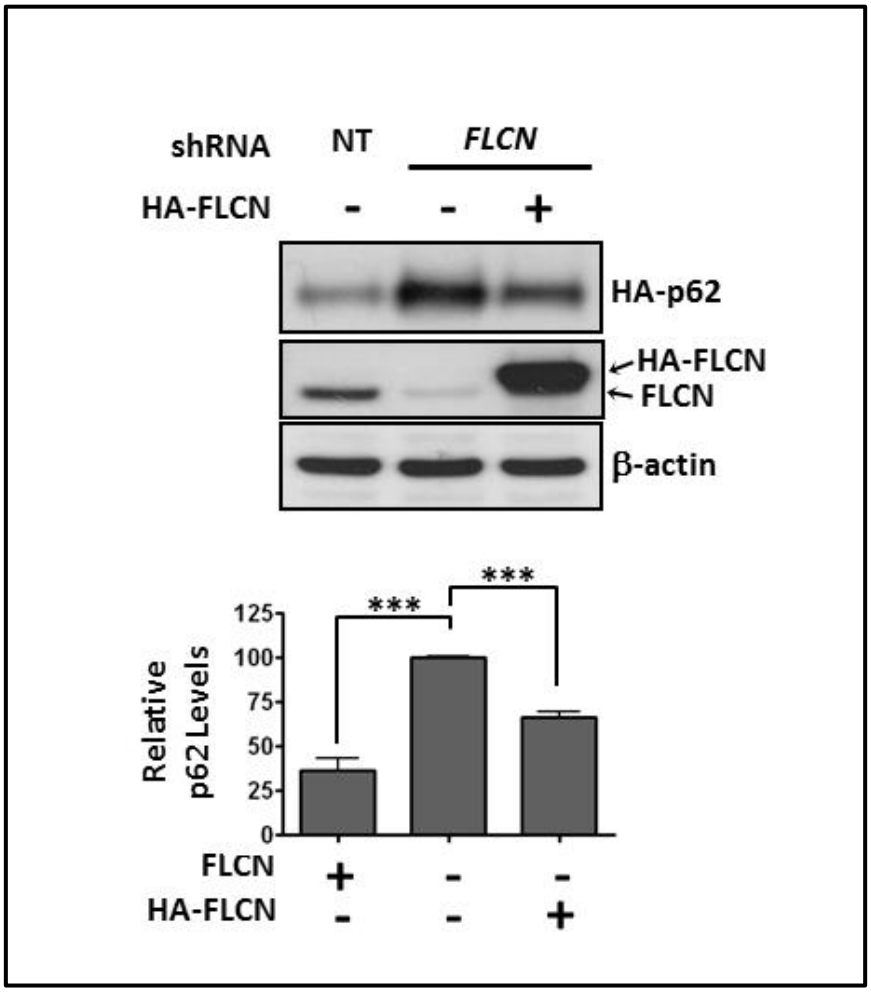

Figure 3.7 Wild-type FLCN rescues basal autophagy in FLCN-deficient cells: HK2 cells that were stably transfected with shRNA towards FLCN or non-target control (NT), autophagy was rescued with HA-tagged FLCN re-expression where indicated. Total levels of p62 (SQSTM1), FLCN and β-actin are shown. Denistometry analysis of p62 levels was carried out and is represented, N=3, *** $P < 0.001$.

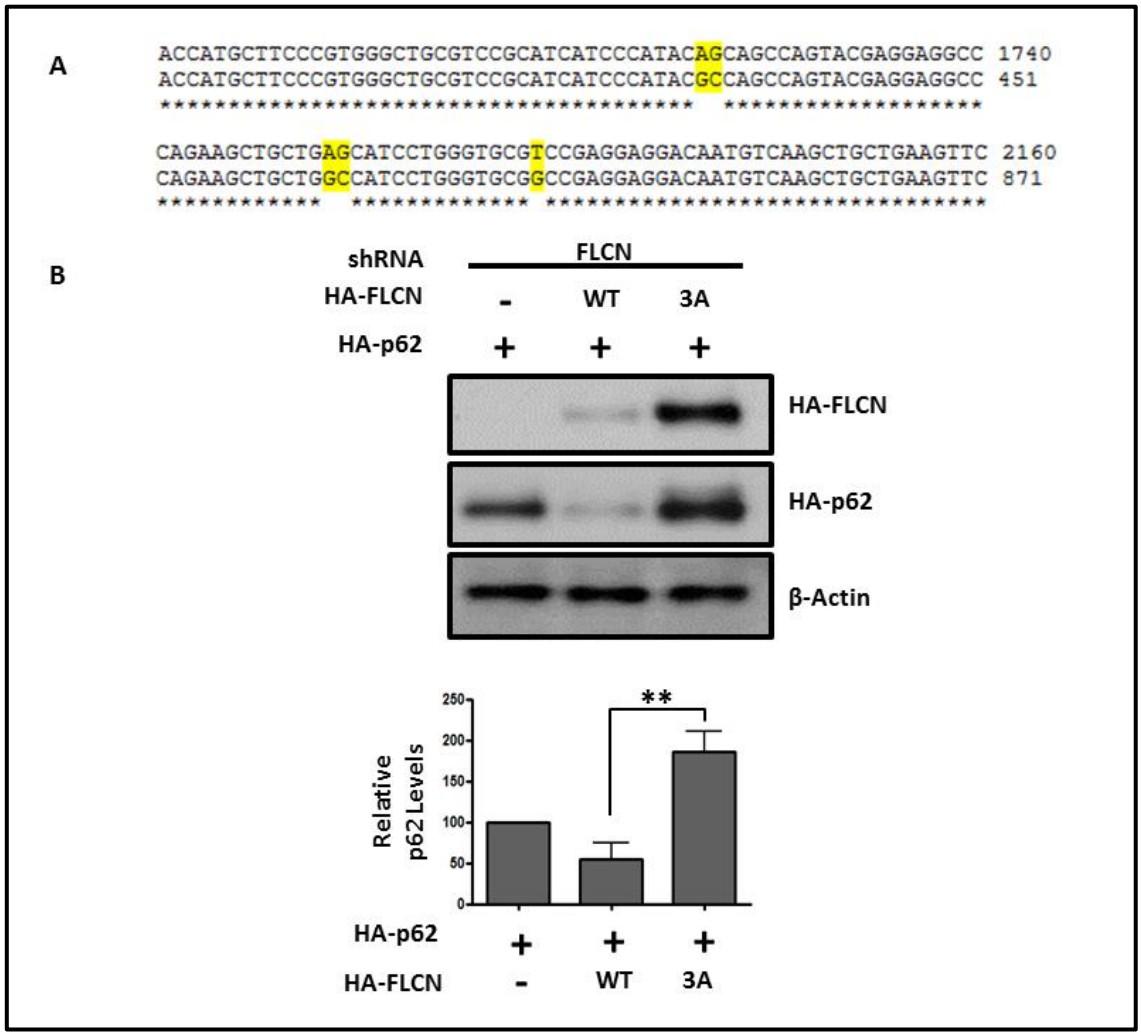

Figure 3.8 3A mutant of FLCN does not rescue basal autophagy in FLCN-deficient cells: (**A**) Nucleotide sequence alignment of the 3A-FLCN mutant (where all three ULK1 phosphorylation sites have been mutated to alanines). (**B**) Either wild-type FLCN or 3A-FLCN mutant were expressed in HK2 cells that were stably expressing FLCN shRNA, where indicated. Total levels of FLCN, p62 (SQSTM1) and β-actin are shown. Denistometry analysis of p62 level was carried out and is represented, N=3, ** $P < 0.01$.

3.3.8 GABARAP interacts with FLCN

The FLCN binding partner, FNIP1, was recently shown to interact with GABARAP (Behrends et al. 2010). GABARAP is mammalian orthologue of Atg8 with a potential role in regulating the sealing process needed for autophagosome maturation (Weidberg et al. 2010). Unbiased GABARAP interaction mass spectrometry was performed and eight high-confidence interacting proteins were identified, including both FNIP1 and FLCN (Figure 3.9A). To confirm this interaction FLCN and GABARAP were co-expressed in HEK293 cells in the presence or absence of FNIP1 or FNIP2. The same experiment was also set for LC3, which is another member of the ATG8 subfamily. It was observed that the immunoprecipitation of FLCN only co-precipitates GABARAP in the presence of FNIP2, but not LC3 (Figure 3.9B). However, the *in vitro* binding assay (done by Dr. Elaine Dunlop, Cardiff University, UK) could detect endogenous FLCN interaction with bacterially generated recombinant GABARAP and LC3 proteins, where there was a stronger interaction between GABARAP and FLCN. Taking into account both the *in vitro* and the *in vivo* results, it suggests the enhanced specificity of FLCN binding for GABARAP family members and that the over-expression of FNIP2 is necessary to strengthen this interaction. Overall, these data reveal that FLCN and its interacting partners FNIP1/2 affect the autophagy machinery through the interaction with GABARAP.

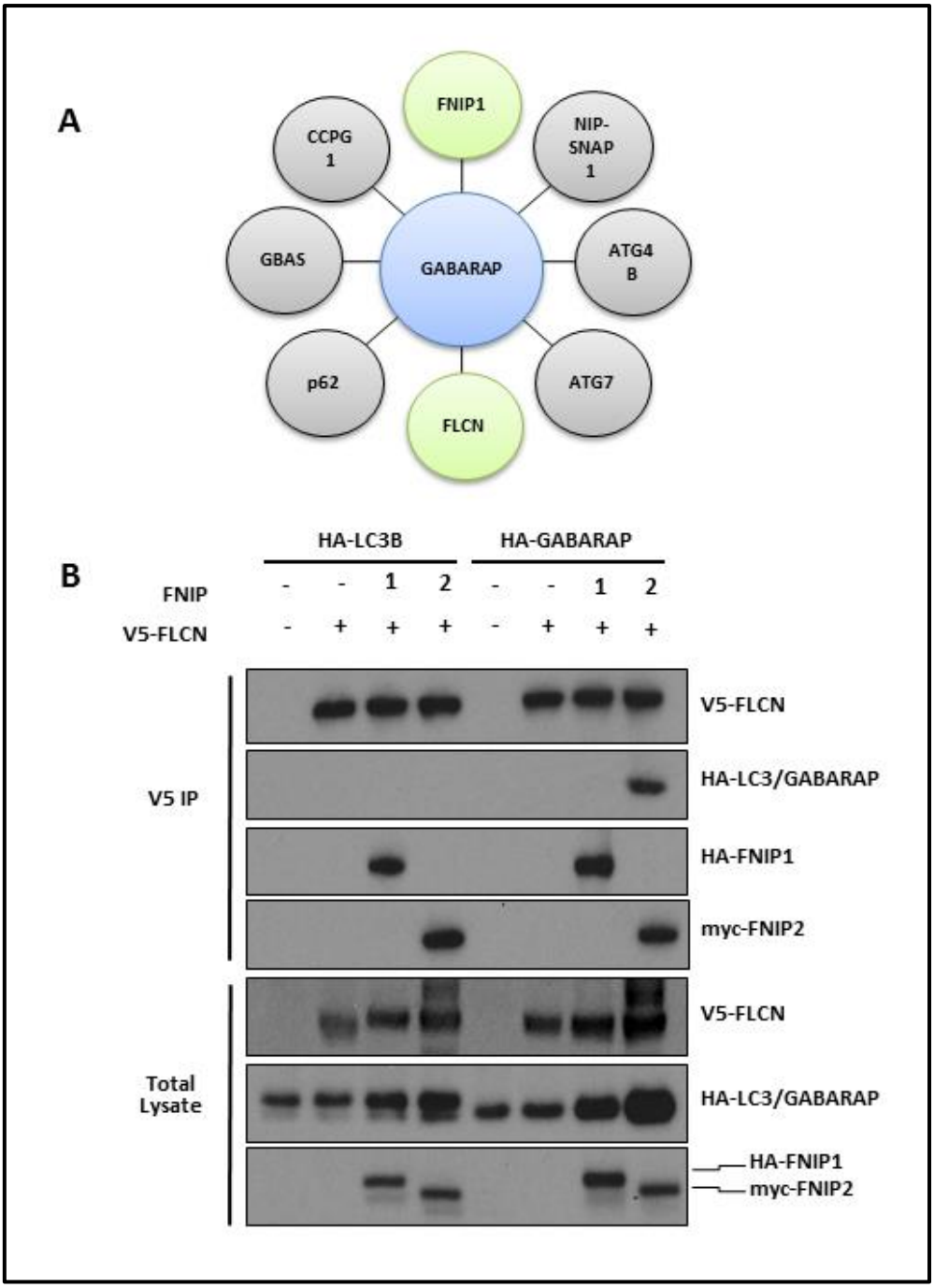

Figure 3.9 GABARAP interacts with FLCN, and this interaction is enhanced when co-expressed with FNIP2: (**A**) GABARAP interactome is presented (carried out through collaboration with Christian Behrends, Goethe University Frankfurt). (**B**) Either HA-tagged LC3B or GABARAP was expressed in HEK293 cells in the presence of V5-FLCN with or without co-expression of either HA-FNIP1 or myc-FNIP2, where indicated. Anti-V5 antibodies were used to immunoprecipitate V5-FLCN, and associated FNIP1, FNIP2 and GABARAP was determined by western blot analysis. Total blots of FLCN, LC3, GABARAP, FNIP1 and FNIP2 were also carried out.

3.3.9 FLCN/GABARAP binding is impaired in BHD patient-derived mutants

Previous work in this study showed that BHD patient-derived mutants of FLCN bound more robustly with ULK1, suggesting the C-terminus of FLCN likely plays a role in dissociation of FLCN from ULK1. Therefore a similar experiment was set to compare the interaction of GABARAP with wild-type and BHD patient-derived mutants of FLCN. In contrast to ULK1 interaction, GABARAP interaction with FLCN was impaired in patient derived mutants (Figure 3.10).

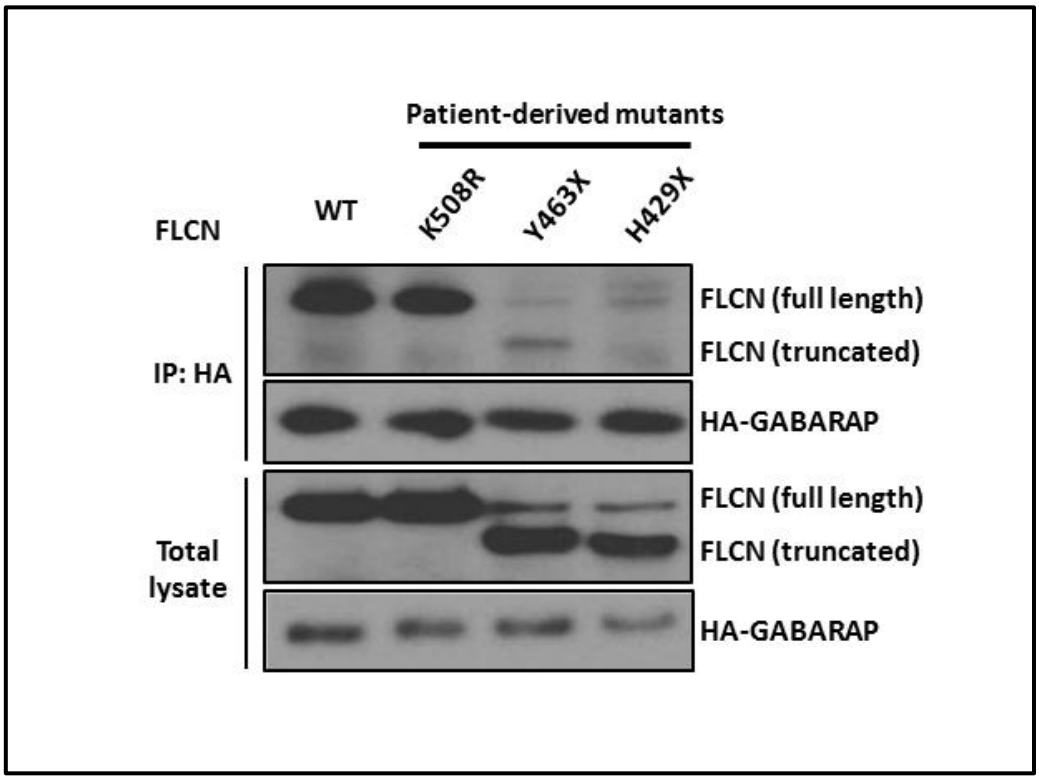

Figure 3.10 FLCN-GABARAP binding is impaired in patient derived mutants: HA-GABARAP was co-expressed with either wild-type FLCN, or FLCN mutant (K508R, Y463X, H429X) in HEK293 cells. Anti-HA antibodies were used to immunoprecipitate HA-GABARAP and associated FLCN was determined by western blot analysis. Total protein expression of FLCN and GABARAP is shown.

3.3.10 FLCN interacts with Rab GTPases associated with autophagy

Previously Nookala *et al.* reported that FLCN functions as a GEF towards Rab35. Although interaction of Rab35 was observed with over-expressed FLCN in HK2 cells, no GEF activity could be detected *in vitro* (data not shown, (carried out by Dr. Andrew Tee, Cardiff University, UK)), suggesting that Rab35 might not be the *bona fide* small G-protein target of FLCN. Having seen the involvement of FLCN in autophagy, it was decided to study the interaction of FLCN with other candidate Rab small G-proteins previously linked to autophagy, *i.e*., Rab7, Rab24, Rab27b and Rab32.

Although the interaction of FLCN with Rab7 and Rab27b was weaker than that of Rab24 and Rab32, over-expressed FLCN appeared to bind to all these autophagy-associated Rab small G-proteins to varying degrees (Figure 3.11). This supports the notion that FLCN may function upstream of several Rab small G-proteins and likely regulates vesicular trafficking events linked to autophagy.

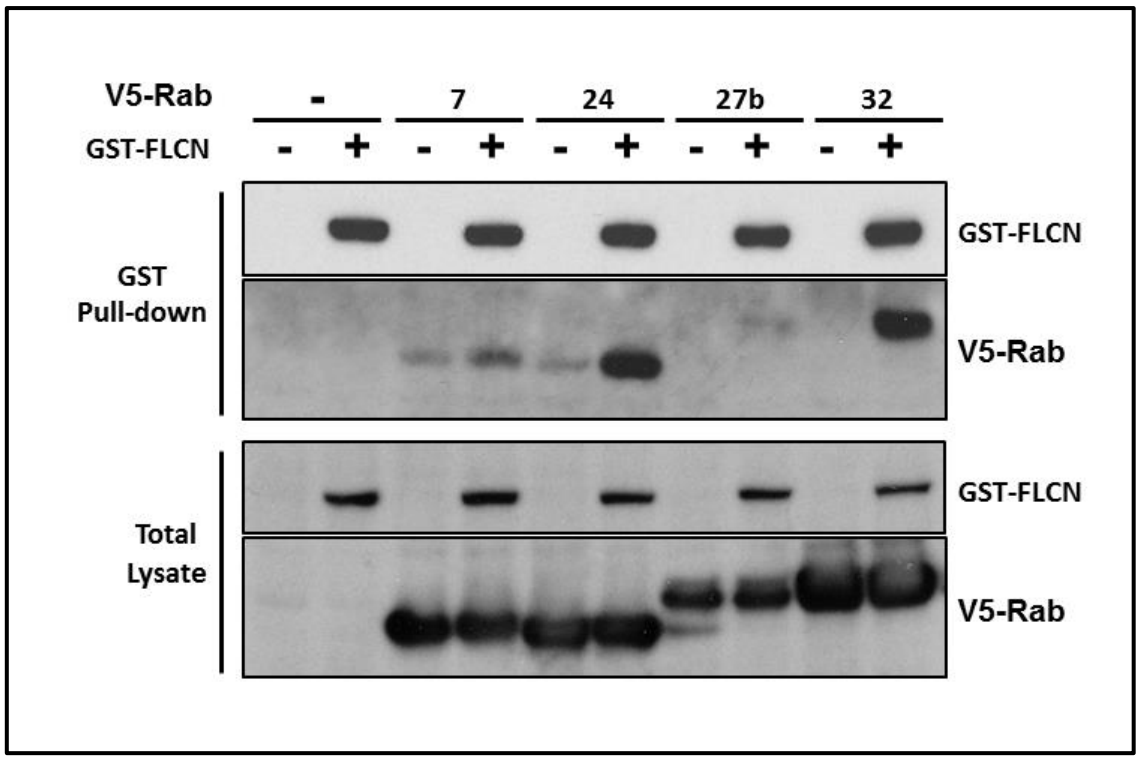

Figure 3.11 FLCN interacts with autophagy associated Rab GTPases: Either Rab7, Rab24, Rab27b or Rab32 was expressed by itself or co-expressed with GST-tagged FLCN, where indicated. GST-FLCN was purified on glutathione-Sepharose beads and associated Rab small G protein was assessed by western blot analysis. Total blots of FLCN and Rab small G-proteins are also shown.

3.3.11 FLCN is not a typical GEF

To further investigate the GEF activity of FLCN towards the Rabs involved in autophagy, inactive mutants of Rab7 and Rab24 were made and their interaction was studied. To make the inactive Rab7 that cannot bind guanine nucleotide, aspartic acid 128 was mutated to asparagine and was called Rab7 D128N. To make the inactive Rab24 aspartic acid D123 was mutated to asparagine and was called Rab4 D123N. GST-tagged FLCN was over-expressed with either wild type or mutant Rab7/24 in HEK293 cells and after GST-pulldown, results were analysed. Since the mutant forms of these Rabs represent the GDP-bound state of the protein in their conformation, a more robust binding of FLCN to Rab mutants was expected if FLCN functioned as a GEF. However after several repeats the level of interaction differed between experiments. Figure 3.12 demonstrates one of the variable results where wild type Rabs were found to bind more avidly to FLCN than the inactive mutants.

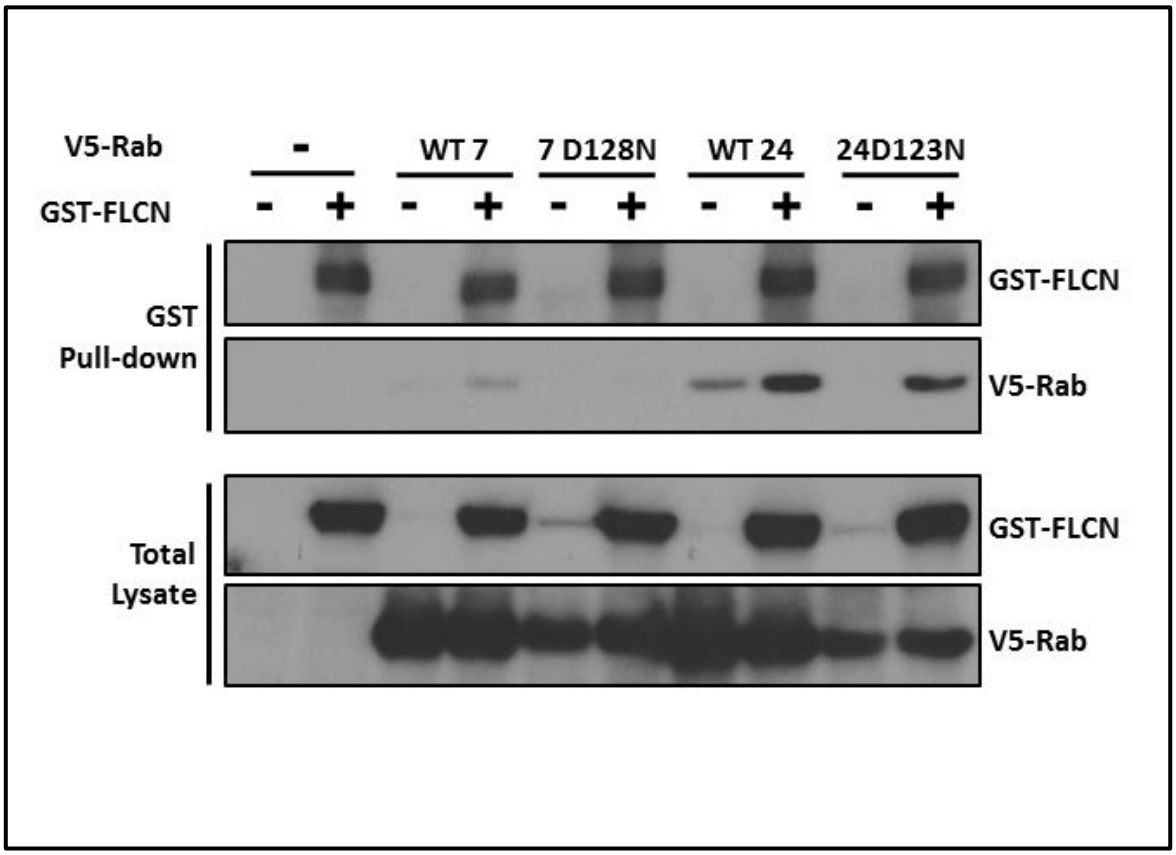

Figure 3.12 FLCN is not a typical GEF: Either Rab7, Rab7 D128N, Rab24 or Rab24 D123N was expressed by itself or co-expressed with GST-tagged FLCN, where indicated. GST-FLCN was purified on glutathione-Sepharose beads and associated Rab small G protein was assessed by western blot analysis. Total blots of FLCN and Rab small G-proteins are also shown.

3.4 Discussion

This chapter shows that FLCN interacts with and is a new downstream substrate of ULK1 and also that phosphorylation by ULK1 modulates the interaction of FLCN with both autophagy components, GABARAP and several Rab small G-proteins linked to autophagy. These interactions with ULK1, GABARAP and Rab proteins link FLCN directly to the autophagy machinery and vesicular trafficking. It is also shown that FLCN plays a positive role in autophagy, where loss of FLCN leads to impaired autophagy. Furthermore, FLCN mutant lacking the ULK1-mediated C-terminal phosphorylation sites could not restore autophagy in FLCN-deficient cells whereas the WT-FLCN could rescue autophagy. Of interest, LST7, the yeast homologue of FLCN, is required for transportation of the amino acid permease, Gap1p, from the Golgi to the cell surface (Roberg et al. 1997). This role of trafficking between cellular compartments in response to nutrients provides an evolutionary link to the proposed function of FLCN as an integral part of the autophagy machinery, probably co-ordinating vesicular trafficking through modulation of Rab activity.

If FLCN functioned as a *bona fide* GEF, it was expected to have an enhanced binding to the non-guanine nucleotide binding mutants of Rabs. However, these Rab mutants sometimes bound less favourably with that of FLCN. Rab activators, GEFs, require a specific mechanism to target them to their site of action (Barr & Lambright 2010). It is possible that the interaction between FLCN and GABARAP functions in an analogous manner to recruit FLCN to the autophagosomal membrane at the appropriate stage of the autophagic process. FLCN does not have a LIR motif; therefore its interaction with GABARAP/LC3 is an indirect interaction through the FNIPs. Although several attempts on FLCN GEF assays were made in our lab by Dr Andrew Tee it did not show any GEF activity for FLCN. It is likely that FLCN in a

complex with FNIP1 and FNIP2 could act as an atypical GAP/GEF (or even a Rab scaffold protein) that helps facilitate vesicular trafficking connected to autophagy.

The binding partners of FLCN, FNIP1 and FNIP2, have previously been connected to B-cell development (Baba et al. 2012), autophagy via GABARAP (Behrends et al. 2010) and the induction of apoptosis following DNA-base mispairing (Lim et al. 2012). Here it is revealed that FNIP2 (and to a lesser extent FNIP1) enhances FLCN-GABARAP binding, implying that FLCN functions as a complex with FNIP proteins to regulate autophagy. GABARAP subfamily members appear to function downstream of autophagosome membrane elongation in a step coupled to dissociation of the Atg12-Atg5-Atg16L complex (Weidberg et al. 2010) and have been hypothesised to recruit and anchor the ULK1 complex on autophagosomes (Kraft et al. 2012) (Alemu et al. 2012).

Although several key advances have been made in BHD syndrome research, such as the determination of an AMPK-FLCN interaction (Baba et al. 2006) and identification of a DENN domain (Nookala et al. 2012), the direct cellular function(s) of FLCN is still unknown. This work refines our understanding of FLCN, where FLCN is revealed to interact with several components integral to autophagy, namely ULK1, GABARAP, Rab7, Rab24 and Rab32. Although it is important to highlight that FLCN function is not just restricted to autophagy. Multiple pathways that drive cancer progression can become dysregulated when FLCN expression is lost, including defects in TGFβ-mediated signalling (S.-B. Hong et al. 2010)(Cash et al. 2011), enhanced hypoxia inducible factor activity (Preston et al. 2011) and TFE3 activity (S. B. Hong et al. 2010).

Recently, both p62 and FLCN have been linked to amino acid sensing through the Rag proteins and mTORC1. p62 was found to bind the Rag proteins to favour formation of the active Rag heterodimer, thereby helping activate mTORC1 at the lysosome (Duran et al. 2011). Although, no altered mTORC1 signalling following FLCN loss could be detected in our lab which could be due to cell type dependant activity of mTORC1 signalling in the context of FLCN-deficiency; three publications have now linked the FLCN/FNIP complex to the Rag small G proteins at the lysosome, linking FLCN to amino acid-dependent mTORC1 signalling (Petit et al. 2013)(Tsun et al. 2013) (Martina et al. 2014).

BHD syndrome has lately been reported to be a ciliopathy, where alteration to FLCN levels can cause changes to the onset of ciliogenesis (Luijten et al. 2013). Changes in FLCN levels are also associated with disruption of planar cell polarity and dysregulation of the canonical Wnt signalling pathway. Pampliega *et al*. suggested a compromised ability to activate the autophagic response as an underlying feature in some ciliopathies (Pampliega et al. 2013). Hence it is possible that there is also an association between cilia and autophagy in BHD syndrome, where impaired autophagy could be a contributing factor to ciliary defects and renal cyst formation in BHD syndrome patients.

Overall this work helps refine our understanding of FLCN by revealing that FLCN interacts with components integral to autophagy, summarised in Figure 3.13, however, it is possible that FLCN could play a broader ‘housekeeping’ role in the cell and is likely to be a fundamental player in autophagy and cellular homeostasis outside the disease setting. Although further studies are required, it seems reasonable to assume that impaired autophagy upon loss of FLCN expression contributes in part to cancer progression in BHD patients.

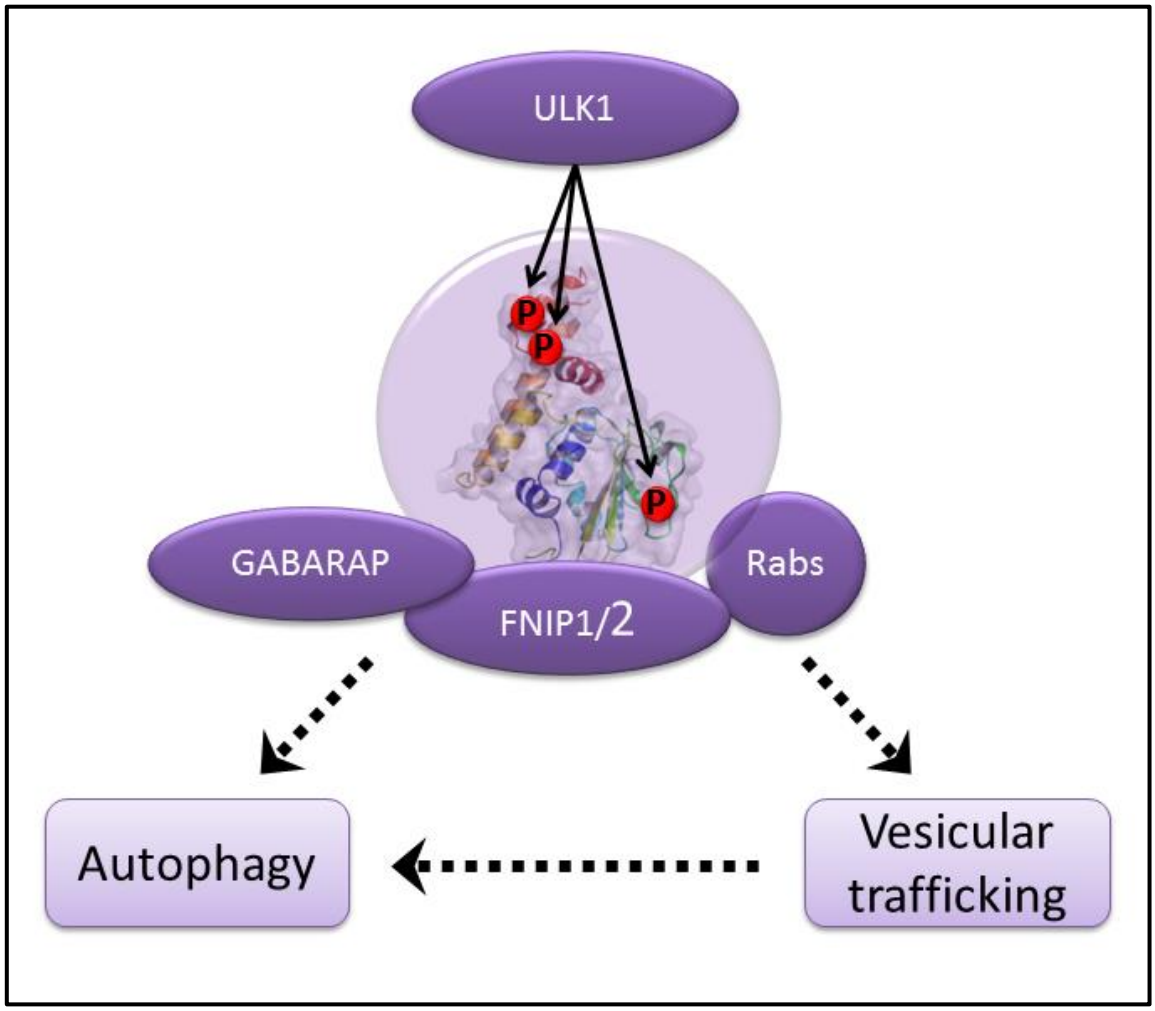

Figure 3.14 Summary diagram, showing critical FLCN interacting proteins involved in autophagy and vesicular trafficking

4 Chapter 4: Familial multiple discoid fibroma (FMDF)

4.1 Introduction

In 2011 a series of families were studied by Starink *et al*. that presented a phenotype similar to BHD. However these families had no pathogenic FLCN germline mutations; furthermore none of these 9 families reported cases of renal cell carcinoma or recurrent pneumothorax. The onset of skin lesions was childhood or in early adulthood as oppose to BHD lesions that have a later onset in life usually occurring in the third decade. Starink *et al*. named this condition familial multiple discoid fibromas (FMDF, OMIM #190340) (Starink et al. 2012).

BHD skin lesions mainly occur on the face and upper torso whereas the FMDF lesions were shown to generally appear on the ears. Familial trichodiscomas have a very similar clinical presentation to fibrofolliculomas but have two distinguishing features: they consist mostly of fibrous stroma and are of childhood onset. Additionally FMDF skin lesions histologically presented a hair follicle at their periphery as oppose to the fibrofolliculomas observed in BHD that often have a distorted hair follicle in the centre of the lesion (Starink et al. 2012).

Another independent study also described two siblings aged 27 and 22 with dischoid fibromas; however they had no family history of skin, lung or renal abnormalities. The 27 year old man had multiple firm papules that had developed primarily over his face and ears, but also on his trunk and limbs since the age of 5 years, whereas his 22 year old sister had an onset in adolescence. Same as in the Starink *et al.* study, no mutation in *FLCN* was found (Wee et al. 2013).

Wee *et al.* first treated the skin lesions with surgical procedures such as shave excision, hyfrecation and curettage and cautery; however the results were not satisfactory. Previously, it has been shown that rapamycin can improve the appearance of skin lesions in TSC (Haemel et al. 2010)(Mutizwa et al. 2011) hence Wee *et al.* treated the facial skin lesions of the affected 27 year old male with application of topical rapamycin at 1 mg/ml. After 8 weeks of treatment there was an evident improvement in the redness and size of the lesions (Wee et al. 2013).

FMDF is an extremely rare genetic disorder and too little is known about the disease. Clinical symptoms, family and medical history play an important role in the diagnosis of the disease. However further research is required to better understand the pathogenesis and genes involved in FMDF to better aid the diagnosis and management of the condition. Therefore the main aim of this chapter was to further study FMDF.

4.2 Methods

Segregation and haplotype analysis – (Carried out by our collaborators in Maastricht) Segregation analysis for the FNIP1 and FNIP2 loci was performed for families 11, 24, and 45 using polymorphic short tandem repeat markers distal and proximal to both genes. Short tandem repeat markers D4S2394, D4S1644, D4S1625, D4S413, D4S2997, D4S1090, D4S2368, D4S2431, D4S2417, D5S1453, D5S2501, D5S1505, D5S2098, D5S2120, D5S2057, D5S2002, D5S2117, D5S816, D5S1480, D5S820, and D5S1471 were amplified by standard procedures with one of the primers labelled with a fluorescent FAM (carboxyfluorescein) label. Fragment length was analysed on an ABI 3130 Genetic Analyzer (Applied Biosystems, Foster City, CA). Haplotype analysis was performed by analysing all available affected and unaffected family members using markers D5S1505, D5S2098, D5S2120, D5S2057, D5S2002, D5S2117, D5S816, and D5S1480 surrounding the FNIP1 locus.

FNIP1 sequence analysis - (Carried out by our collaborators in Maastricht) Polymerase chain reaction (PCR) primers were designed to cover all 18 exons and exon/ intron boundaries of FNIP1. PCR products were sequenced using the BigDyeTerminator Cycle sequencing kit (Applied Biosystems) and an automated sequencer (ABI 3730 DNA analyzer). Sequencing data was analysed using Mutation Surveyor software (www.softgenetics.com) and by visual inspection.

Primers:

cloning FNIP1 fw: 5’TCTCGAGCTATGGCCCCTACGCTGTTCCAG3’

cloning FNIP1 rv: 5’CAGATCTTTAAAGGAGTATTTGTGCAAC3’

site-directed mutagenesis fw:

5'-TCTTAATTTATCTCTGTACTGTTTACATCAACAGCATTTTCTTCTTGG-3’

site-directed mutagenesis rv:

5'-CCAAGAAGAAAATGCTGTTGATGTAAACAGTACAGAGATAAATTAAGA-3'

Sequencing FNIP1 mutation: 5’CCACAACCATTCCTGTGGAT3’

Cell lines and cell culture - Primary skin fibroblasts with FNIP1 mutation were obtained from a skin biopsy taken from a consenting 27-year-old male subject diagnosed with FMDF (Carried out by our collaborators in Maastricht). All cells were cultured in DMEM supplemented with 10 % (v/v) foetal calf serum, 100 U/ml penicillin and 100 µg/ml streptomycin (Life Technologies).

DNA constructs, transfections and antibodies - Human FNIP1 wild-type was amplified by PCR. FNIP1 mutant Val663fs were made by site-directed mutagenesis using the Quikchange II Site Directed Mutagenesis kit according to the manufacturer’s instructions (Agilent).

Co-immunoprecipitation and Western blotting - HEK293 cells transiently transfected with appropriate plasmids were lysed in BHD lysis buffer (20 mM Tris, 135 mM NaCl, 5% (v/v) glycerol, 50 mM NaF and 0.1% (v/v) Triton X-100, pH 7.5 supplemented with protease inhibitors), centrifuged and protein quantified using Bradford reagent (Sigma-Aldrich). Anti-HA and anti-V5 coupled to Protein G-Sepharose beads (GE Healthcare Life Sciences) were used to immunoprecipitate HA- and V5-tagged proteins as appropriate. Immunoprecipitates were washed three times in lysis buffer and resuspended in NuPAGE LDS sample buffer (Life

Technologies). Western blotting was performed as previously described. Blots shown are representative of at least three independent experiments.

4.3 Results

4.3.1 Families with FMDF have common ancestors and affected members have FNIP1 c.1989delT mutation

Eight out of nine families in this study (same families as the Starink *et al*. study) originate from the same Dutch village, which forms a small ethnic isolate. Genealogical studies confirmed common ancestry of these families, suggesting a founder effect (Figure 4.2). Clinical re-evaluation with a specific focus on lungs and kidneys again did not reveal any systemic abnormalities. Consequently, co-segregation of FMDF with the FNIP1 locus in nine Dutch families was found, while excluding FNIP2. In these families, all available FMDF cases (n=27) carried a heterozygous germline mutation in *FNIP1* (c.1989delT), which was not present in any of the unaffected family members.

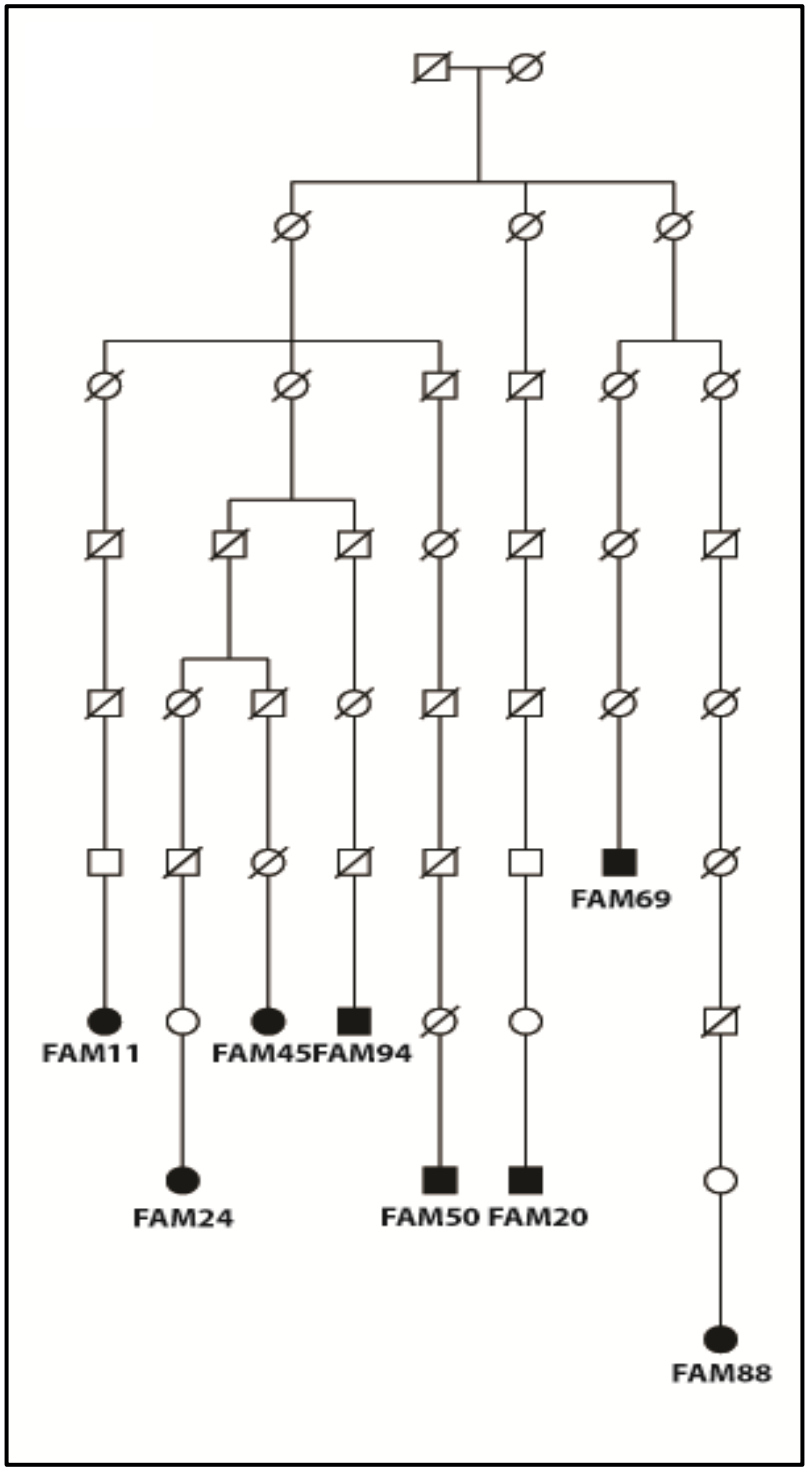

Figure 4.2 Families with FMDF have common ancestors and affected members have FNIP1 c.1989delT mutation: Pedigree showing the relation between FMDF kindreds identified on the Island of Urk. Linkage analysis confirmed common ancestry for all FMDF patients with the FNIP1 c.1989delT mutation.

4.3.2 The c.1989delT mutation predicts the frameshift p.Val663fsX which is a conserved residue in vertebrates

FNIP1 is an evolutionary conserved protein especially at the C-terminus (Figure 4.3 A). The c.1989delT mutation found in FMDF families causes a frameshift at valine 663 (p.Val663fsX) which leads to a C-terminal deletion. valine 663 is also an evolutionary conserved residue (Figure 4.3 B).

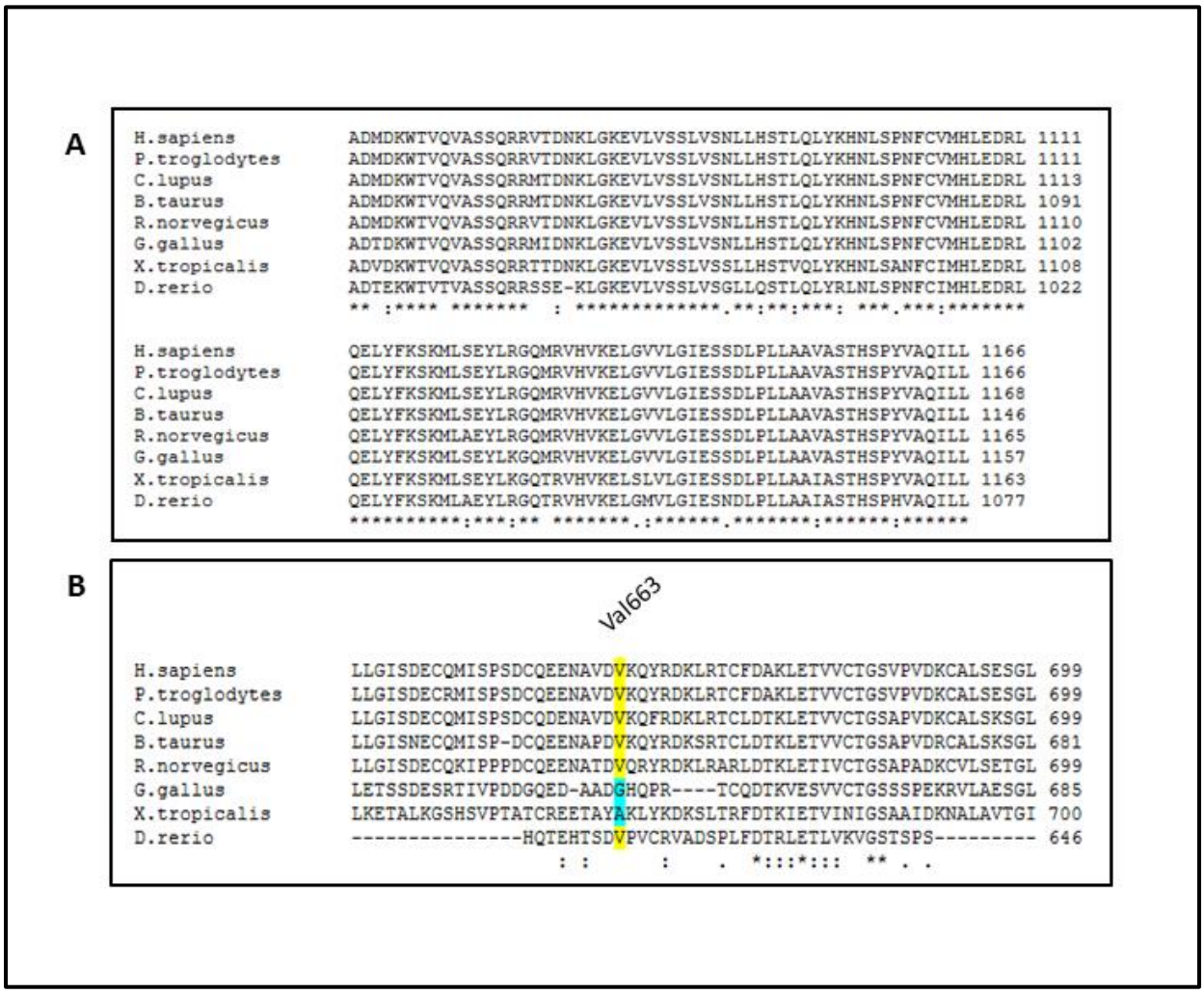

Figure 4.3 FNIP1 protein alignment: FNIP1 is a highly conserved protein across species especially at the C-terminus (**A**) valine 663 which is mutated in FMDF families, is an evolutionary conserved residue (**B**)

4.3.3 FLCN/FNIP1 interaction is impaired by c.1989delT mutation

FNIP1 is a poorly studied protein and its function is not fully understood. FNIP1 has been reported to interact with FLCN where deletion of the 237 C-terminal amino acids of FNIP1 was shown to result in decreased FLCN binding (Baba et al. 2006). Accordingly, using co-immunoprecipitation the interaction of endogenous FLCN with both wild type FNIP1 and FNIP1-Val663fsX was studied. FLCN interaction with FNIP1-Val663fsX was shown to be completely abolished (Figure 4.4), which was expected according to the Baba *et.al.* study. However, in a reciprocal experiment where overexpressed FLCN was immunoprecipitated, only partial impairment of FNIP1-Val663fsX interaction with FLCN was observed (Figure 4.5). This could be explained if FNIP1-Val663fsX was interacting with FLCN via FNIP2.

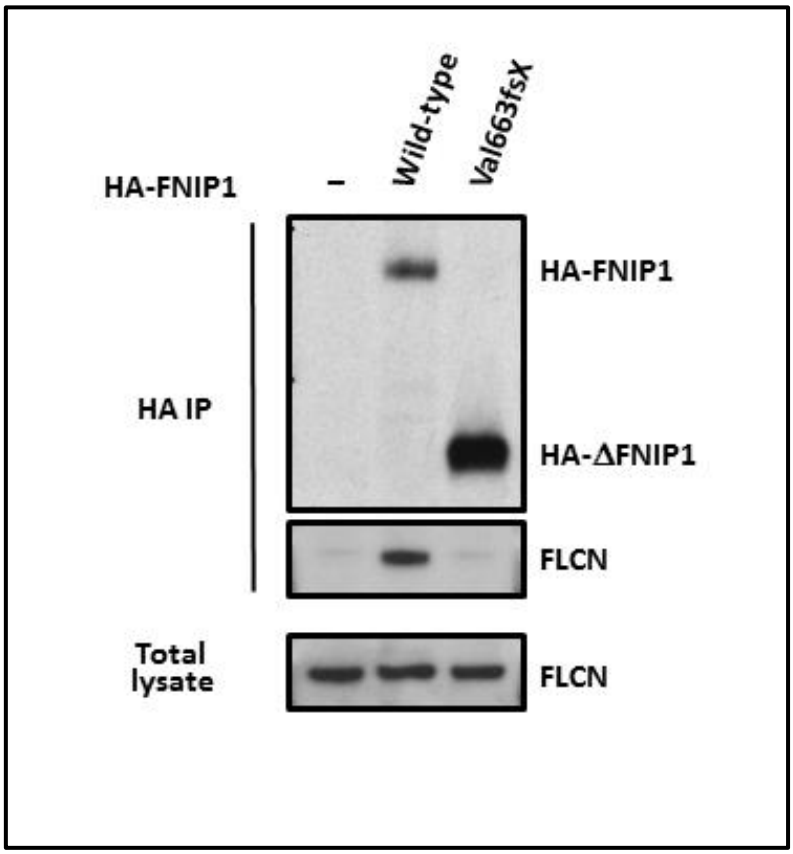

Figure 4.4 FLCN/FNIP1 interaction is impaired by c.1989delT mutation: HA-FNIP1 (wild-type and Val663fsX6) was expressed in HEK293 cells. HA antibody was used to immunoprecipitate both HA-FNIP1 and HA-ΔFNIP1 in generated cell lysates. Associated endogenous FLCN was determined by western blotting, showing decreased binding of endogenous FLCN to FNIP1-Val663fsX6 (ΔFNIP1) compared to FNIP1 wild-type.

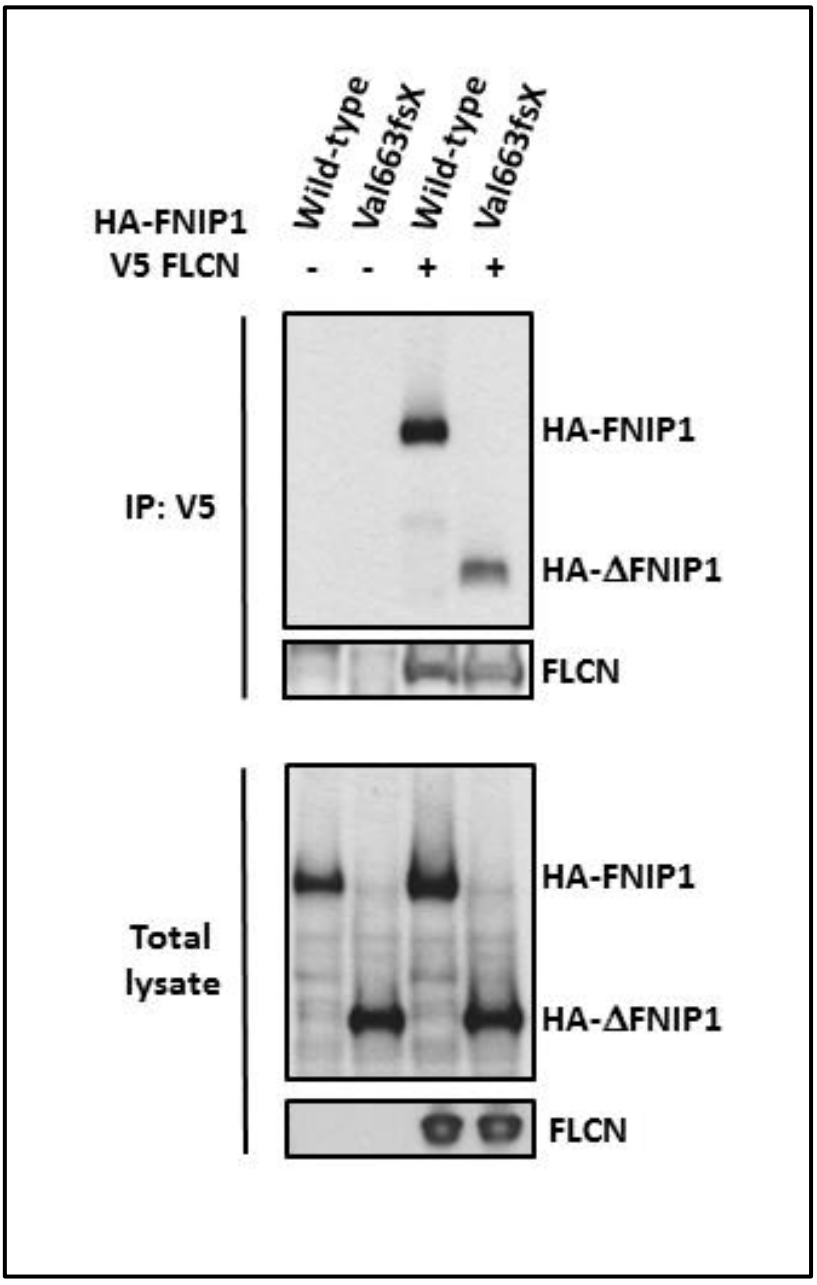

Figure 4.5 FLCN/FNIP1 interaction is impaired by c.1989delT mutation: HA-FNIP1 (wild-type and Val663fsX6) was expressed in HEK293 cells with or without V5-FLCN. V5 antibody was used to immunoprecipitate FLCN in generated cell lysates. Decreased binding of ΔFNIP1 compared to FNIP1 wild-type can be observed.

4.3.4 FNIP1/FNIP2 interaction is not modified by c.1989delT mutation

Previously it has been shown that deletion of all of the five conserved domains of FNIP1 is necessary to abolish FNIP2 binding (Hasumi et al. 2008). To test if the interaction of FNIP1 with FNIP2 is affected in FMDF families, wild-type FNIP1 and Val663fsX6 FNIP1 was over-expressed in HEK293 cells with or without myc-FNIP2. From the generated cell lysate either FNIP1 (Figure 4.6 A) or FNIP2 (Figure 4.6 B) was immunoprecipitated. It was observed that both wild-type and mutant FNIP1 interact with FNIP2.

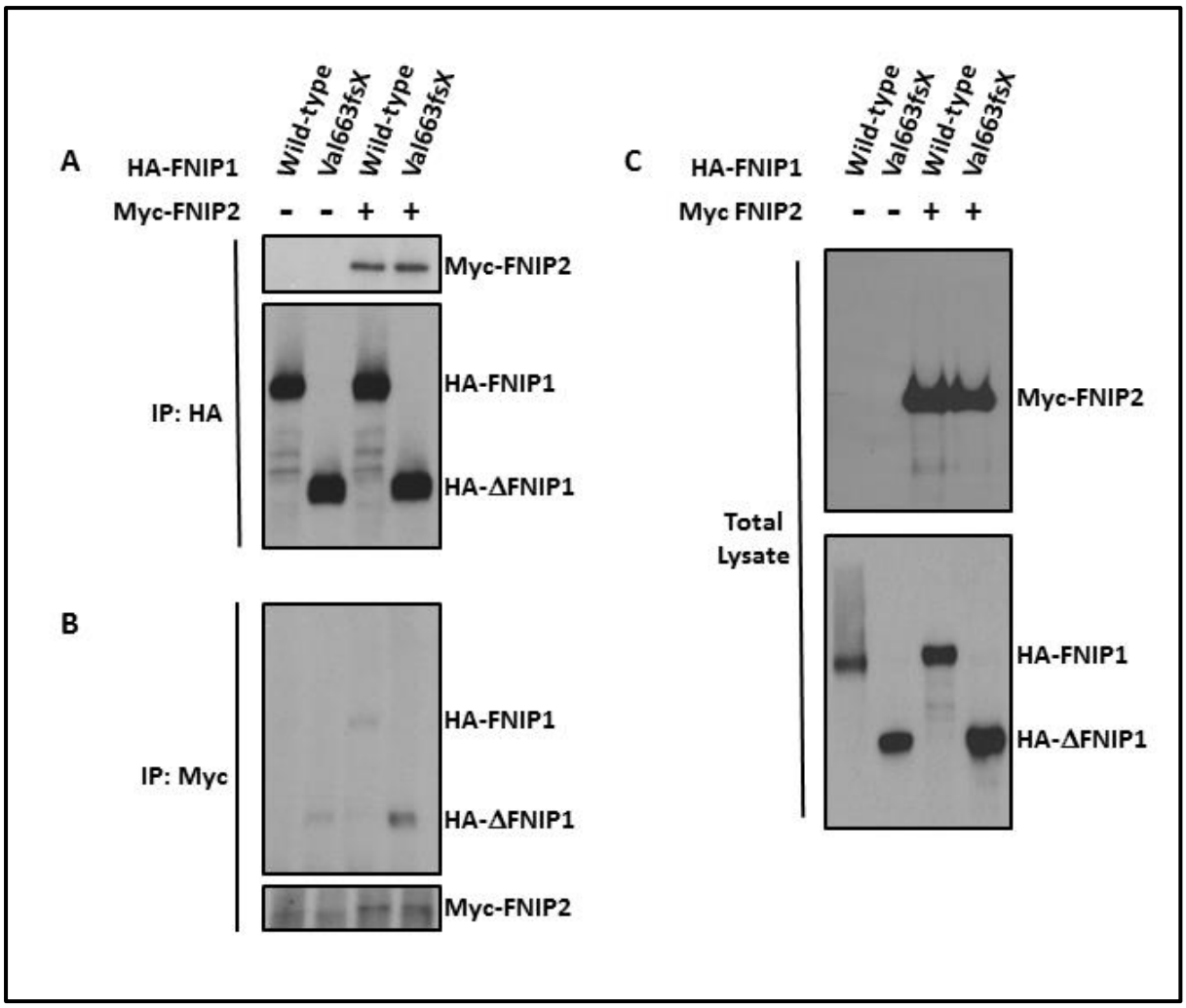

Figure 4.6 FNIP1/FNIP2 interaction is not modified by c.1989delT mutation: wild-type FNIP1 and Val663fsX6 FNIP1 were over-expressed in HEK293 cells with or without myc-FNIP2. Either HA immunoprecipitation (**A**) or Myc immunoprecipitation (**B**) was performed on the cell lysate generated (**C**).

4.4 Discussion

Although the clinical presentation of the fibrofolliculomas and discoid fibromas is similar, histologically they are distinct. In addition, none of the FMDF patients show any extracutaneous manifestations, suggesting that FNIP1 is only critical in the skin. Of interest, FNIP1 has been reported to be expressed at low levels in the lung and kidney, while FNIP2 is expressed at higher levels in these organs (Takagi et al. 2008)(Hasumi et al. 2008). In other tissues, loss of FNIP1 might be tolerated, or the mutant protein might be expressed at higher levels than in the skin tissue. These observations suggest of differing functions for FLCN and FNIP1; this is further supported by the high degree of variation in phenotype observed with FLCN and FNIP1 mutations in humans. FNIP1 Val663fsX has impaired binding to FLCN, but not to FNIP2 and therefore might maintain partial functionality. Alternatively lack of systemic phenotype could be explained by compensation through FNIP2.

Collectively these findings represent the first human disorder caused by a mutation in one of the folliculin interacting proteins, with a phenotype distinct from BHD. Whether the FNIP1 mutation in these patients would function in a similar regard to that of BHD patient mutations within the FLCN-deficient cells is doubtful.

To determine if FNIP1-Val663fsX6 is expressed or broken down by nonsense mediated mRNA decay, fibroblasts were obtained from discoid fibroma biopsy material by our collaborators in Maastricht. Genomic sequencing of the *FNIP1* locus confirmed presence of heterozygous c.1989delT; no somatic second hits were detected. Sequencing of cDNA from these fibroblasts showed minimal presence of mutant mRNA, which increased after incubation with puromycin (an inhibitor of nonsense-mediated mRNA decay). In addition, no wild-type or Val663fsX6 FNIP1

was detected by Western blot in these cells (data not shown). Together, these data indicate that FMDF could be caused by *FNIP1* haploinsufficiency.

However, recently Prof Julian Sampson and his group were presented with a family consisting of four members, with a germline whole gene deletion of FNIP1 in addition to loss of the 5' region of RAPGEF6 encompassing exon 1, and the 3' region of LOC728637, encompassing the last 4 exons (exon 9-12). In contrast to the FMDF patients, this FNIP1 deletion, does not give rise to the characteristic of discoid fibromas that are associated with a FNIP1 single base-pair deletion in FMDF (unpublished data). Therefore, it is less likely that the disease is caused by haploinsufficienciency of *FNIP1*.

Given that loss of FNIP1 in these patients does not appear to result in cancer, there is possible redundancy between FNIP1 and FNIP2. To further study and compare the cellular function of FNIP1 and FNIP2, *FNIP1* and *FNIP2* knockdown cells were created in Chapter 5.

5 Chapter 5: Characterising FNIP1, FNIP2 and FLCN interactions

5.1 Introduction

Very little is known about FLCN interacting proteins, FNIP1 and FNIP2. FNIP2 was the first of the two interacting proteins to be identified. Nagase *et al.,* in a study of human cDNA library identified the *FNIP2* gene, which was then designated KIAA1450 (Nagase et al. 1998). However it wasn't until 2008 that Hasumi *et al.* identified it as FLCN interacting protein 2 (Hasumi et al. 2008).

FNIP1 was first identified by Baba *et al.* 2006 where they showed that it interacts directly with FLCN and also facilitates phosphorylation of FLCN by AMPK. Baba *et al.,* also demonstrated that FNIP1 binds to AMPK and that both FLCN and FNIP1 are phosphorylated by AMPK (Baba et al. 2006). Furthermore FLCN/FNIP1 interaction has been shown to be altered by treatment of AMPK inhibitor (compound C), and also with rapamycin and amino acid starvation (Baba et al. 2006). Other post-translational modification of FNIP1 published to date include phosphorylation by mTOR (Yu et al. 2011) and ubiquitination at lysine 161 (Wagner et al. 2011).

Both FLCN interacting proteins, FNIP1 and FNIP2, have been shown to be essential for recruitment of FLCN to the lysosomes during amino acid starvation, it has also been demonstrated that FNIP1 and FNIP2 are required for interaction between FLCN and the Rag small G proteins facilitating the activation of Rags by FLCN (Petit et al. 2013)(Tsun et al. 2013).

FNIP1 has been linked to B cell development in mice by two independent studies published in 2012 (Park et al. 2012)(Baba et al. 2012). Park *et al.* found dysregulation of both AMPK and mTOR activity in FNIP1-null pre-B cells, which

resulted in excessive cell growth and enhanced sensitivity to apoptosis. Consequently they suggested that energy stress as a result of FNIP1 loss is the cause of B cell arrest (Park et al. 2012). In contrast the FNIP1-null mice generated by Baba *et al.* did not demonstrate any alterations in mTOR activity. However they also observed a substantial increase in apoptosis, hence suggesting that a caspase induced pre-B cell death as the cause of defects in B cell development in FNIP1-null mice (Baba et al. 2012).

In the follow-up study Park *et al*. demonstrated that invariant Natural Killer T (iNKT) cells do not develop to full maturation in FNIP1-null mice either. FACS analysis of the iNKTs from the FNIP1-null mice in this study revealed that stage 1 and stage 2 iNKT cells are present whereas very few stage 3 iNKT cells could be found. This finding suggests that the maturation of these cells in the absence of FNIP1 is blocked between stage 2 and stage 3. There was also a significant increase in caspase 3-positive cells in stage 2 and stage 3 iNKTs. mTOR activity in FNIP1-null iNKT cells was shown to be increased and the number of mitochondria to be decreased despite the low ATP levels. These results could suggest that FNIP1 plays an important role development of iNKTs by regulating their metabolic homeostasis (Park et al. 2014).

In a mega proteomic study of the human autophagy network in 2010 Behrends *et al*. found FNIP1 to interact with GABARAP (Behrends et al. 2010). GABARAP together with LC3 and GATE16 are the human orthologs of ATG8 family of proteins that are crucial for autophagosome formation (Shpilka et al. 2011).

In 2012 it was revealed that FNIP1 and FNIP2, both contain a DENN domain, similar to FLCN, implicating them in membrane trafficking which could be during various stages of autophagy (Zhang et al. 2012).

One of the earliest pathways that FNIP2 was reported to be involved in was O6-methylguanine triggered apoptosis (Komori et al. 2009). Further studies revealed that upon treatment with N-methyl-Nnitrosourea (MNU) FNIP2 levels in the cells increased due to stabilisation of the FNIP2 protein, since mRNA level was not changed (Lim et al. 2012)(Sano et al. 2013).

The most diverse role suggested for FNIP2 is its requirement for myelination in the central nervous system (Pemberton et al. 2014). In Pemberton *et al*. study the Weimaraner dog was found to have a frameshift mutation in *FNIP2* gene which resulted in a C-terminal truncation of the protein. This truncated FNIP2 protein was shown to cause hypomyelination of the brain and myelin defects in the spinal cord. It was also demonstrated that FNIP2 expression in oligodendrocytes was regulated by the transcription factor Sox10 (Pemberton et al. 2014).

Two independent studies have shown that similar to FNIP1, FNIP2 also binds to and is phosphorylated directly by AMPK (Hasumi et al. 2008)(Takagi et al. 2008). FNIP1 and FNIP2 are homologous proteins that have been shown to be able to form both homodimers and hetrodimers (Takagi et al. 2008).

It has been published that both FLCN interacting partners FNIP1 and FNIP2 interact with FLCN through its C-terminal (Baba et al. 2006)(Hasumi et al. 2008)(Takagi et al. 2008). Of interest, most of the disease causing mutations in BHD syndrome produce a C-terminal truncated form of FLCN (Schmidt et al. 2005). It is not known if the truncated form of FLCN is left within the cell with defective function

or it undergoes nonsense-mediated decay, however the latter is less likely to be true as deletion of the whole FLCN gene, which is observed in Smith-Magenis syndrome (SMS) (OMIM182290), does not produce any of the BHD symptoms (Bi et al. 2002). SMS is a congenital disorder caused by a mutation in the *RAI1* gene; though the majority of the patients lose this gene by a heterozygous deletion of part of chromosome locus 17p11.2 (Bi et al. 2002). This region includes the *FLCN* gene, which leaves these patients with only one wild-type FLCN allele. The absence of any obvious BHD associated symptoms in SMS patients would suggest that the presence of a mutant FLCN allele is required for BHD symptoms to develop. Whilst the mechanism driving tumourigenesis in BHD remains unclear, it is apparent that the majority of disease causing mutations result from C-terminus truncations to the FLCN protein. These truncated proteins are unable to interact with both FNIP1 and FNIP2, suggesting that this FLCN: FNIP1/FNIP2 interaction could be of functional significance within cells. There could also be other unknown C-terminus interactors which have yet to be discovered.

Since FNIP1 and FNIP2 and their interaction with FLCN seems to be vital for the normal physiology of the cell, the main aim of this result chapter was to further study the role of FNIP1 and FNIP2 within cells.

5.2 Methods

Cell culture - All cell lines were cultured in DMEM supplemented with 10 % (v/v) foetal calf serum, 100 U/ml penicillin and 100 µg/ml streptomycin (Life Technologies).

Transfection - Lipofectamine® 2000 Reagent (Life Technologies) was used for transfection according to the manufacturer's protocol. Cells were 70-90 % confluent at the time of transfection. Cells were harvested 24–36 h post-transfection. Experiments were performed under normal growth conditions, unless otherwise stated. For complete starvation, cells were washed twice in phosphate buffered saline (PBS) and incubated in Krebs Ringer buffer (KRB) (20 mM HEPES (pH 7.4), 115 mM NaCl, 5 mM KCl, 10 mM $NaHCO_3$, 2.5 mM $MgCl_2$, 2.5 mM $CaCl_2$) for 4 h.

Since a large number of cells needed to be transfected for GST purification, $CaCl_2$ transfection was used. DNA complexes were prepared by combining the DNA with ddH_2O, $CaCl_2$ was then added and the solution was vortexed. BES solution was then slowly added drop-wise whilst aerating the sample with a drawn glass pasteur pipette. Mixtures were left to stand at room temperature for 15-20 min (until precipitate becomes visible) then added drop-wise to the cells.

MISSION shRNAs to knockdown each FNIP1 and FNIP2 were purchased from Sigma Aldrich as follows:

FNIP1:

pLKO.1puro-shRNA0369

pLKO.1puro-shRNA9563

pLKO.1puro-shRNA9412

pLKO.1puro-shRNA9414

pLKO.1puro-shRNA9515

FNIP2:

pLKO.1puro-shRNA5772

pLKO.1puro-shRNA5784

pLKO.1puro-shRNA6305

pLKO.1puro-shRNA6306

pLKO.1puro-shRNA6307

Immunoprecipitation, GST-pulldown, western blotting - Cells were lysed in BHD lysis buffer (20 mM Tris, 135 mM NaCl, 5 % (v/v) glycerol, 50 mM NaF and 0.1 % (v/v) Triton X-100, pH 7.5 plus protease inhibitors), centrifuged and protein levels standardised using a Bradford assay (Sigma-Aldrich). Anti-HA and anti-Flag coupled to Protein G-Sepharose beads (GE Healthcare Life Sciences) were used to immunoprecipitate HA and Flag-tagged proteins as appropriate. Immunoprecipitates were washed three times in lysis buffer and resuspended in NuPAGE LDS sample buffer (Life Technologies). Samples for GST-pulldown were lysed in Buffer B (40 mM HEPES (pH 7.5), 120 mM NaCl, 1 mM EDTA, 10 mM pyrophosphate, 10 mM β-glycerophosphate, 50 mM NaF, 1.5 mM Na3VO4, 0.3% (w/v) CHAPS plus protease inhibitors) and incubated with glutathione-Sepharose beads (GE Healthcare Life Sciences). Beads were washed three times in lysis buffer, and GST-tagged proteins were eluted using 10 mM glutathione. Western blotting was performed as previously described. Blots shown are representative of at least three independent experiments.

Mass spectrometry - GST-FLCN, GST-FNIP1 and GST-FNIP2 were purified from HEK293 cells. Samples were separated by SDS-PAGE and excised bands were subjected to mass spectrometry in collaboration with Dr Bryan Balliff (Vermount University).

RNA extraction, qPCR - cells were lysed in RNA protect Cell Reagent and centrifuged at 5000 rpm for 5 min, the pellet was saved for mRNA extraction. mRNA was extracted using the Qiagen mRNA extraction kit in accordance with manufacturer's protocol, QIA shredders (QIAGEN) were utilised to homogenise the pellet. Resulting mRNA concentration was determined using the nanodrop spectrophotometer. cDNA was prepared using the QIAGEN reverse transcription kit according to the manufacturer's protocol. Quantitative real-time PCR reactions were performed in 96-well plates using appropriate primers and Sybr Green PCR Master mix (QIAGEN). All primers were purchased from QIAGEN as follows:

Hs_FLCN_1_SG QuantiTect Primer Assay, cat no: QT00088417

Hs_FNIP1_1_SG QuantiTect Primer Assay, cat no: QT01029063

Hs_FNIP2_1_SG QuantiTect Primer Assay, cat no: QT01672629

Hs_GABARAP_1_SG QuantiTect Primer Assay, cat no: QT00203532

Hs_SQSTM1_1_SG QuantiTect Primer Assay, cat no: QT00095676

Protein alignment - Clustal Omega provided by The European Bioinformatics Institute (EMBL-EBI) was used for all multiple alignments.

5.3 Results

5.3.1 Generation of FNIP1 and FNIP2 stable knockdown cell lines

To characterise and better understand the role of FLCN interacting proteins, two stable knockdown cell lines were generated using both FNIP1 and FNIP2 shRNAs. To make an efficient knockdown cell line, first a series of five different FNIP1 and FNIP2 shRNAs were transiently transfected into HEK293 cells to determine which of these shRNAs were most effective. The cells were harvested after 48 h and RNA was extracted from the cells. qPCR was carried out and the two shRNAs which demonstrated the best knock down for each FNIP (Figure 5.1A,B), were selected to generate the stable FNIP1 and FNIP2 knockdown cell lines.

For reasons previously described in chapter 3, HK2 cells were used to generate FNIP1 and FNIP2 stable knockdown cell lines. HK2 cells were transfected with both selected shRNA plasmids (sh9563 and sh9412 for FNIP1, sh5784 and sh6305 for FNIP2) and after 48 h the selection media containing 2µg/mL of puromycin, was added to the cells. Subsequently 16 clones from each knockdown were isolated to grow. After 2-3 month the clones that had survived were selected. Gene expression levels of FNIP1 and FNIP2 mRNAs were examined in all selected clones to ensure the efficiency of knockdown (Figure 5.2A,B).

FNIP1 clones A8 and B2 had 82% and 85% knockdown, respectively (Figure 5.2A), while FNIP2 clones A6 and B5 had 88% and 83% (Figure 5.2B). These cell lines with the most effective knockdown were used for further experiments.

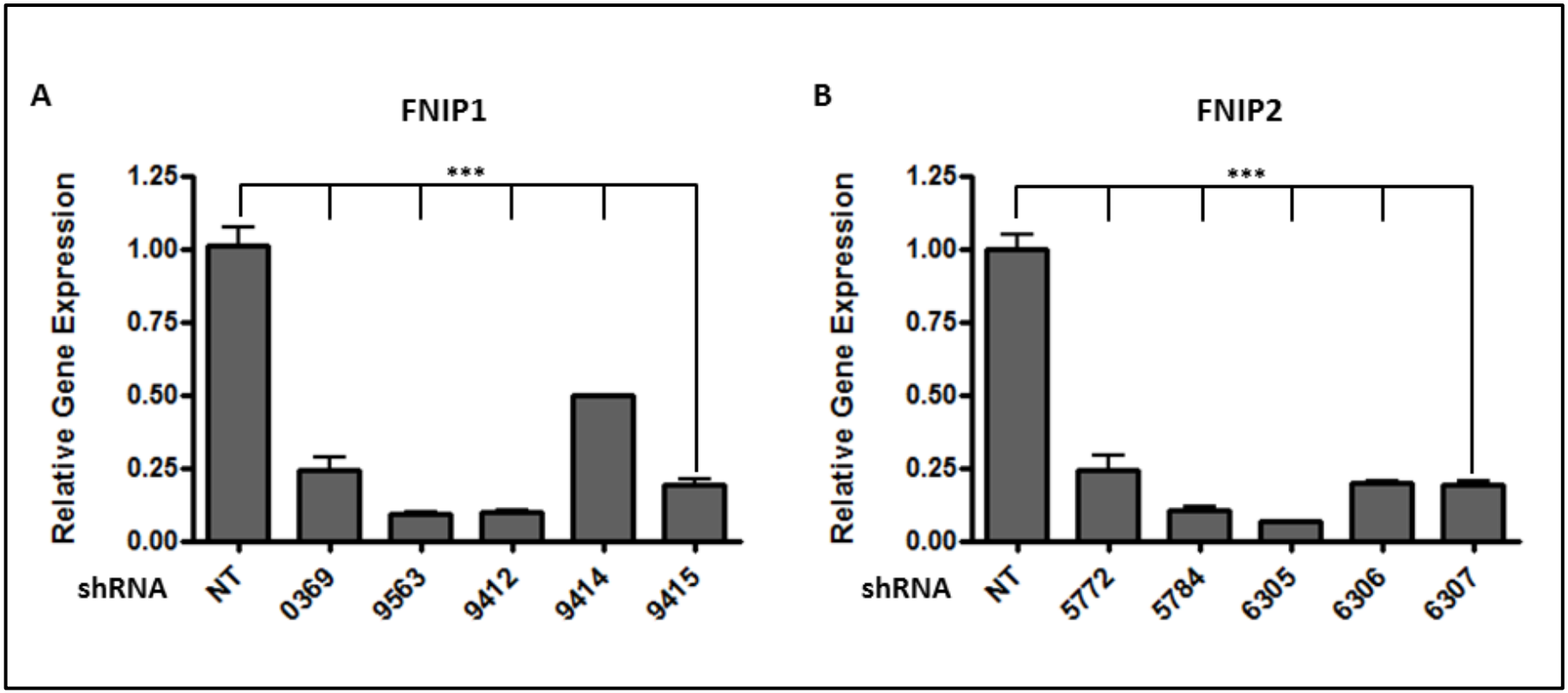

Figure 5.1 Transient knockdown of HEK293 cells with FNIP shRNAs: 5 different shRNA vectors targeting either FNIP1 or FNIP2, with non-target shRNA as a control were transiently transfected into HEK293 cells to test for efficiency of knockdown. mRNA extracted was analysed by Q-PCR to determine relative levels of either (**A**) FNIP1 or (**B**) FNIP2 expression, which was standardised against β-actin. N = 3. *** $P < 0.001$.

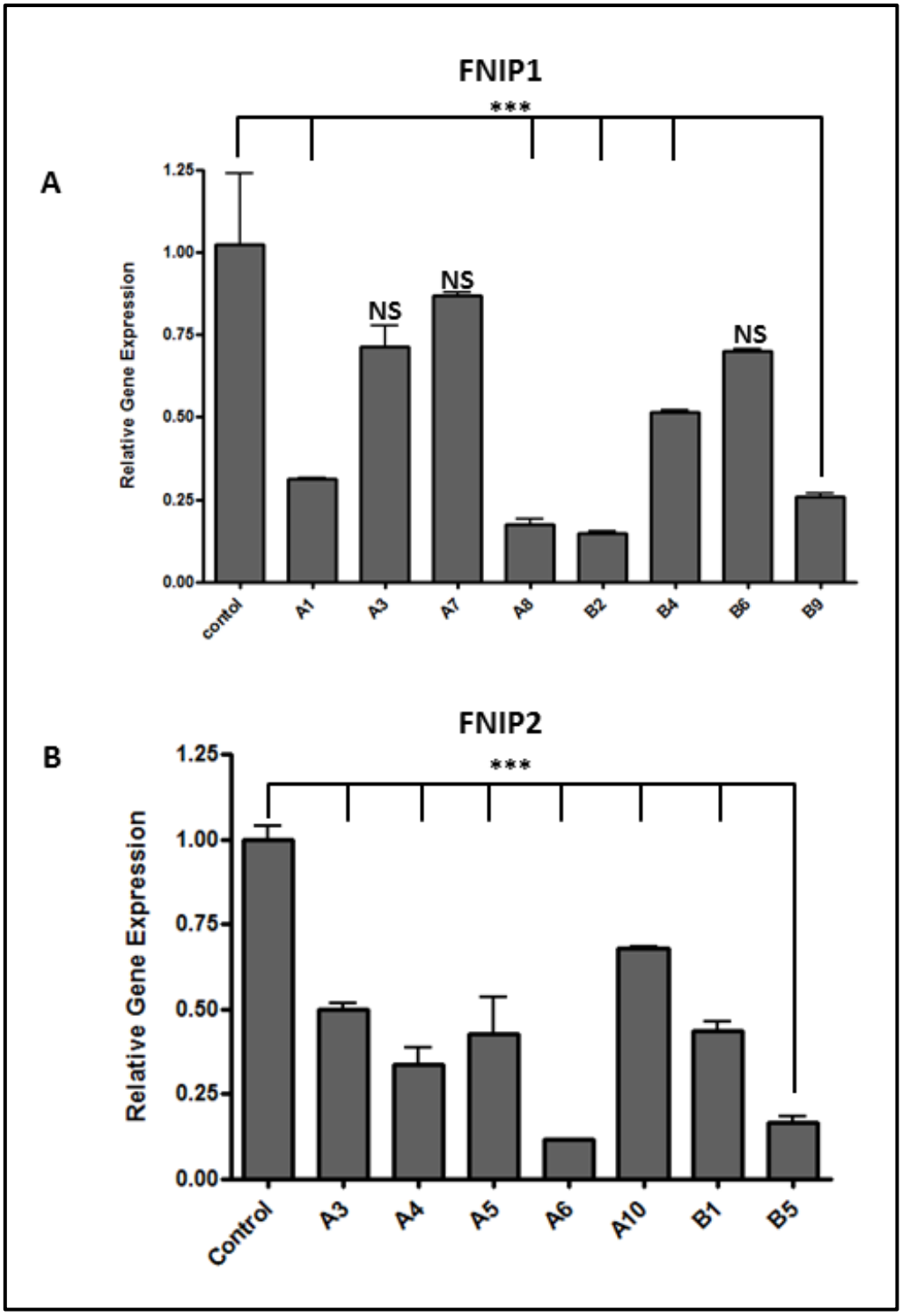

Figure 5.2 Stable knockdown of HK2 cells with FNIP shRNAs: Stable cell lines expressing either (**A**) FNIP1 or (**B**) FNIP2 selected shRNAs were created and validated for efficient knockdown after selection. mRNA extracted was analysed by Q-PCR to determine relative levels of either FNIP1 or FNIP2 , where indicated, which was standardised against β-actin. N = 3. *** $P < 0.001$.

5.3.2 Early morphological changes were observed in FNIP1 stable knockdown cell lines

During the first few weeks after the knockdown of FNIP1 in the HK2 cells, many FNIP1 shRNA expressing cells underwent a drastic morphological change (Figure 5.3A) compared to the normal HK2 cells expressing non-target shRNA (Figure 5.3B). The growth of these FNIP1 knockdown cells was dramatically reduced and the cells appeared expanded and full of fatty acid deposits. Also quite a few ghosts cells were observed, where these cells had likely ruptured leaving membrane structures (Figure 5.3A). The accumulation of fatty acid deposits in the cells could be an indication of FNIP1's involvement in metabolic pathways such as lipolysis /lipogenesis. However after a couple of months of selection the growth rate returned to a level equivalent to the control HK2 cell lines, and the morphological changes were abolished. This suggests the existence of compensatory signalling mechanisms within these cells in order to overcome the lack of FNIP1. It is likely that the slow growing cells were undergoing a level of crisis, and/or homeostatic imbalance that was rectified through a low level of FNIP1 re-expression. Indeed, complete loss of FNIP1 expression was not observed.

Although the FNIP2 knockdown cells also grew slowly initially, unlike the FNIP1 knockdowns they did not demonstrate obvious morphological changes. However some minor changes could be observed including spiky cytoplasmic projections (Figure 5.4A), compared to control HK2 cells (Figure 5.4B). It is possible that these cytoplasmic projections are as a result of incomplete cell division which in turn could indicate the involvement of FNIP2 in cytokinesis.

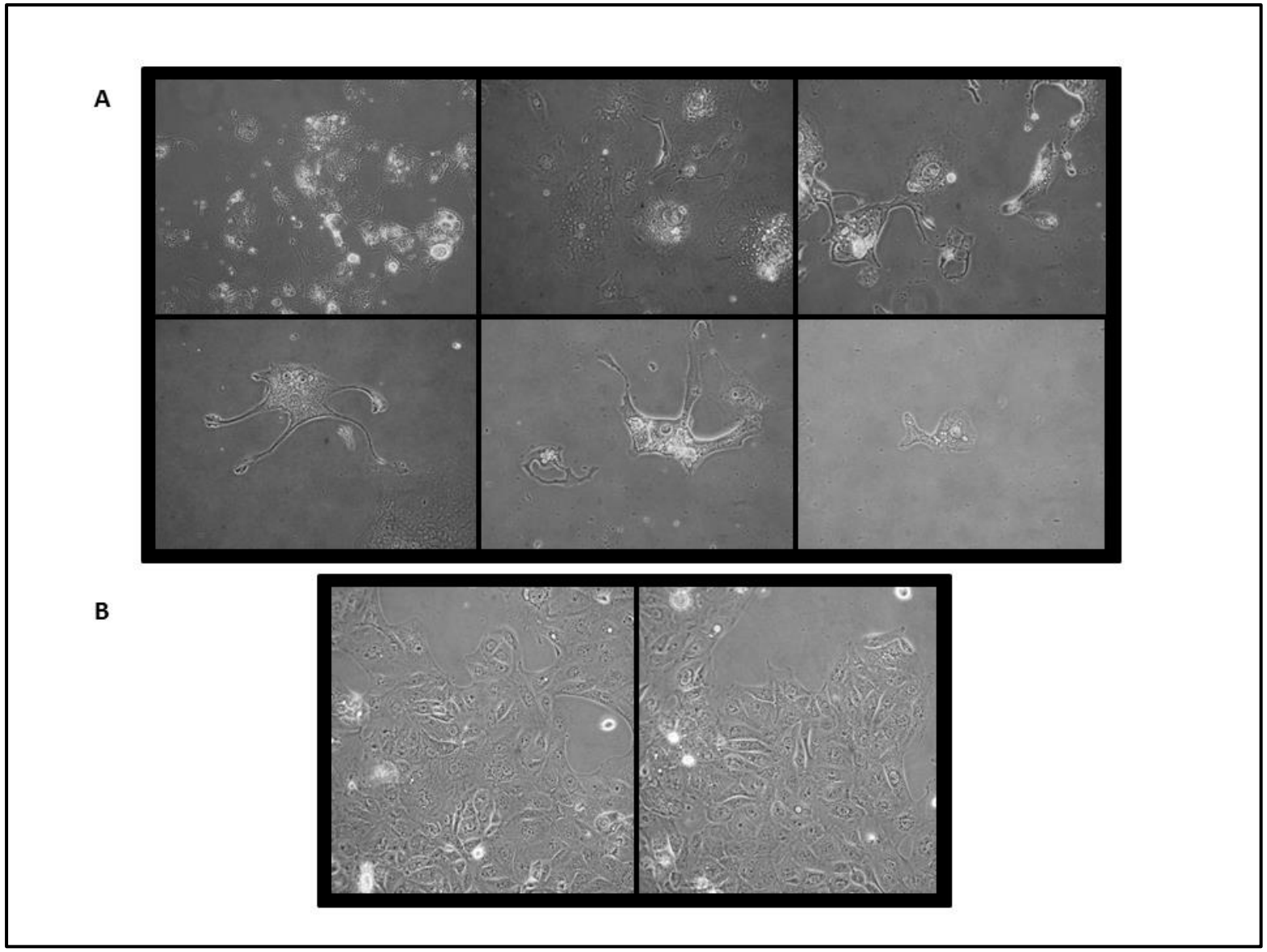

Figure 5.3 Early morphological changes were observed in FNIP1 stable knockdown cell lines: Phase contrast images (x40) of clonal populations were taken during the selection of HK2 cells that were transfected with FNIP1 double shRNA, where (**A**) shows cells that are enlarged and appear to be undergoing cellular crisis and (**B**) control HK2 cells expressing non-target shRNA.

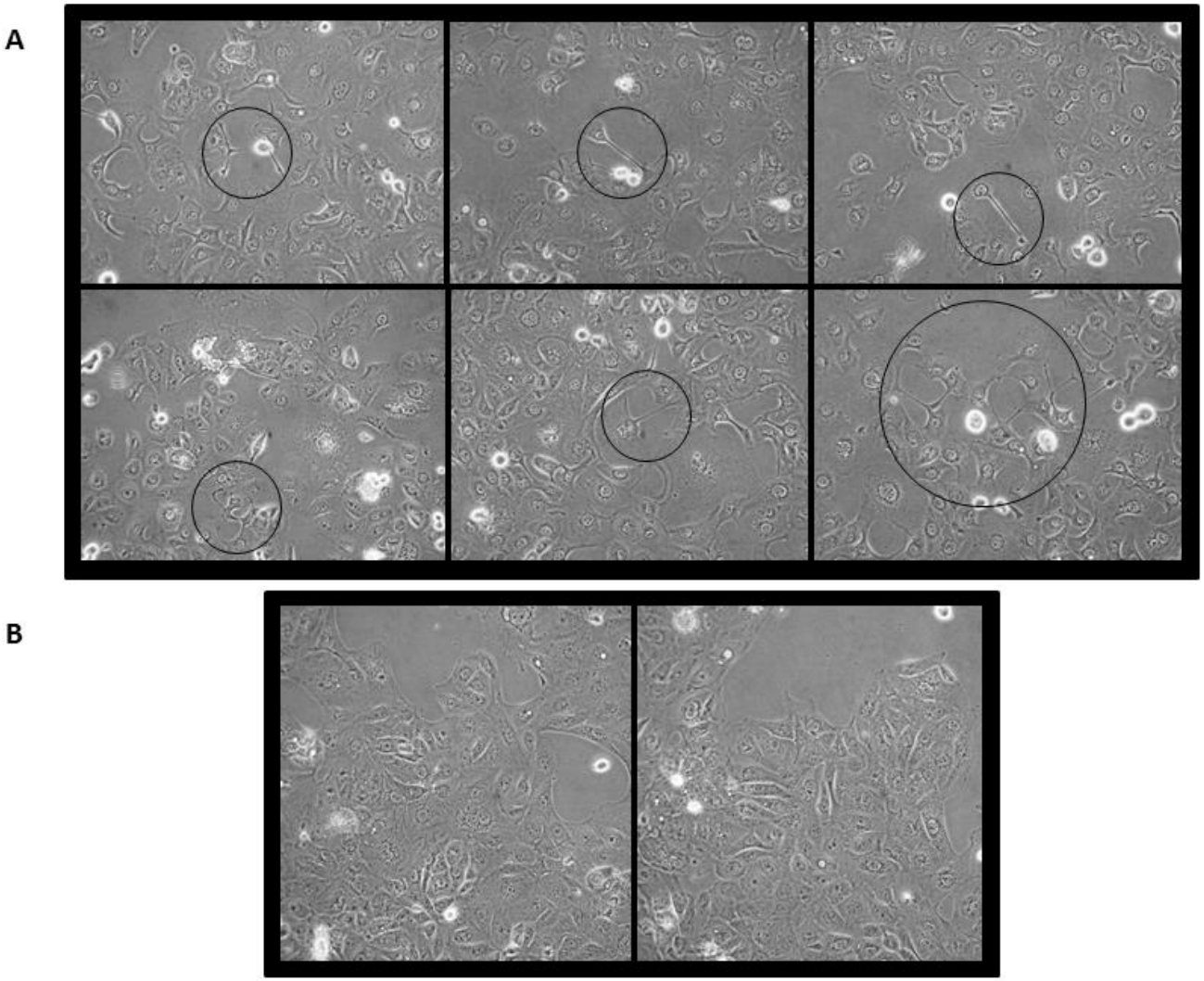

Figure 5.4 Minor morphological changes were observed in FNIP2 stable knockdown cell lines: Phase contrast images (x40) of clonal populations were taken during the selection of HK2 cells that were transfected with FNIP2 double shRNA. (**A**) Images highlight minor morphological changes while clonal expansion of cells taken within (**B**) control HK2 cells expressing non-target shRNA.

5.3.3 When FNIP2 is knocked down, other components of the complex, i.e., FLCN and FNIP1 were observed to be present at higher levels in the cell

To characterise the *FNIP1/2* stable knockdown cell lines, the initial step was to closely study the components of the FLCN/FNIP complex. Unfortunately a specific working FNIP2 antibody suitable for western blotting could not be obtained, therefore only FLCN and FNIP1 protein levels were examined. Figure 5.5A reveals a significant level of FNIP1 protein knockdown was achieved in these stable knockdown cell lines (Figure 5.5A). The results clearly demonstrate that in the *FNIP2* knockdown cells, FNIP1 protein levels were significantly higher compared to control HK2 cells (Figure 5.5B). FLCN protein levels were also observed at higher levels in *FNIP2* knockdown cell lines, showing up to 2.6 fold higher in clone A6 (Figure 5.5D). However *FNIP1* knockdown cell lines did not show any significant change in FLCN protein levels (Figure 5.5C).

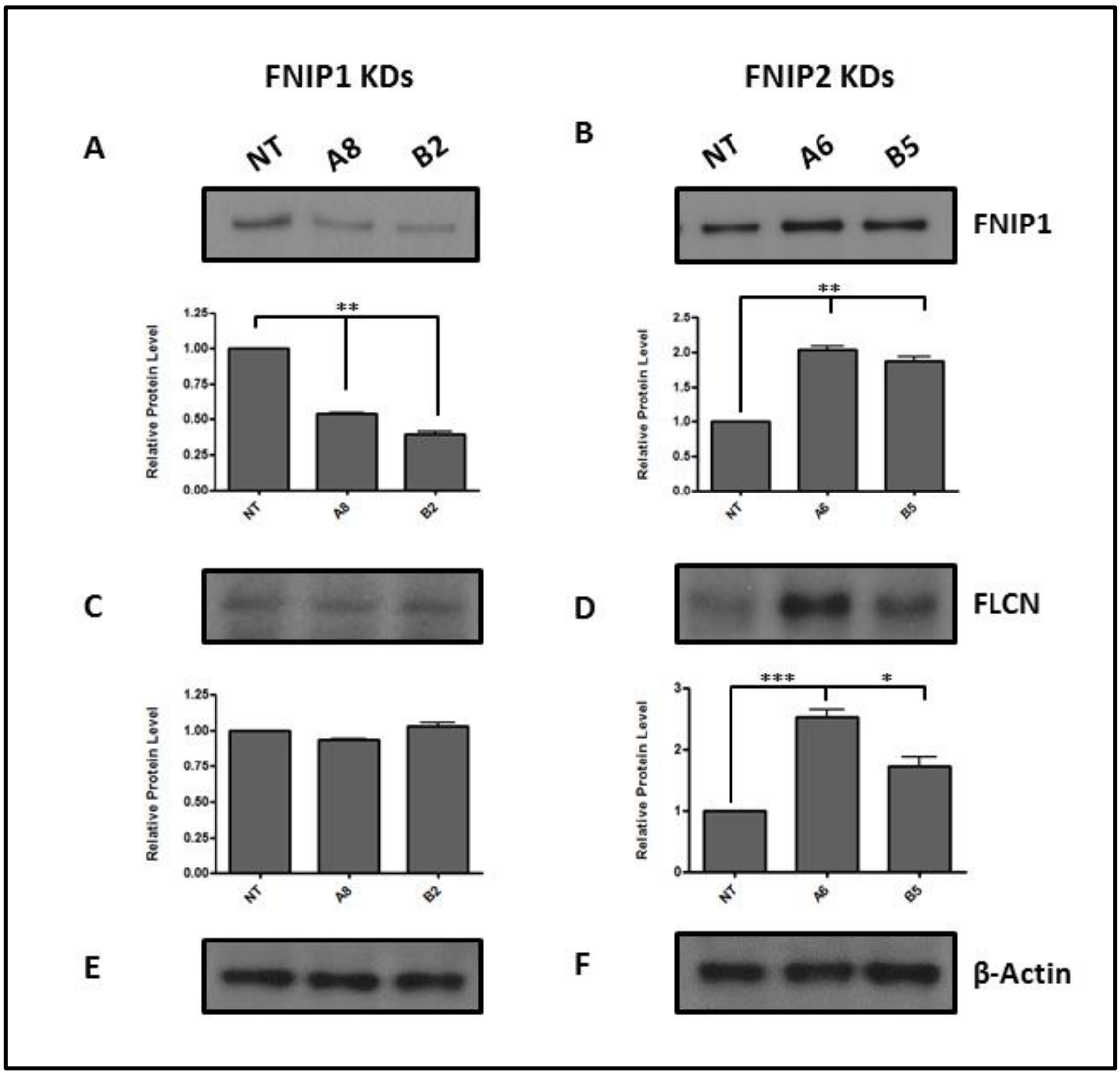

Figure 5.5 Loss of FNIP2 expression is compensated by enhanced expression of FNIP1 and FLCN: Clonal cell lines for (**A**) *FNIP1* (clones A8 and B2) and (**B**) *FNIP2* (clones A6 and B5) knockdown were analysed for expression of FNIP1 protein by western blot analysis and were compared to non-target control HK2 cells. Total FLCN expression within these (**C**) *FNIP1* and (**D**) *FNIP2* clones were also determined. (**E**-**F**) β-Actin was used a loading control. Densitometry was carried out to determine relative protein levels between samples and is graphed. N = 3, * $P < 0.05$, *** $P < 0.001$.

5.3.4 FNIP1 and FNIP2 both possess conserved LIR motifs

Both FNIP1 and FNIP2 are highly conserved across species (Figure 5.6A-C). Of interest, in less developed species like worms and flies, there is only one FNIP protein. Although the worm/fly FNIP shows homology to both human FNIP1 and FNIP2, it is more closely related to the FNIP2 protein (Hasumi et al. 2008). Correspondingly, both proteins contain a LIR motif. Figure 5.6D demonstrates known classic LIR motifs amino acid sequences. The LIR motif in FNIP2 is the classic F-type, which is an evolutionary conserved LIR motif; whereas FNIP1 has a partial LIR motif (Figure 5.6A). The F-type LIR motifs are known to have a higher affinity to bind the GABARAP subfamily of Atg8s (Alemu *et al.* 2012). This could be the reason why the presence of FNIP2 is necessary for GABARAP/ FLCN interaction demonstrated in chapter 3, while FNIP1 had less of an impact.

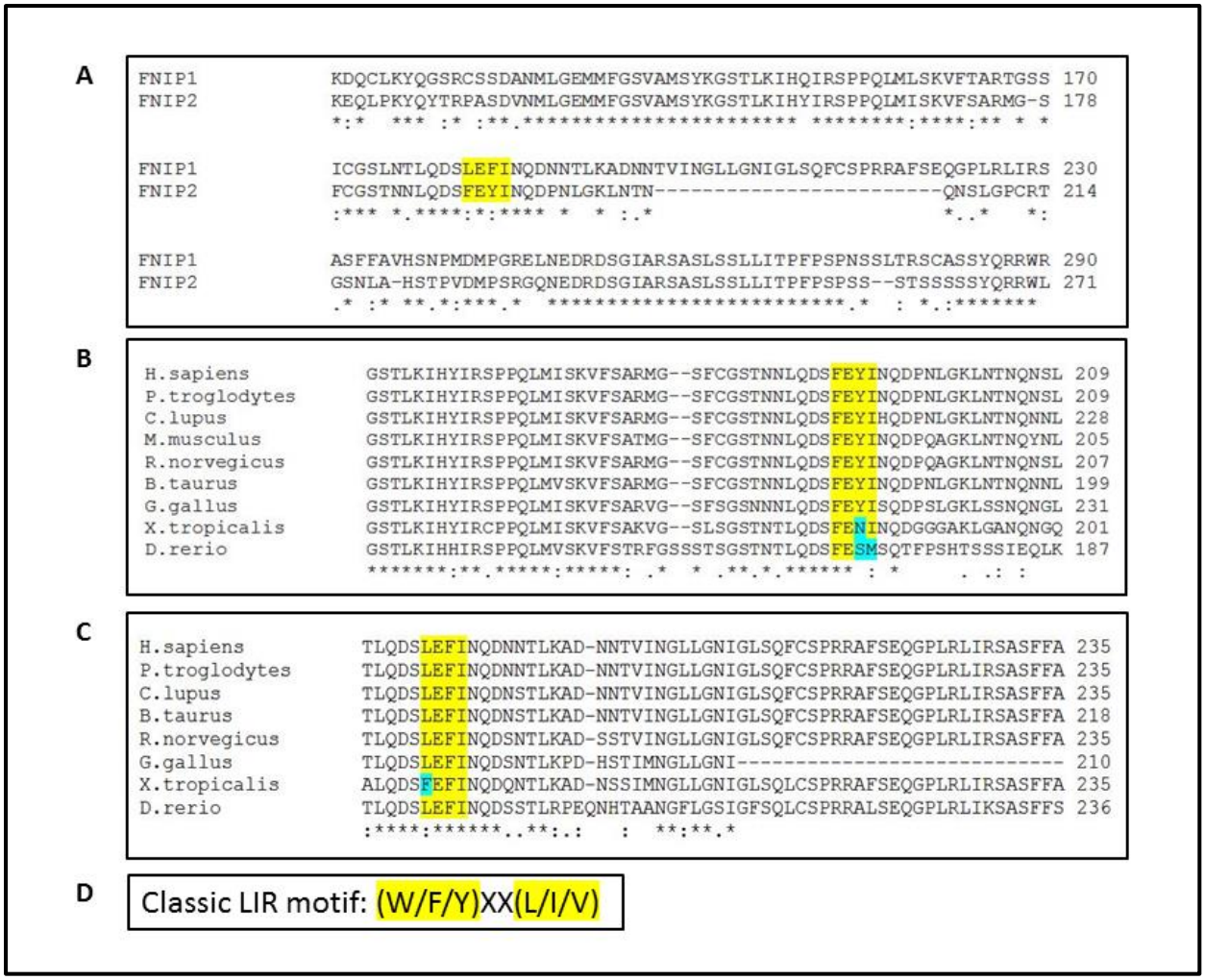

Figure 5.6 FNIP1 and FNIP2 are highly conserved proteins across species and both contain a LIR motif: Amino acid alignments of the potential LIR motif comparing (**A**) human FNIP1 and FNIP2, either (**B**) FNIP2 or (**C**) FNIP1 between species as indicated, and a (**D**) classic consensus sequence of a LIR motif are shown.

5.3.5 Starvation of HK2 cells induces FNIP1 and FNIP2 expression

It was shown earlier that *FLCN* mRNA expression was significantly higher upon induction of autophagy via nutrient and energy starvation. To see whether or not the FNIP proteins are also involved in autophagy, HK2 cells were cultured under three different conditions, normal DMEM, serum free DMEM and Krebs Ringer buffer (lacking both amino acids and glucose). The cells were harvested after 24 hours and mRNA was extracted from the cells. Both *FNIP1* and *FNIP2* mRNA levels showed a significant increase upon serum starvation compared to normal growth conditions (Figure 5.7), this was further increased with amino acid/glucose starvation.

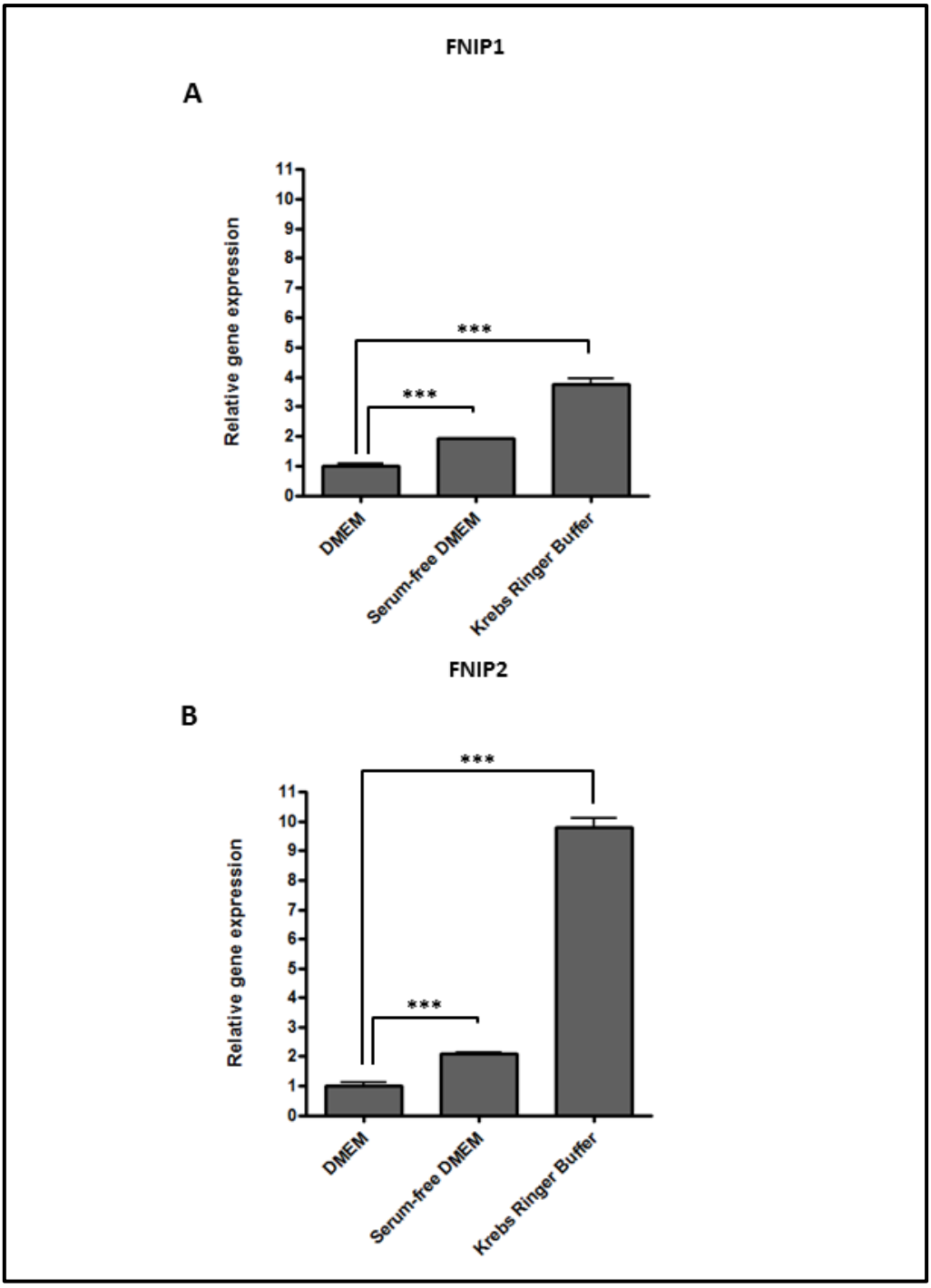

Figure 5.7 Glucose and amino acid starvation causes higher gene expression of *FNIP1* and *FNIP2* within normal HK2 cells: HK2 cells were grown in the presence of either DMEM with and without serum, or Krebs Ringer Buffer (without amino acids and glucose), where indicated. mRNA extracted was assessed for either (**A**) *FNIP1* mRNA or (**B**) *FNIP2* mRNA by Q-PCR to determine relative gene expression that was standardised to β-actin. N = 3, *** $P < 0.001$.

5.3.6 FNIP2 knockdown shows similar molecular defect characteristic to FLCN knockdown cells

It was shown in chapter 3 that autophagy is down regulated in FLCN deficient cells. Evidence suggests that FNIP1 and FNIP2 may also play a role in autophagy, given that both FNIP1 and FNIP2 contain a conserved LIR motif, FNIP1 interacts directly with GABARAP. Additionally both *FNIP1* and *FNIP2* gene expression levels were higher upon starvation induced autophagy. Therefore autophagy was studied in FNIP1/2 deficient cells by measuring GABARAP and p62 protein levels in these cell lines. Both GABARAP and p62 protein levels were observed to be significantly higher in *FNIP2* knockdown cells (Figure 5.8B,D) whereas no significant results were observed for FNIP1 knockdown cells (Figure 5.8A,C). p62 protein levels in FNIP1 knockdown cells were inconsistent after several repeats. GABARAP levels appeared to increase, however these results were not significant. Collectively, these results indicate that FNIP2 might play a more critical role in the regulation of autophagy when complexed with FLCN.

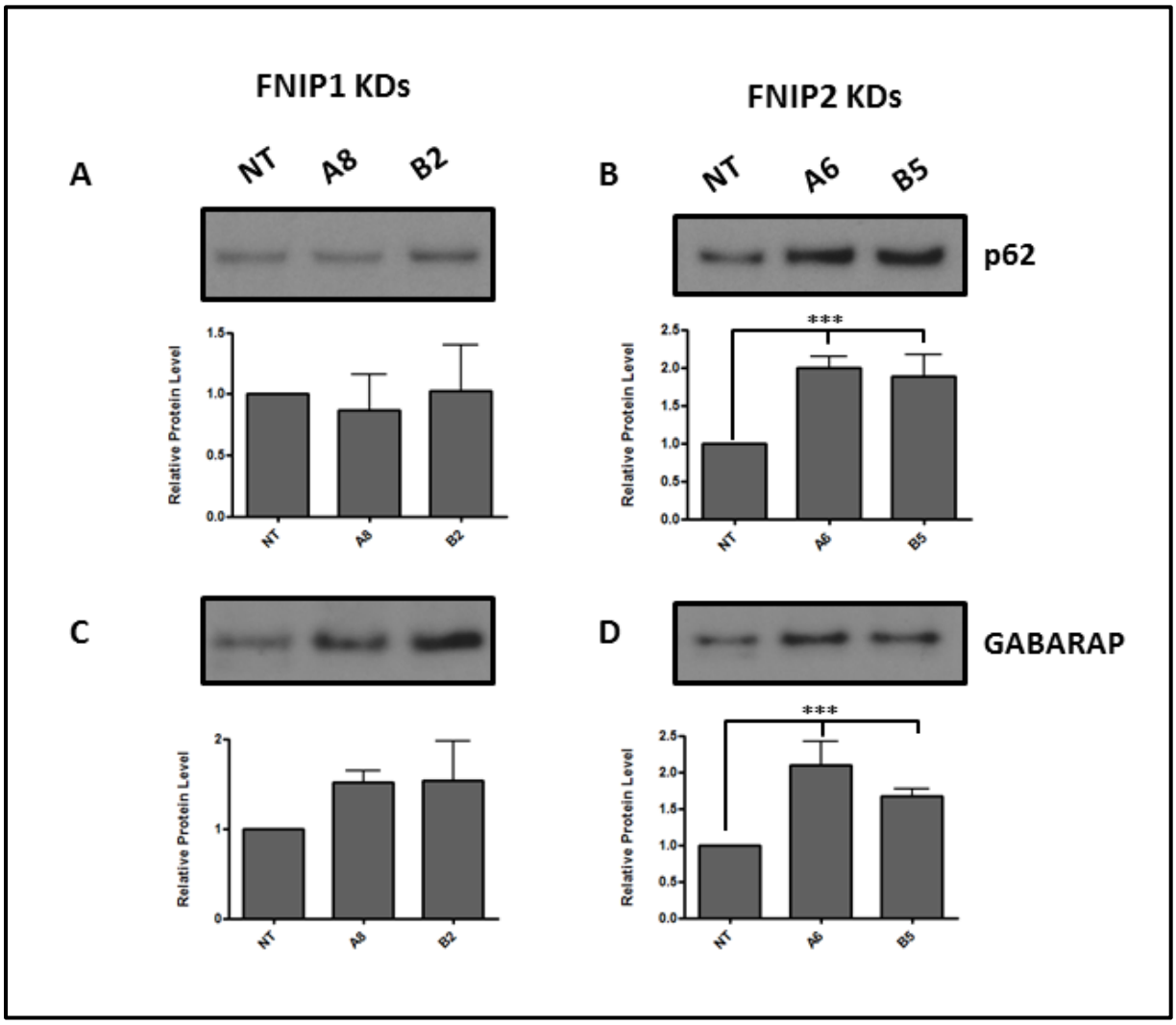

Figure 5.8 *FNIP2* knockdown causes autophagy defects similar to FLCN knockdown: Both *FNIP1* knockdown HK2 clones (A8 and B2) and *FNIP2* (clones A6 and B5) were assessed for (**A-B**) p62 (SQSTM1) and (**C-D**) GABARAP, expression, respectively. Non-target shRNA expressing HK2 cells were used as a control. Densitometry was carried out to determine relative protein levels between samples and is graphed. N = 3, * $P < 0.05$, *** $P < 0.001$.

5.3.7 FNIP knockdown alters expression of selected autophagy proteins

To find out if the differences seen in protein levels within *FNIP* knockdown cell lines were as a result of transcriptional changes, gene expression levels were examined by measuring mRNA levels in these cell lines. Although FNIP1 protein levels were significantly higher in FNIP2 deficient cells, *FNIP1* gene expression was not significantly different compared to control HK2 cells (Figure 5.9A). In contrast, *FNIP2* mRNA expression was shown to be significantly higher in FNIP1 deficient cells (Figure 5.9B). In line with protein level analysis of FLCN in *FNIP* knockdown cell lines, *FLCN* gene expression was shown to be significantly higher in FNIP2 deficient cells but not in FNIP1 deficient cells (Figure 5.9C). *GABARAP* gene expression also mirrored the protein levels, where the expression level was significantly higher in FNIP2 deficient cells but no significant change was observed in FNIP1 deficient cells (Figure 5.9D).

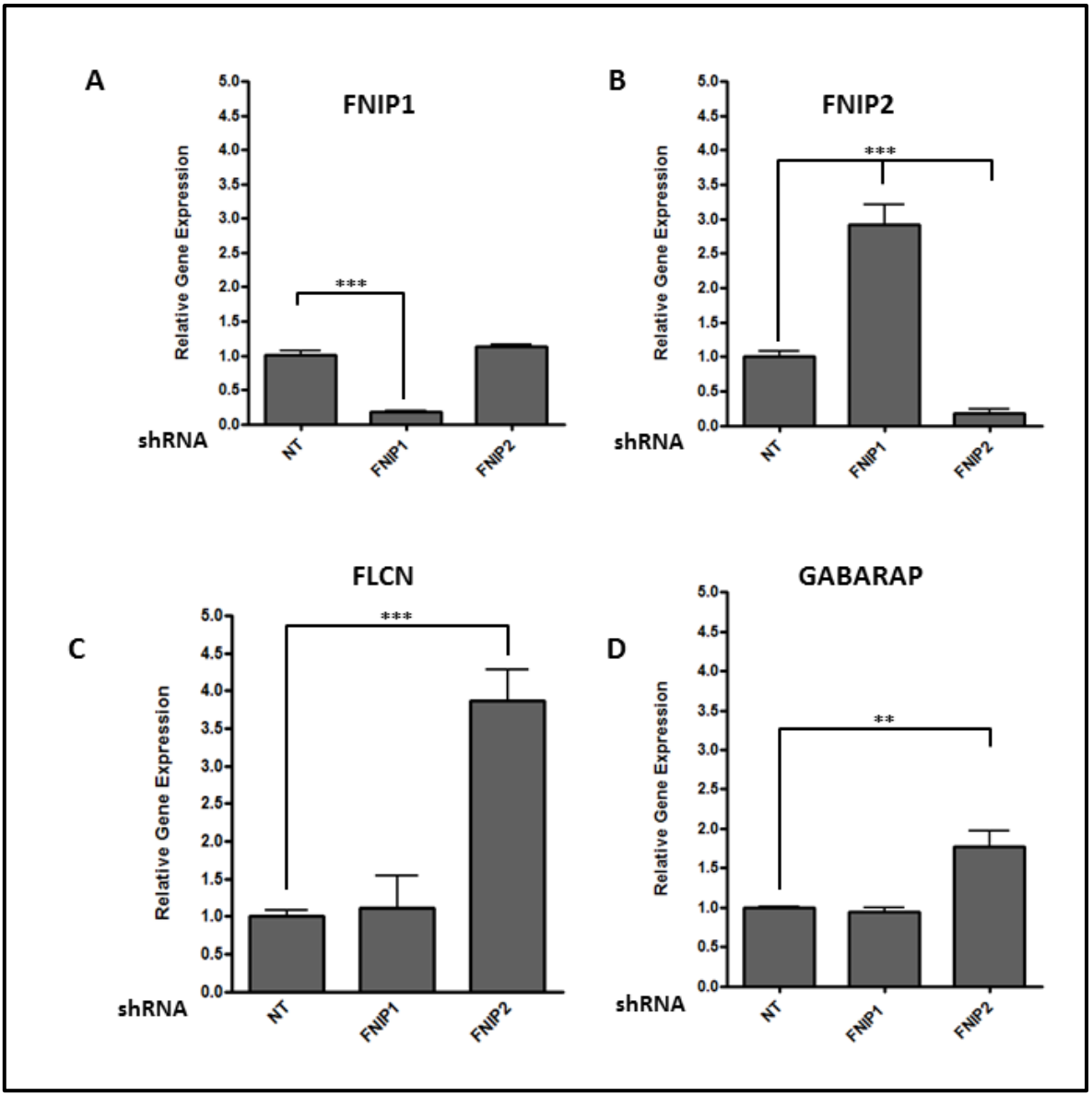

<u>Figure 5.9 Gene expression levels on the FNIP knockdowns</u>: mRNA expression levels of (**A**) *FNIP1*, (**B**) *FNIP2*, (**C**) *FLCN* and (**D**) *GABARAP* were assessed in both a *FNIP1* (HK2 *FNIP1* shRNA clone A8) and *FNIP2* (HK2 *FNIP2* shRNA clone B5) with non-target shRNA HK2 cells used as a control. N = 3, * $P < 0.05$, ** $P < 0.01$, *** $P < 0.001$

5.3.8 GST purification of FLCN, FNIP1 and FNIP2

Very little is known regarding protein interactions of FLCN, FNIP1 and FNIP2. Therefore, to study protein associations with FLCN/FNIPs in an unbiased manner, mass spectrometry was performed on samples enriched for FLCN, FNIP1 and FNIP2. GST-tagged FLCN, GST-tagged FNIP1, and GST-tagged FNIP2 were over-expressed in HEK293 cells. The cells were harvested 48 h post transfection. FLCN, FNIP1 and FNIP2 were purified using Glutathione Sepharose beads and then eluted using free glutathione. The eluent was then run on a 4-12% SDS-PAGE gel. Each lane was cut into 6 fractions as shown in Figure 5.10. and these fractions were subjected to mass spectrometry (in collaboration with Dr Bryan Balliff (University of Vermount)). A list of protein interactors which had at least one unique peptide hit for each protein is shown in Table 5.1 (FLCN interactors shown in this table are combined results of two independent studies). As it can be observed in Figure 5.10, FNIP1 is not over-expressed as well as FNIP2 or FLCN, hence not as many strong interactions could be detected. Some of the more prominent and more interesting interactors identified are as follows:

Nuclear proteins: Component of the Nuclear Pore Complex interacting with FLCN such as NUP155, NUP205, NUP35, NUP188 that are part of the adaptor nucleoporin group, NUP160, NUP133 that are part of the coat, NUP54 that is part of the channel, NUP153, NUP50 and TPR that are parts of the nuclear basket, RAE1 and RanBP2 that are parts of cytoplasmic filaments.

In addition, other nuclear related proteins that are part of the nuclear import/export machinery were also found to interact with FLCN: two exportin proteins, XPO1 and XPO5, two importin proteins, IPO5 and IPO7, and some Histones; HIST1H1C, HIST1H4J, HIST2H2BE.

Mitochondrial proteins: a few members of the mitochondrial membrane ATP synthase family such as ATP5O, ATP5A1, ATP5B and ATP5C1 were found to interact with FLCN and ATP5F1 co-immunoprecipitated with FNIP2. ATXN10 interacts with FLCN, which may play role in activation of mitogen-activated protein kinase cascade. It has also been hypothesised that ATXN10 is involved in maintenance of the intracellular glycosylation level and homeostasis.

A range of translation factors and RNA related proteins: a number of Eukaryotic Initiation Factors including, EIF4G1, EIF4G1, EIF4G3, EIF4G3, EIF4E and EIF4E2 all interacting with FLCN and EIF4ENIF1 that interacts with FNIP2. Eukaryotic elongation factors; EEF1G and EEF1A2 were both found to interact with FLCN. SERPINE1 mRNA Binding Protein 1 (SERBP1) also interacting with FLCN.

Ubiquitin related proteins: Ubiquitin-activating enzyme E1, UBA1, interacting with FLCN. Ubiquitin specific peptidase 9, X-linked, USP9X, interacting with FLCN. UBC; RPS27A; UBB interacting with both FLCN and FNIP2.

BAG proteins: BAG2 interacting with both FLCN and FNIP2, BAG4 and BAG5 interacting with FLCN. BAG proteins are highly conserved chaperone regulating proteins.

A cilia related protein interacting both with FLCN and FNIP1: KIAA1751 (CFAP74), (Cilia and Flagella Associated Protein 74) which is part of the central apparatus of the cilium axoneme.

Rho GTPase Activating Proteins (ARHGAP): ARHGAP5 interacting with FLCN and ARHGAP15 interacting with FNIP2. They convert Rho GTPases to inactive GDP-bound state.

Tyrosine 3-Monooxygenase/Tryptophan 5-Monooxygenase Activation Protein, Theta (YWHAQ): YWHAQ interacts with both FLCN and FNIP2. It belongs to a big family of activation proteins that mediates signal transduction by binding phospho-serine/phospho-threonine proteins and is involved in cell proliferation, cell survival, apoptosis and stress signalling pathways.

Apoptosis-Related Cysteine Protease, CASP7: interacting with FNIP2. CASP7 is an Effector caspase that interacts with and cleaves downstream substrates.

Cytoskeleton Associated Protein 5, CKAP5: interacting with FLCN. CKAP5 is a spindle protein that is involved in mitosis.

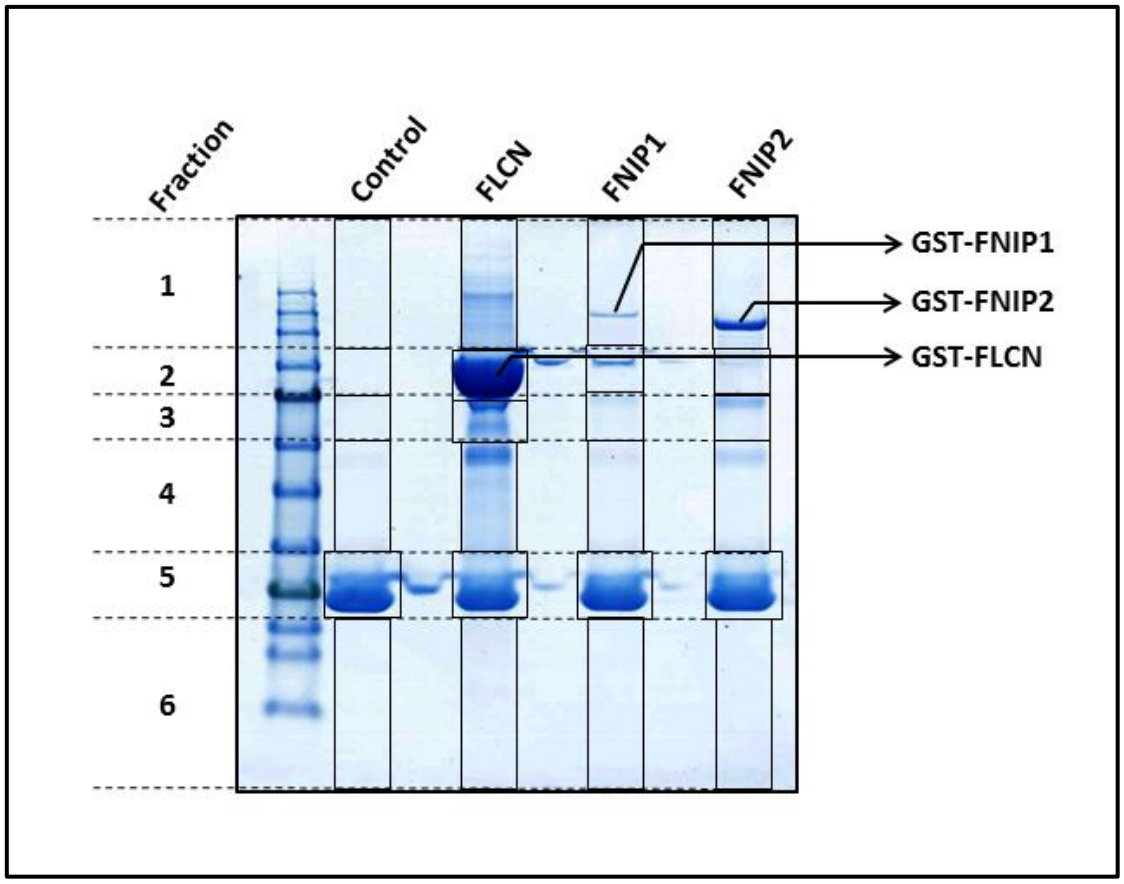

Figure 5.10 GST purification of FLCN, FNIP1 and FNIP2: HEK293 cells expressing either GST-FLCN, GST-FNIP1 or GST-FNIP2, with non-transfected cells as a control, were subjected to GST purification after lysis, with Glutathione-Sepharose. GST-tagged proteins and protein interactors were eluted with free Glutathione and resolved on SDS-PAGE and stained with Coomassie Brilliant Blue. Gel lanes were excised in strips (fraction 1-6), and sent to our collaborators (Dr. Brian Ballif, University of Vermont) for protein ID by mass-spec.

Table 5.1 protein interactions of FLCN, FNIP1 and FNIP2 detected by mass spectrometry.

FLCN			FNIP1	FNIP2		
ANKRD44	HSPA1A;HSPA1B	RAE1	ACAP2	AEBP2	KCNQ3	SUZ12
ATP5O	HSPA1L	RANBP2	ARAP2	AHNAK2	LMOD2	SYNE1
ATXN10	HSPA7	RBM39	CDC20B	ARHGAP15	MAP3K7	THOC2
BAG2	HSPA8	RBM39	DNAH7	ATP5F1	MCM4	TIAM2
CAD	KHDRBS1	RNF135	DST	BAG2	MYO10	TRAF6
CKAP5	KIF20B	RPL10L	FLCN	BRD3	NAV3	TREH
DCD	KPNA1	RPL26L1	FNIP2	C12orf66	NCOR2	TTN
DIAPH3	MYH9	RPL23	IL33	C19orf44	NEFM	UBC;RPS27A;UBB
DSP	NUP155	RPS3	KIAA1751	CASP7	PIGM	URB1
DYNC1H1	NUP188	SERBP1	MYH9	CCAR1	PIP5K1A	YWHAQ
FASN	NUP50	TPR	PPFIBP1	CCDC88C	PRDX3	ZFP57
FLNA	NUP160	TRIM29	PRDX3	DNAH7	RASSF8	ZNF468
FNIP1	NUP133	USP9X	RPS6KA4	DNAH8	RB1	
FNIP2	NUP205	WDR31	SHC4	EHBP1L1	RGS18	
GCN1L1	NUP153	XPO1	SLC38A4	EIF4ENIF1	RPL4	
HIST1H1C	NUP54	XPO5	SPTBN5	FLCN	RPL6	
HIST1H4J	NUP35	YWHAQ		FNIP1	RUFY3	
HIST2H2BE	OTUD3	ZNF638		HFM1	SAMD8	
HNRNPK	PPP2R1A			HNRNPUL2	SP4	
HNRNPUL2	PRDX1			HSPA1A;HSPA1B	STXBP5L	
HSD17B10	PRDX2			HSPA8	SUDS3	

5.3.9 NUP155 IP co-purifies FLCN, and more robustly in the presence of FNIP2

Unfortunately there was not enough time or resources to follow up all the potential protein interactions identified in the mass spectrometry analysis.

Several members of the nuclear pore complex were shown to interact with FLCN, suggesting a role for FLCN in nuclear transport. NUP155 was one of the most prominent interacting proteins with FLCN (24 total peptide and 11 unique hits); hence it was selected to validate the interactions shown in mass spectrometry results, and to study the role of FLCN in the nuclear pore complex further.

The nuclear pore complex is the only mode of transport for molecules over 40 kDa in and out of the nucleus. It is composed of about 30 different proteins that are referred to as nucleoporins. The structure of the nuclear pore complex consists of a central pore, cytoplasmic filaments and nuclear basket (Hoelz et al. 2011). Nucleoporins are classified into 6 different categories: integral membrane nucleoporins (POMs) that integrate the nuclear envelope membrane, coat nucleoporins, adaptor nucleoporins, channel nucleoporins, nuclear basket nucleoporins, and cytoplasmic filament nucleoporins (Figure 5.11).

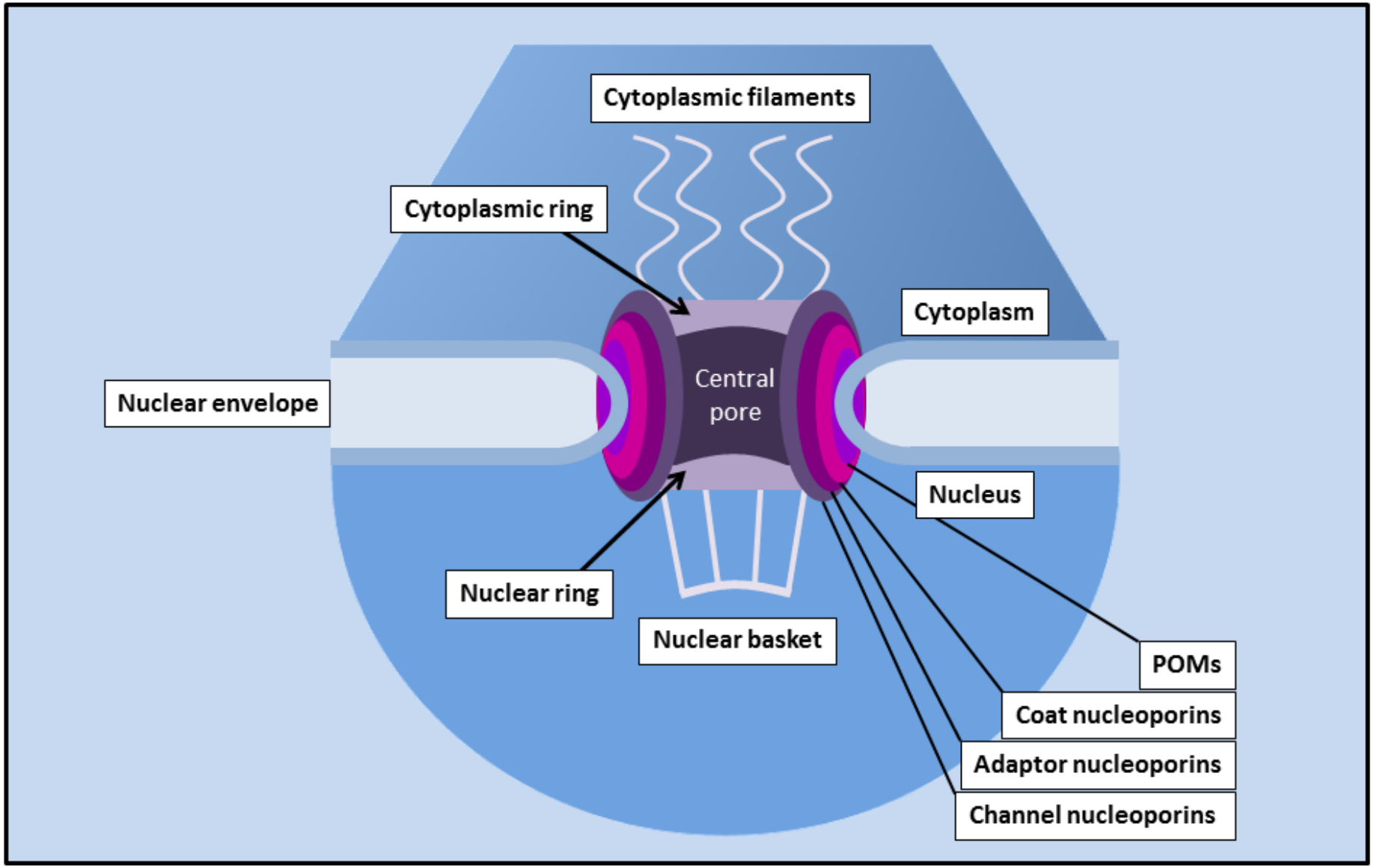

Figure 5.11 Nuclear Pore Complex: A diagram of the nuclear pore complex spanning the nuclear envelope.

An experiment was set to study the interaction of NUP155 with wild type FLCN and patient derived mutants of FLCN. Over-expressed Flag-tagged NUP155 co-purifies with HA-tagged FLCN both wild type and patient derived mutants, however the interaction is stronger with the patient mutants that have a truncated C-terminus (Figure 5.12A). Since the positive effect of FNIP2 expression upon FLCN interaction has been observed in quite a few of the experiments so far, FLCN/NUP155 interaction was also tested in the presence of over-expressed Myc-tagged FNIP2. FLCN/NUP155 interaction proved to be more robust in the presence of FNIP2, which was increased further with the patient mutants with a truncated C-terminus (Figure 5.12B).

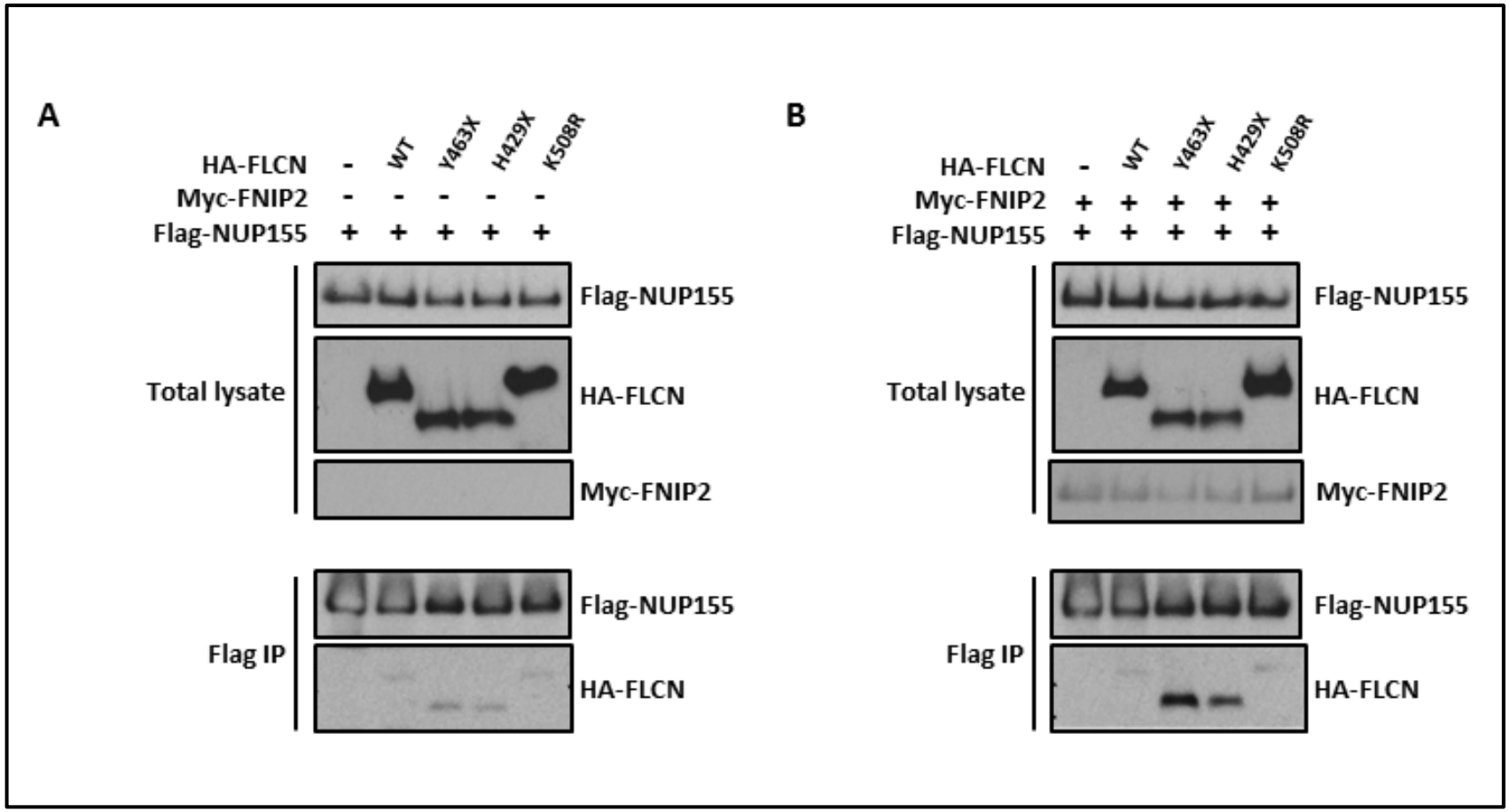

Figure 5.12 NUP155 IP co-purifies FLCN more robustly in the presence of FNIP2: Flag-NUP155 was co-expressed with either wild-type FLCN, or FLCN mutant (Y463X, H429X, K508R) (**A**) without Myc-FNIP2 or (**B**) in the presence of Myc-FNIP2 in HEK293 cells. Anti-Flag antibody was used to immunoprecipitate Flag-NUP155 and associated HA-FLCN (and Myc-FNIP2, where appropriate) was determined by western blot analysis. Total protein expression of NUP155, FLCN and FNIP2 is shown.

5.3.10 FLCN IP also co-purifies NUP155, and more robustly in the presence of FNIP2

To confirm the interaction between FLCN and NUP155, a reciprocal experiment was setup where over-expressed HA-tagged FLCN was immunoprecipitated. As it is observed in Figure 5.13A the FLCN IP co-purified Flag-tagged NUP155. Similar to the previous experiment this interaction is stronger with truncated patient mutants and is more robust in the presence of FNIP2 (Figure 5.13 A,B).

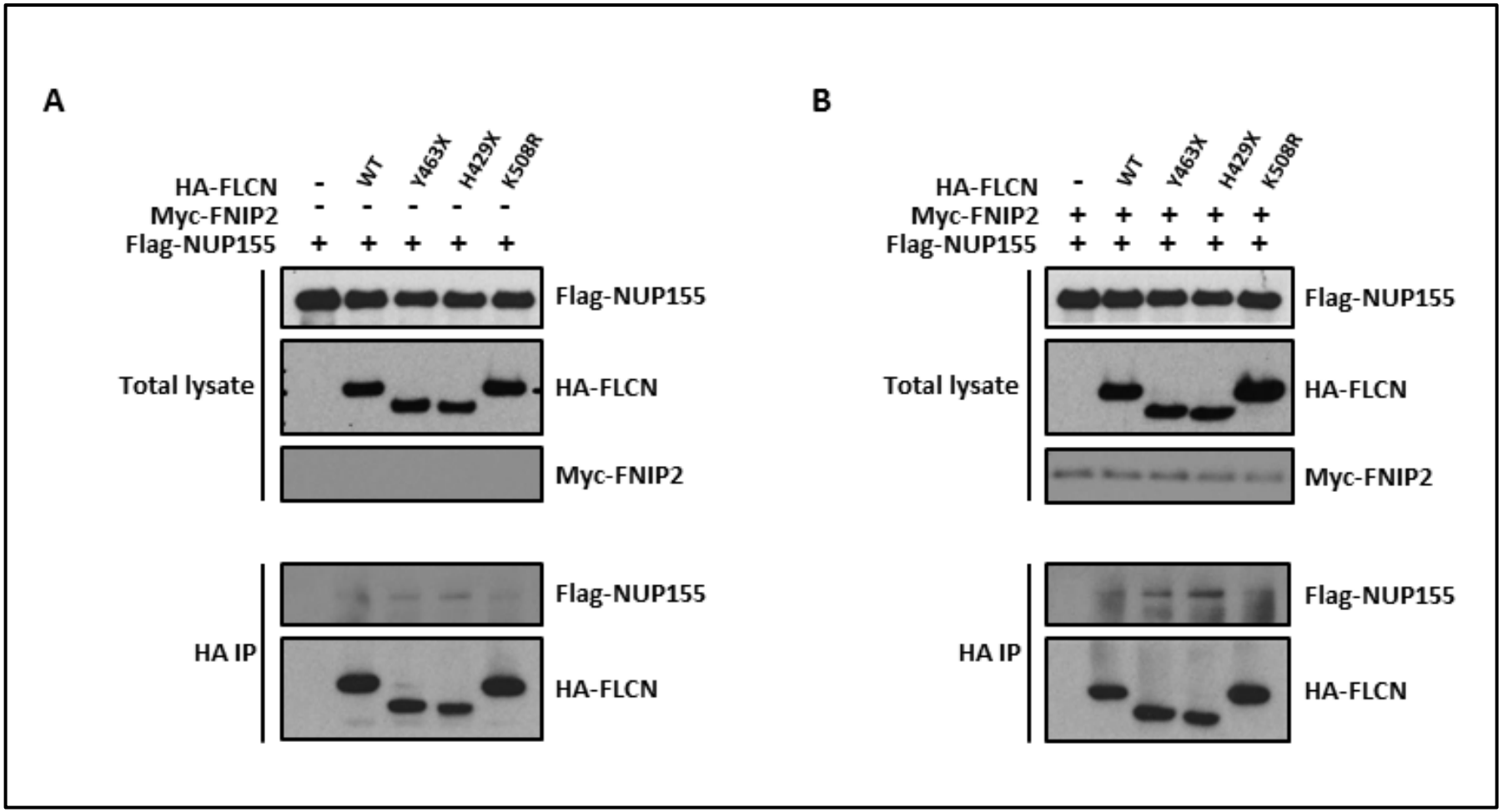

Figure 5.13 FLCN IP also co-purifies NUP155, and more robustly in the presence of FNIP2: Flag-NUP155 was co-expressed with either wild-type FLCN, or FLCN mutant (Y463X, H429X, K508R) (**A**) without Myc-FNIP2 or (**B**) in the presence of Myc-FNIP2 in HEK293 cells. Anti-HA antibody was used to immunoprecipitate HA-FLCN and associated Flag-NUP155 (and Myc-FNIP2, where appropriate) was determined by western blot analysis. Total protein expression of NUP155, FLCN and FNIP2 is shown.

According to the mass spectrometry data (revealing the interactions), co-IPs and immunofluorescence (IF) co-localisation data by our collaborators (data not shown), figure 5.14 shows the suggested localisation of FLCN within the nuclear pore complex.

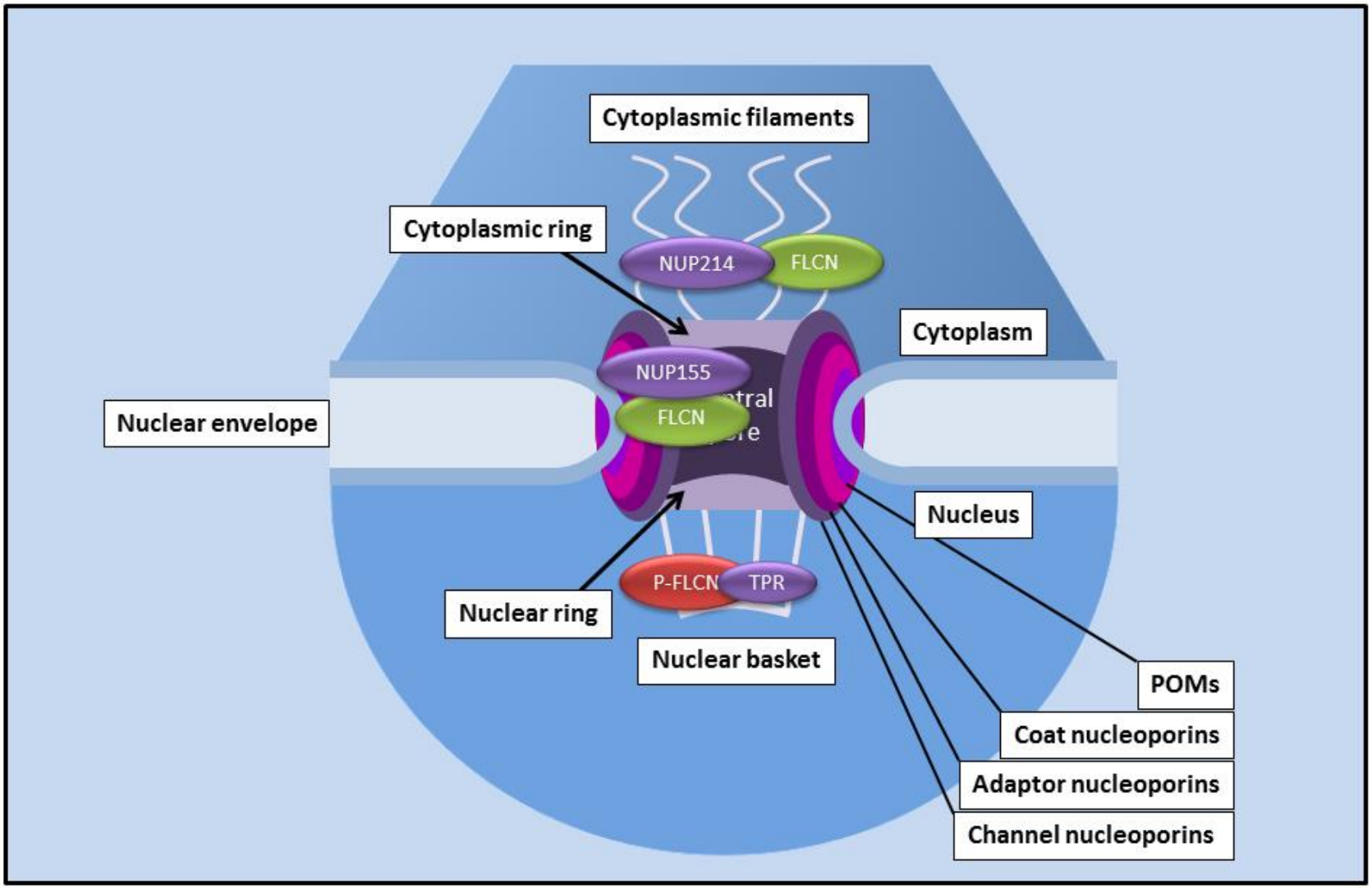

Figure 5.14 Nuclear Pore Complex and FLCN: A diagram depicting a model where FLCN is associated with integral components of the nuclear pore complex.

5.3.11 HIF1α protein level is significantly higher in old FLCN knockdown cells and new FNIP2 knockdown cells

In the context of renal cell carcinoma, which is metabolically driven through Hypoxia Inducible Factor (HIF) activation, it is possible that loss of FLCN might lead to indirect dysregulation of HIF through many of these new interactions. As BHD patients acquire RCC late in life (The average age of onset is 50), dysregulation of HIF may take time to occur. To test this hypothesis, *FLCN* knockdown HK2 cells were grown in continuous culture for a year (>155 passage number) and compared to younger cells after selection (<10 passage number) for levels of HIF protein. It is clearly observed that HIF-1α level is significantly higher in the old *FLCN* knockdown cells compared to the control HK2 cells, whereas there is no significant difference between new *FLCN* knockdown cells and new control HK2 cells (Figure 5.15). Interestingly *FNIP2* knockdown cells demonstrate the same significant increase in HIF-1α protein level observed in old *FLCN* knockdown cells (Figure 5.15).

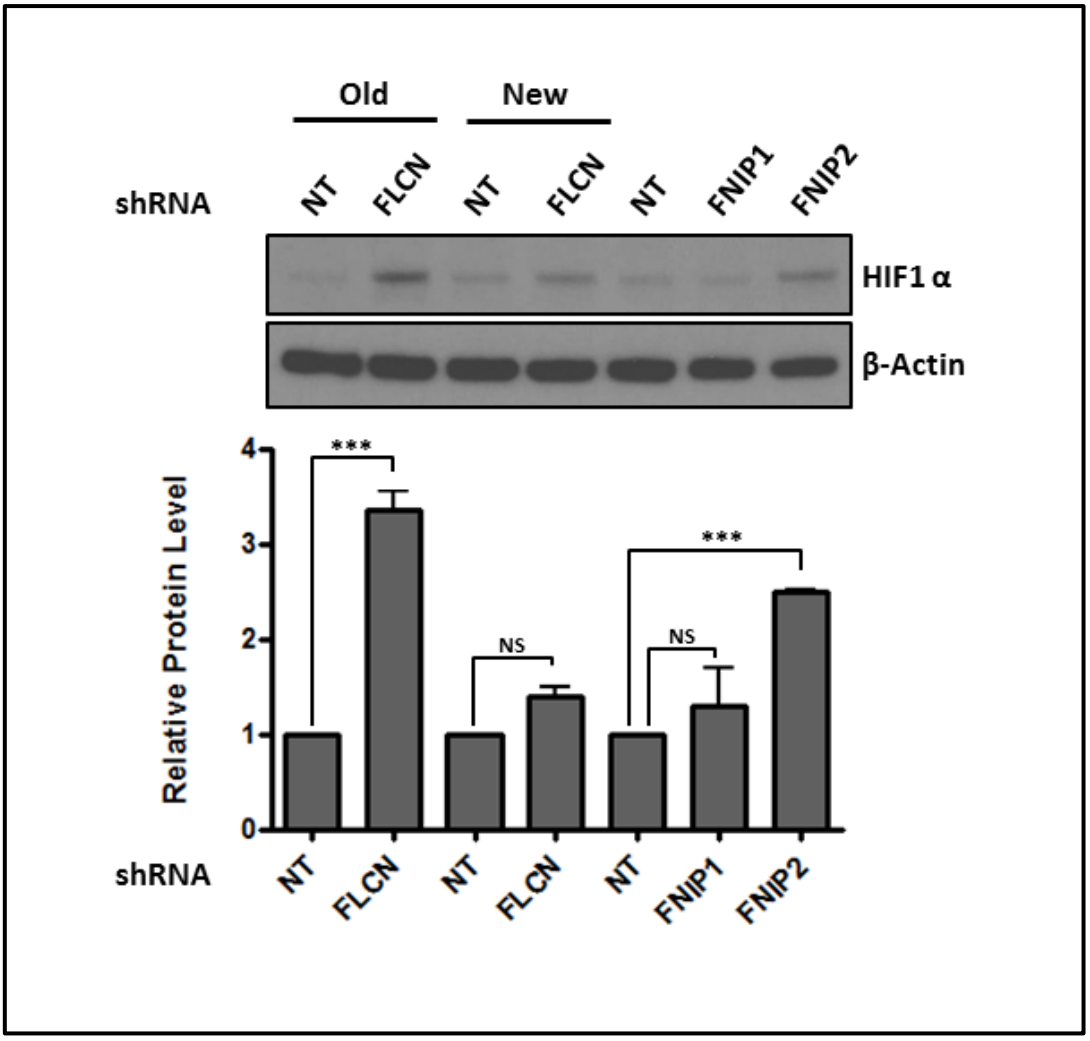

Figure 5.15 HIF1α protein level is significantly higher in old FLCN knockdown cells and new FNIP2 knockdown cells: Old *FLCN* knockdown and control HK2 (>155 passage number) were assessed for HIF-1α and were compared to new *FLCN* knockdown and control HK2 (<10 passage number). HIF-1α was also assessed in newly made *FNIP1* and *FNIP2* knockdown cells. Densitometry was carried out to determine relative protein levels between samples and is graphed. N = 3, *** P < 0.001.

5.4 Discussion

Upon generating the *FNIP* knockdown HK2 cells, it was observed that the cells with *FNIP1* knockdown underwent drastic morphological changes at the early stage, which then later normalised. This observation indicates that the cells go through an initial crisis phase after losing *FNIP1*; however the loss of *FNIP1* seems to be compensated for after a few months. Accumulation of fatty droplets during this shock period places *FNIP1* in metabolic pathways, specifically fatty acid oxidation and/or lipogenesis. However it has to be said that due to the slow growth and small number of the cells present at this crisis stage, they could not be tested to confirm the presence of fatty droplets by other means such as Oil Red O dye. Furthermore, it is possible that the cells went into the crisis stage as a result of other technical difficulties (such as clonal selection, not having the optimal proximity to each other *etc*.), not just lack of *FNIP1*. Although the *FNIP2* knockdown cells did not demonstrate such extreme morphological changes, the growth was slowed and some minor morphological changes were also observed. The presence of spiky cytoplasmic projections observed in *FNIP2* knockdown cells could indicate a role for *FNIP2* in cytokinesis. Remarkably in line with these observations, in *FNIP1* and *FNIP2* knockdown mice generated by Hasumi *et.al.,* there was no pathogenic phenotype observed with *FNIP2* knockdown, whereas the *FNIP1* mouse exhibits a similar phenotype to the FLCN mouse model (Hasumi et al. 2015).

Interestingly, protein levels of FNIP1 and FLCN were significantly higher in FNIP2 knockdown cell lines, which could be as a result of compensatory mechanisms in the cells that try to overcome the loss of FNIP2. Increased protein expression in the cell could be due to 3 possibilities; increased gene transcription, increased protein translation or increased protein stability. To determine the reason

for this increase in protein levels, mRNA levels of each gene were also measured in the knockdown cell lines. In contrast to higher levels of FNIP1 protein in *FNIP2* knockdown cells, gene expression of *FNIP1* was not significantly higher in FNIP2 deficient cells. This rules out the possibility of increased transcription as the cause of elevated protein levels. Therefore, FNIP1 degradation could be reduced in the absence of FNIP2, or there may be an increase in *FNIP1* mRNA translation due to FNIP2 loss. Conversely, *FLCN* gene expression, similar to its protein level, was significantly higher in *FNIP2* knockdown cells. Hence increased transcription is driving a higher protein level in this case. Consequently, it could be concluded that FNIP2 is involved in the regulation of *FLCN* transcription and is also possibly involved in FNIP1 translation. Although protein levels of FNIP2 in *FNIP* knockdown cell lines could not be measured, gene expression of *FNIP2* exhibited a significant increase in FNIP1-deficient cells. Since lack of FNIP1 results in increased *FNIP2* transcription, it could be possible that FNIP1 plays a role in regulating *FNIP2* transcription in a negative feedback manner where lack of FNIP1 results in higher *FNIP2* transcription. Although more research into the FLCN/FNIP complex is needed, it can be speculated that FLCN/FNIP is a tightly self-regulated complex.

FNIP1 and FNIP2 are homologous proteins with 49% identity and 74% similarity, indicating that they both likely share some functions within the cell, while each may also have additional and specific functions (Hasumi et al. 2008). Both FNIP1 and FNIP2 are highly conserved proteins that contain a LIR motif which connects them to autophagy. Generally a classic LIR motif has the protein sequence of (W/F/Y)XX(L/I/V). The LIR motif sequence on FNIP2 is FEYI which is a classic F-type LIR motif that evolutionarily has a higher affinity for the GABARAP subfamily of Atg8s (Alemu et al. 2012). However FNIP1 only has a partial LIR motif with the

sequence of LEFI. This could explain the FNIP2 requirement for GABARAP/FLCN binding, whilst FNIP1 has less impact (shown in Chapter 3). Several attempts were made to insert FNIP2's LIR motif into FNIP1 by site-directed mutagenesis, to check if it would enhance FLCN's binding to GABARAP in the same manner as FNIP2. Unfortunately, creating the mutant was not successful which is probably due to the number of base changes that had to be made at once.

Similarly to *FLCN* gene expression levels, expression of both *FNIP1* and *FNIP2* were significantly increased upon starvation in normal HK2 cells, further suggesting a role for the FNIP proteins in autophagy. *FNIP2* mRNA level displayed a drastic increase (up to 9 fold), when the cells were depleted of nutrients; which together with the classic F-type LIR motif suggests a more prominent role for FNIP2 in autophagy. Of interest, when the knockdown cell lines were studied for autophagy markers, GABARAP and p62, *FNIP2* knockdown cells demonstrated a significant increase in both p62 and GABARAP protein levels, suggesting an impaired autophagy response in *FNIP2* knockdown cells. In this context *FNIP2* knockdown cells mimic the autophagy defects observed in *FLCN* knockdown cells. However these results on their own do not confirm autophagy defects in *FNIP2* knockdown cells and further experiments such as autophagic flux and LC3 blots are needed to conclusively place FNIP2 in autophagy, which due to time restrictions could not be done in this study. *FNIP1* knockdown cell lines did not show any significant changes in GABARAP or p62 protein levels, although GABARAP protein levels exhibited an increasing trend. Inconclusively, p62 protein levels in the *FNIP1* knockdown cells were either higher or lower compared to control HK2 cells in different experimental repeats, and did not demonstrate any consistency.

Since FNIP1 and FNIP2 have a high degree of sequence homology, especially at the N-terminal and the last 158 C-terminal residues, it is speculated they may have similar cellular functions, which suggests that they can compensate for each other with these overlapping functions. Interestingly, Hasumi *et.al.* showed that only a kidney specific double knockout of *FNIP1* and *FNIP2* led to production of enlarged polycystic kidneys (Hasumi et al. 2015). Therefore, the next logical step for this study would be to produce a double knockdown of *FNIP1* and *FNIP2* to further analyse the effect of these two proteins in a human cell.

In general, most of the proteins that FLCN, FNIP1 and FNIP2 interact with are involved in major physiological cellular processes, including apoptosis, stress response, cell cycle/ cell differentiation and in some cases tumourigenesis.

NUP155 is one of the nucleoporins located in the central pore of the nuclear pore complex that interacts with FLCN. It was observed that the interaction of FLCN/NUP155 was stronger in the disease setting, *i.e.,* presence of patient-derived FLCN mutants. The same result was also observed for the reciprocal experiment. Furthermore, in both experiments, the presence of FNIP2 made the interaction more robust. It could be speculated that the presence of the FLCN C-terminus is essential for dissociation of NUP155 from FLCN and smooth transport of FLCN in and out of nucleus.

Given the multiple interactions that FLCN and the FNIPs are involved in, it would appear that FLCN might have a general housekeeping role in a cell, which when lost may lead to cancer. Also taking into account that the onset of RCC in BHD syndrome is >50 years of age, the effects of FLCN loss takes time to occur. One of the pathways that FLCN is involved in which might be altered over time, probably

due to long term production of ROS, is the HIF signalling pathway. To mimic the long term effects of FLCN loss in BHD patients, *FLCN* knockdown cells were grown in continuous culture for a year, resulting in increased HIF-1α protein levels compared with the control HK2 cells that were grown for the same length of time. Further investigation is required to determine whether this is a direct result of FLCN loss or due to sporadic mutations occurring due to long term culturing of these cells.

6 Chapter 6: Final discussion

The aim of this research was to better characterise the function of FLCN and its associated proteins, FNIP1 and FNIP2, in cellular processes such as autophagy and their dysregulation in genetic diseases such as BHD.

6.1 FLCN is a positive driver of autophagy

During the course of this study it was shown that FLCN interacts with and is a new downstream substrate of ULK1. FLCN also interacts with GABARAP and several Rab small G proteins linked to autophagy and these interactions were shown to be modulated via ULK1 phosphorylation of FLCN. Additionally it was demonstrated that FLCN has a positive role in the regulation of autophagy where a FLCN mutant lacking the ULK1-mediated C-terminal phosphorylation sites could not restore autophagy in FLCN-deficient cells whereas the WT-FLCN could rescue autophagy. Furthermore, p62 expression was shown to be increased in renal tumours from BHD patients compared to the normal renal tissue. However, FLCN's role in autophagy does not seem to be straight forward as other studies have observed increased autophagy in FLCN-deficient cells. Liu *et al.* observed increased autophagy in *dBHD*$^{-/-}$ larvae with growth defects; however treating the *Drosophila* with the autophagy inhibitor, 3-Methyladenine, did not restore the normal growth whereas it could be rescued by nutrients (leucine in particular) (Liu et al. 2013). FLCN similar to VHL was shown to suppress LC3B-mediated autophagy and stimulate LC3C autophagic activity. *FLCN* knockdown in VHL-null cells caused considerable reduction in the accumulation of LC3C with an increase in LC3B (Bastola et al. 2013). Furthermore, Zhang *et al.* found FLCN-deficient UOK257 and ACHN-5968 cells were more sensitive to treatment with paclitaxel (a

chemotherapeutic drug that induces apoptosis) due to their enhanced autophagy compared to *FLCN* expressing cells (Zhang et al. 2013). As discussed earlier in chapter one, all the pathways that FLCN has been shown to be involved in seem to be highly cell type dependent and varied between experimental procedures.

Previously, FLCN was linked to autophagy via GABARAP interaction (Behrends et al. 2010). In this study it was shown that the FLCN/ GABARAP binding was enhanced in the presence of FNIP2 (and to a lesser extent FNIP1), which further indicates that FLCN in a complex with FNIP1 and FNIP2 functions to regulate autophagy. Weidberg *et al*. demonstrated that GABARAP subfamily members function downstream of autophagosome membrane elongation and maturation (Weidberg et al. 2010). This could also suggest the involvement of FLCN and FNIPs in maturation of autophagosomes.

It was observed that FLCN interactions were markedly influenced upon direct ULK1 phosphorylation within the DENN domain of FLCN. Therefore ULK1 likely requires FLCN for efficient modulation of the autophagy machinery. The finding that FLCN could interact with a multitude of Rab small G proteins already involved in autophagy and trafficking events could suggest that FLCN's main role in autophagy is to coordinate autophagic flux and vesicular trafficking through Rabs. Of interest, LST7, the yeast homologue of FLCN, has been shown to be essential for transportation of the amino acid permease, Gap1p, from the Golgi to the cell surface (Roberg et al. 1997). This role of trafficking between cellular compartments provides an evolutionary link to the proposed function of FLCN as an integral part of the autophagy machinery.

Guanine nucleotide exchange factors (GEFs) are regulators of small G proteins that mediate their activation. In higher eukaryotes, differentially expressed normal versus neoplastic (DENN) domain proteins are known to have Rab GEF activity and require a specific mechanism to target them to their site of action (Barr & Lambright 2010). The crystal structure of the C-terminal domain of FLCN revealed that FLCN contains a DENN domain suggesting that FLCN could have GEF activity towards Rabs (Nookala et al. 2012). However investigation of the GEF activity of FLCN in this study towards the Rabs involved in autophagy proved to be inconclusive. Enhanced binding to the non-guanine nucleotide binding mutants of Rabs is expected to be observed from a GEF, however, these Rab mutants bound sometimes less favourably and sometimes more favourably to FLCN. It could be hypothesised that FLCN, associated with different FNIP1 and FNIP2 proteins (as multimers), would act as a small G protein scaffold to control the direction of autophagosome/lysosome travel through appropriate activation of Rabs. In support of this, the finding that FNIP1 and FNIP2 also have DENN domains (Zhang et al. 2012) would imply that these larger FLCN/FNIP complexes are multifunctional small G protein regulators. Furthermore, Tsun *et al.* found FLCN to be a GAP for the RagC/D GTPases (Tsun et al. 2013). FLCN could be considered as an atypical GAP/GEF protein, where the GEF domain is C-terminal and the GAP domain could be postulated to be found within the N-terminus. With the addition of the DENN domains in both FNIP1 and FNIP2, this might explain why FLCN/FNIP complexes can bind to a range of different small G proteins. This dual function of FLCN to be able to bind to the same small G protein irrespective of its GTP- or GDP-bound status is what makes it atypical. This dual function would explain why FLCN was able to bind the Rab small G proteins in both GTP- and GDP-bound states.

6.2 Role of FNIP1 in familial multiple discoid fibromas (FMDF)

During the course of this study, a new patient disease incurring mutations to FNIP1 was discovered (FMDF), which provided a useful genetic tool to further characterise FNIP1's interactions within the FLCN/FNIP complex. This is the first human genetic disease caused by FLCN interacting proteins, however the mechanism of its pathogenesis is not yet fully understood. The fact that FMDF patients only display skin abnormalities suggests that FNIP1 plays a critical role in the skin. Takagi *et al.* and Hasumi *et al.* demonstrated that FNIP2 is expressed at higher levels than FNIP1 in lung and kidney tissues (Takagi et al. 2008)(Hasumi et al. 2008) which could be the reason why loss of FNIP1 function does not cause any phenotype abnormalities in these organs. It is also possible that FNIP1 Val663fsX is expressed at higher levels in the skin and its impaired FLCN binding is causing the skin phenotype in FMDF patients. However, it was shown that FNIP1 Val663fsX retains the ability to bind FNIP2 through which the altered protein could maintain partial functionality. Alternatively, lack of a systemic phenotype could be explained by compensation through FNIP2. Since the complete deletion of *FNIP1* gene was shown not to cause any of the FMDF symptoms, haplo-insufficienciency could be ruled out as the pathogenesis mechanism. Furthermore, lack of cancer within the FMDF patient population is good genetic evidence that loss of *FNIP1* is not sufficient in itself to cause cancer.

6.3 Characterising FNIP1 and FNIP2

To better characterise FLCN interacting partners, FNIP1 and FNIP2, HK2 stable knockdown cells were generated and studied. At the early stages of the *FNIP1* knockdown the cells displayed extreme morphological changes which were normalised later. These results indicate that after the initial shock of *FNIP1* loss the cells can subsequently compensate. However, lack of *FNIP2* did not cause such initial crisis in the cell, although some minor morphological changes could still be observed. Of interest, Hasumi *et al.* reported that the *FNIP1* mouse model could produce kidney cysts whereas a *FNIP2* mouse model did not produce any pathogenic phenotype (Hasumi et al. 2015).

FNIP2 knockdown caused a significant increase in FNIP1 and FLCN protein levels. After mRNA levels were measured, it was revealed that in contrast to an increased protein level, *FNIP1* gene expression was not significantly increased in *FNIP2* knockdown cells. This data suggests that FNIP2 deficiency could result in increased mRNA translation, or FNIP1 could become a more stable protein in the absence of FNIP2. However, FLCN mRNA level comparable to its protein level was significantly increased upon loss of FNIP2 which is suggestive of an increased transcription as the cause of this high level of protein. Hence it could be concluded that FNIP2 is involved in the regulation of FLCN transcription and it is possibly involved in FNIP1 translation or stability.

Although lack of *FNIP1* did not result in any significant changes in FLCN protein or mRNA levels, *FNIP2* gene expression showed a significant increase in FNIP1-deficient cells. Since the transcription of FNIP2 mRNA is significantly increased upon loss of *FNIP1*, FNIP1 could be regulating FNIP2's transcription in a negative feedback manner.

FNIP1 and FNIP2 are highly conserved proteins that both contain a LIR motif. The LIR consists of a short hydrophobic region with sequence of (W/F/Y)XX(L/I/V). LIR-containing proteins are known to be involved in selective autophagy (Alemu et al. 2012)(Birgisdottir et al. 2013). FNIP2's LIR motif has the sequence of FEYI, which is a classic F-type LIR motif that evolutionarily has a higher affinity for the GABARAP subfamily of Atg8s; whereas FNIP1's LIR motif is partial with the sequence of LEFI. The necessary presence of FNIP2 for the interaction of FLCN and GABARAP demonstrated in Chapter 3, could be as a result of this LIR motif.

FNIP1 and *FNIP 2* gene expression were found to be significantly increased when normal HK2 cells were starved, which further implicates the FNIP proteins in autophagy. Furthermore, in the *FNIP2* knockdown cell lines both p62 and GABARAP protein levels demonstrated a significant increase suggestive of impaired autophagy. However, no significant changes of GABARAP or p62 protein levels were observed in *FNIP1* knockdown cell lines.

FNIP1 and FNIP2 have a high degree of sequence homology with 49% identity and 74% similarity, it is likely that have some shared functions while both may also have individual functions (Hasumi et al. 2008). This shared sequence suggests that they likely compensate for each other within their overlapping functions. Hasumi *et al.* has recently demonstrated that a kidney specific *FNIP1* knockout mouse only produced small kidney cysts while a kidney specific *FNIP2* knock out mouse did not produce any pathogenic phenotype. However, when both *FNIP1* and *FNIP2* were knocked out specifically in the kidney it caused enlarged polycystic kidneys (Hasumi et al. 2015). Similarly, to further study the role of both FNIP1 and FNIP2 in human cells it would be rational to generate a double knockdown of *FNIP1* and *FNIP2*.

6.4 FLCN, FNIP1 and FNIP2 and the interacting partners

Unbiased screens for protein interactors of FLCN, FNIP1 as well as FNIP2, implicate that FLCN and its associated FNIP proteins are involved in a wide range of cellular processes.

The nuclear envelope protects and restricts access to the genetic material in the nucleus in eukaryotes. Nuclear pore complexes (NPCs) are large protein complexes within the nuclear envelope that provide a mode of transport for proteins and RNAs to and from the nucleus. NPCs consist of multiple nucleoporins (NUPs) that when fully assembled (with mass of ~125 MDa) is one of the largest protein complexes within the cell (Alber et al. 2007)(Kabachinski & Schwartz 2015). FLCN was found to interact with a number of proteins within the nuclear pore complex. NUP155 is one of the nucleoporins located on the central pore of the nuclear pore complex which was found to interact with FLCN. NUP155 was found to associate more robustly with the C-terminal truncated (BHD patient-derived mutant) form of FLCN. Furthermore, the presence of FNIP2 made this NUP155/FLCN interaction stronger. The nuclear pore is the principal gateway between the nucleus and cytoplasm that permits highly regulated protein and mRNA transport. It is possible that the stronger interaction of NUP155 with FLCN in the disease setting could compromise active transport across the nuclear pore. It could also be speculated that the C-terminal of FLCN is necessary for the dissociation of FLCN from the NUP155 and transport of FLCN in and out of nucleus.

The median age of BHD patients developing renal cell carcinoma is 50 years of age (Shuch et al. 2014). Therefore, following loss of FLCN it takes time for cancer to progress. FLCN has been shown to be involved in the HIF signalling pathway (Preston et al. 2011)(Yan et al. 2014) and long term production of ROS and

metabolic transformation could be one of the contributing factors to RCC in BHD patients. To simulate the long term effects of FLCN loss, *FLCN* knockdown HK2 cells were grown in continuous culture for a year. Western blot analysis revealed that HIF-1α protein levels were increased in *FLCN* knockdown cells compared to the control HK2 cells that were grown for the same length of time. Further investigation is required to determine whether this is a direct result of FLCN loss or due to sporadic mutations occurring due to long term culturing of these cells.

In general, FLCN and the FNIPs are involved in multiple interactions in the cell which could mean that FLCN and its interacting partners might have a more universal housekeeping role, which when lost may lead to cancer.

6.5 Future Work

The implication of FLCN in the autophagy pathway has provided a great tool to explore therapeutic targets for treating BHD patients. However autophagy can be a double edged sword in regard to cancer where impaired autophagy at the early stages can lead to cancer, while higher levels of autophagy could function as a survival mechanism. Therefore, the effect of both autophagy inhibitors and activators needs to be investigated on FLCN-deficient cell lines.

Moreover several interesting FLCN and FNIP interactors were identified by mass spectrometry, which need to be further investigated to better understand the diverse functions of FLCN, FNIP1 and FNIP2 within the cell.

To fully examine the role of FNIP1 and FNIP2 and to characterise their cellular function better, a double knockdown cell line needs to be made and investigated.

The data in this thesis, combined with recent publications showing FLCN's potential GAP/GEF activity implies that FLCN or most probably the FLCN/FNIP complex could function to regulate small G proteins within the cell and therefore co-ordinate trafficking. This possibility needs to be further investigated.

7 References

Agarwal, P.P. et al., 2011. Thoracic CT findings in Birt-Hogg-Dube syndrome. *AJR. American journal of roentgenology*, 196(2), pp.349–52.

Alber, F. et al., 2007. The molecular architecture of the nuclear pore complex. *Nature*, 450(7170), pp.695–701.

Alemu, E.A. et al., 2012. ATG8 family proteins act as scaffolds for assembly of the ULK complex: Sequence requirements for LC3-interacting region (LIR) motifs. *Journal of Biological Chemistry*, 287(47), pp.39275–39290.

Alers, S. et al., 2012. Role of AMPK-mTOR-Ulk1/2 in the Regulation of Autophagy: Cross Talk, Shortcuts, and Feedbacks. *Molecular and Cellular Biology*, 32(1), pp.2–11.

Ao, X., Zou, L. & Wu, Y., 2014. Regulation of autophagy by the Rab GTPase network. *Cell death and differentiation*, 21(3), pp.348–58.

Ávalos, Y. et al., 2014. Tumor suppression and promotion by autophagy. *BioMed research international*, 2014, p.603980.

Baba, M. et al., 2006. Folliculin encoded by the BHD gene interacts with a binding protein, FNIP1, and AMPK, and is involved in AMPK and mTOR signaling. *Proceedings of the National Academy of Sciences of the United States of America*, 103(42), pp.15552–7.

Baba, M. et al., 2008. Kidney-targeted Birt-Hogg-Dube gene inactivation in a mouse model: Erk1/2 and Akt-mTOR activation, cell hyperproliferation, and polycystic kidneys. *Journal of the National Cancer Institute*, 100(2), pp.140–54.

Baba, M. et al., 2012. The folliculin-FNIP1 pathway deleted in human Birt-Hogg-Dubé syndrome is required for murine B-cell development. *Blood*, 120(6), pp.1254–1261.

Bach, M. et al., 2011. The serine/threonine kinase ULK1 is a target of multiple phosphorylation events. *Biochemical Journal*, 440(2), pp.283–291.

Barr, F. & Lambright, D.G., 2010. Rab GEFs and GAPs. *Current opinion in cell biology*, 22(4), pp.461–70.

Bastola, P. et al., 2013. Folliculin Contributes to VHL Tumor Suppressing Activity in Renal Cancer through Regulation of Autophagy. *PLoS ONE*, 8(7), pp.1–8.

Behrends, C. et al., 2010. Network organization of the human autophagy system. *Nature*, 466(7302), pp.68–76.

Benhammou, J.N. et al., 2011. Identification of intragenic deletions and duplication in the FLCN gene in Birt-Hogg-Dubé syndrome. *Genes, chromosomes & cancer*, 50(6), pp.466–77.

Bento, C.F. et al., 2013. The role of membrane-trafficking small GTPases in the regulation of autophagy. *Journal of cell science*, 126(Pt 5), pp.1059–69.

Benusiglio, P.R., Gad, S., et al., 2014. Case Report: Expanding the tumour spectrum associated with the Birt-Hogg-Dubé cancer susceptibility syndrome. *F1000Research*, 3, p.159.

Benusiglio, P.R., Giraud, S., et al., 2014. Renal cell tumour characteristics in patients with the Birt-Hogg-Dubé cancer susceptibility syndrome: a retrospective, multicentre study. *Orphanet journal of rare diseases*, 9, p.163.

Bessis, D., Giraud, S. & Richard, S., 2006. A novel familial germline mutation in the initiator codon of the BHD gene in a patient with Birt-Hogg-Dubé syndrome. *The British journal of dermatology*, 155(5), pp.1067–9.

Bi, W. et al., 2002. Genes in a refined Smith-Magenis syndrome critical deletion interval on chromosome 17p11.2 and the syntenic region of the mouse. *Genome research*, 12(5), pp.713–28.

Birgisdottir, Å.B., Lamark, T. & Johansen, T., 2013. The LIR motif - crucial for selective autophagy. *Journal of cell science*, 126(Pt 15), pp.3237–47.

Birt, A.R., Hogg, G.R. & Dubé, W.J., 1977. Hereditary multiple fibrofolliculomas with trichodiscomas and acrochordons. *Archives of dermatology*, 113(12), pp.1674–7.

Byrne, M. et al., 2012. Birt-Hogg-Dubé syndrome with a renal angiomyolipoma: further evidence of a relationship between Birt-Hogg-Dubé syndrome and tuberous sclerosis complex. *The Australasian journal of dermatology*, 53(2), pp.151–4.

Cash, T.P. et al., 2011. Loss of the Birt-Hogg-Dubé tumor suppressor results in apoptotic resistance due to aberrant TGFβ-mediated transcription. *Oncogene*, 30(22), pp.2534–2546.

Chen, J. et al., 2008. Deficiency of FLCN in mouse kidney led to development of polycystic kidneys and renal neoplasia. *PloS one*, 3(10), p.e3581.

Choi, A.M.K., Ryter, S.W. & Levine, B., 2013. Autophagy in human health and disease. *The New England journal of medicine*, 368(7), pp.651–62.

Chua, C.E.L., Gan, B.Q. & Tang, B.L., 2011. Involvement of members of the Rab family and related small GTPases in autophagosome formation and maturation. *Cellular and molecular life sciences : CMLS*, 68(20), pp.3349–58.

Cocciolone, R.A. et al., 2010. Multiple desmoplastic melanomas in Birt-Hogg-Dubé syndrome and a proposed signaling link between folliculin, the mTOR pathway, and melanoma susceptibility. *Archives of dermatology*, 146(11), pp.1316–8.

Creighton, C.J. et al., 2013. Comprehensive molecular characterization of clear cell renal cell carcinoma. *Nature*, 499(7456), pp.43–49.

Danielsen, J.M.R. et al., 2011. Mass spectrometric analysis of lysine ubiquitylation reveals promiscuity at site level. *Molecular & cellular proteomics : MCP*, 10(3), p.M110.003590.

De la Torre, C. et al., 1999. Acrochordons are not a component of the Birt-Hogg-Dubé syndrome: does this syndrome exist? Case reports and review of the literature. *The American Journal of dermatopathology*, 21(4), pp.369–74.

Demetriades, C., Doumpas, N. & Teleman, A.A., 2014. Regulation of TORC1 in response to amino acid starvation via lysosomal recruitment of TSC2. *Cell*, 156(4), pp.786–99.

Dephoure, N. et al., 2008. A quantitative atlas of mitotic phosphorylation. *Proceedings of the National Academy of Sciences*, 105(31), pp.10762–10767.

Dhillon, A.S. et al., 2007. MAP kinase signalling pathways in cancer. *Oncogene*, 26(22), pp.3279–90.

Dodding, M.P. et al., 2011. A kinesin-1 binding motif in vaccinia virus that is

widespread throughout the human genome. *The EMBO journal*, 30(22), pp.4523–38.

Dorsey, F.C. et al., 2009. Mapping the phosphorylation sites of Ulk1. *Journal of proteome research*, 8(11), pp.5253–63.

Dunlop, E. a. et al., 2011. ULK1 inhibits mTORC1 signaling, promotes multisite Raptor phosphorylation and hinders substrate binding. *Autophagy*, 7(7), pp.737–747.

Duran, A. et al., 2011. p62 Is a Key Regulator of Nutrient Sensing in the mTORC1 Pathway. *Molecular Cell*, 44(1), pp.134–146.

Egami, Y. et al., 2005. Induced expressions of Rab24 GTPase and LC3 in nerve-injured motor neurons. *Biochemical and biophysical research communications*, 337(4), pp.1206–13.

Egan, D.F. et al., 2011. Phosphorylation of ULK1 (hATG1) by AMP-activated protein kinase connects energy sensing to mitophagy. *Science (New York, N.Y.)*, 331(6016), pp.456–61.

Elazar, Z., Scherz-Shouval, R. & Shorer, H., 2003. Involvement of LMA1 and GATE-16 family members in intracellular membrane dynamics. *Biochimica et biophysica acta*, 1641(2-3), pp.145–56.

Erdi, B. et al., 2012. Loss of the starvation-induced gene Rack1 leads to glycogen deficiency and impaired autophagic responses in Drosophila. *Autophagy*, 8(7), pp.1124–35.

Fujita, W.H., Barr, R.J. & Headley, J.L., 1981. Multiple fibrofolliculomas with

trichodiscomas and acrochordons. *Archives of dermatology*, 117(1), pp.32–5.

Furuya, M. et al., 2012. Pulmonary cysts of Birt-Hogg-Dubé syndrome: a clinicopathologic and immunohistochemical study of 9 families. *The American journal of surgical pathology*, 36(4), pp.589–600.

Gad, S. et al., 2007. Mutations in BHD and TP53 genes, but not in HNF1beta gene, in a large series of sporadic chromophobe renal cell carcinoma. *British journal of cancer*, 96(2), pp.336–40.

Ganley, I.G., 2013. Autophagosome maturation and lysosomal fusion. *Essays in biochemistry*, 55, pp.65–78.

Ganley, I.G. et al., 2009. ULK1·ATG13·FIP200 complex mediates mTOR signaling and is essential for autophagy. *Journal of Biological Chemistry*, 284(18), pp.12297–12305.

Gauci, S. et al., 2009. Lys-N and trypsin cover complementary parts of the phosphoproteome in a refined SCX-based approach. *Analytical chemistry*, 81(11), pp.4493–501.

Gaur, K. et al., 2013. The Birt-Hogg-Dub?? tumor suppressor folliculin negatively regulates ribosomal RNA synthesis. *Human Molecular Genetics*, 22(2), pp.284–299.

Goncharova, E.A. et al., 2014. Folliculin controls lung alveolar enlargement and epithelial cell survival through E-cadherin, LKB1, and AMPK. *Cell reports*, 7(2), pp.412–23.

Gunji, Y. et al., 2007. Mutations of the Birt Hogg Dube gene in patients with multiple

lung cysts and recurrent pneumothorax. *Journal of medical genetics*, 44(9), pp.588–93.

Gutierrez, M.G. et al., 2004. Rab7 is required for the normal progression of the autophagic pathway in mammalian cells. *Journal of cell science*, 117(Pt 13), pp.2687–97.

Haemel, A.K., O'Brian, A.L. & Teng, J.M., 2010. Topical rapamycin: a novel approach to facial angiofibromas in tuberous sclerosis. *Archives of dermatology*, 146(7), pp.715–8.

Hardie, D.G., 2007. AMP-activated/SNF1 protein kinases: conserved guardians of cellular energy. *Nature Reviews Molecular Cell Biology*, 8(10), pp.774–785.

Hardie, D.G., Schaffer, B.E. & Brunet, A., 2015. AMPK: An Energy-Sensing Pathway with Multiple Inputs and Outputs. *Trends in cell biology*.

Hartman, T.R. et al., 2009. The role of the Birt-Hogg-Dubé protein in mTOR activation and renal tumorigenesis. *Oncogene*, 28(13), pp.1594–604.

Hasumi, H. et al., 2015. Folliculin-interacting proteins Fnip1 and Fnip2 play critical roles in kidney tumor suppression in cooperation with Flcn. *Proceedings of the National Academy of Sciences of the United States of America*, 112(13), pp.E1624–31.

Hasumi, H. et al., 2008. Identification and characterization of a novel folliculin-interacting protein FNIP2. *Gene*, 415(1-2), pp.60–7.

Hasumi, H. et al., 2009. NIH Public Access. , 415, pp.60–67.

Hasumi, Y. et al., 2014. Folliculin (Flcn) inactivation leads to murine cardiac

hypertrophy through mTORC1 deregulation. *Human molecular genetics*, 23(21), pp.5706–19.

Hasumi, Y. et al., 2009. Homozygous loss of BHD causes early embryonic lethality and kidney tumor development with activation of mTORC1 and mTORC2. *Proceedings of the National Academy of Sciences of the United States of America*, 106(44), pp.18722–18727.

He, C. & Klionsky, D.J., 2009. Regulation mechanisms and signaling pathways of autophagy. *Annual review of genetics*, 43, pp.67–93.

Heitman, J., Movva, N.R. & Hall, M.N., 1991. Targets for cell cycle arrest by the immunosuppressant rapamycin in yeast. *Science (New York, N.Y.)*, 253(5022), pp.905–9.

Herrero-Martín, G. et al., 2009. TAK1 activates AMPK-dependent cytoprotective autophagy in TRAIL-treated epithelial cells. *The EMBO journal*, 28(6), pp.677–85.

Hirota, Y. & Tanaka, Y., 2009. A small GTPase, human Rab32, is required for the formation of autophagic vacuoles under basal conditions. *Cellular and molecular life sciences : CMLS*, 66(17), pp.2913–32.

Hoelz, A., Debler, E.W. & Blobel, G., 2011. The structure of the nuclear pore complex. *Annual review of biochemistry*, 80, pp.613–643.

Hong, S.B. et al., 2010. Inactivation of the FLCN tumor suppressor gene induces TFE3 transcriptional activity by increasing its nuclear localization. *PLoS ONE*, 5(12).

Hong, S.-B. et al., 2010. Tumor suppressor FLCN inhibits tumorigenesis of a FLCN-null renal cancer cell line and regulates expression of key molecules in TGF-beta signaling. *Molecular cancer*, 9, p.160.

Hornstein, O.P., 1976. Generalized dermal perifollicular fibromas with polyps of the colon. *Human genetics*, 33(2), pp.193–7.

Hornstein, O.P. & Knickenberg, M., 1975. Perifollicular fibromatosis cutis with polyps of the colon--a cutaneo-intestinal syndrome sui generis. *Archives for dermatological research = Archiv für dermatologische Forschung*, 253(2), pp.161–75.

Hosokawa, N. et al., 2009. Nutrient-dependent mTORC1 Association with the ULK1-Atg13-FIP200 Complex Required for Autophagy. *Molecular Biology of the Cell*, 20(7), pp.1981–1991.

Houweling, A.C. et al., 2011. Renal cancer and pneumothorax risk in Birt-Hogg-Dubé syndrome; an analysis of 115 FLCN mutation carriers from 35 BHD families. *British journal of cancer*, 105(12), pp.1912–9.

Høyer-Hansen, M. et al., 2007. Control of macroautophagy by calcium, calmodulin-dependent kinase kinase-beta, and Bcl-2. *Molecular cell*, 25(2), pp.193–205.

Hsu, R.-J. et al., 2012. WNT10A plays an oncogenic role in renal cell carcinoma by activating WNT/β-catenin pathway. *PloS one*, 7(10), p.e47649.

Huang, J. & Manning, B.D., 2009. A complex interplay between Akt, TSC2 and the two mTOR complexes. *Biochemical Society transactions*, 37(Pt 1), pp.217–22.

Huang, K. & Fingar, D.C., 2014. Growing knowledge of the mTOR signaling network.

Seminars in cell & developmental biology, 36, pp.79–90.

Hudon, V. et al., 2010. Renal tumour suppressor function of the Birt-Hogg-Dubé syndrome gene product folliculin. *Journal of medical genetics*, 47(3), pp.182–9.

Ichimura, Y. et al., 2008. Structural basis for sorting mechanism of p62 in selective autophagy. *The Journal of biological chemistry*, 283(33), pp.22847–57.

Itakura, E. & Mizushima, N., 2010. Characterization of autophagosome formation site by a hierarchical analysis of mammalian Atg proteins. *Autophagy*, 6(6), pp.764–76.

Jäger, S. et al., 2004. Role for Rab7 in maturation of late autophagic vacuoles. *Journal of cell science*, 117(Pt 20), pp.4837–48.

Jeanes, A., Gottardi, C.J. & Yap, A.S., 2008. Cadherins and cancer: how does cadherin dysfunction promote tumor progression? *Oncogene*, 27(55), pp.6920–9.

Jin, Z. et al., 2009. Cullin3-based polyubiquitination and p62-dependent aggregation of caspase-8 mediate extrinsic apoptosis signaling. *Cell*, 137(4), pp.721–35.

Johannesma, P.C. et al., 2014. Spontaneous pneumothorax as indicator for Birt-Hogg-Dubé syndrome in paediatric patients. *BMC pediatrics*, 14, p.171.

Johansen, T. & Lamark, T., 2011. Selective autophagy mediated by autophagic adapter proteins. *Autophagy*, 7(3), pp.279–96.

Jung, C.H. et al., 2011. ULK1 inhibits the kinase activity of mTORC1 and cell proliferation. *Autophagy*, 7(10), pp.1212–21.

Jung, C.H. et al., 2009. ULK-Atg13-FIP200 complexes mediate mTOR signaling to

the autophagy machinery. *Molecular biology of the cell*, 20(7), pp.1992–2003.

Kabachinski, G. & Schwartz, T.U., 2015. The nuclear pore complex--structure and function at a glance. *Journal of cell science*, 128(3), pp.423–9.

Kabeya, Y. et al., 2004. LC3, GABARAP and GATE16 localize to autophagosomal membrane depending on form-II formation. *Journal of cell science*, 117(Pt 13), pp.2805–12.

Kang, S.A. et al., 2013. mTORC1 phosphorylation sites encode their sensitivity to starvation and rapamycin. *Science (New York, N.Y.)*, 341(6144), p.1236566.

Khabibullin, D. et al., 2014. Folliculin regulates cell-cell adhesion, AMPK, and mTORC1 in a cell-type-specific manner in lung-derived cells. *Physiological reports*, 2(8).

Khoo, S.K. et al., 2001. Birt-Hogg-Dubé syndrome: mapping of a novel hereditary neoplasia gene to chromosome 17p12-q11.2. *Oncogene*, 20(37), pp.5239–42.

Khoo, S.K. et al., 2002. Clinical and genetic studies of Birt-Hogg-Dubé syndrome. *Journal of medical genetics*, 39(12), pp.906–12.

Khoo, S.K. et al., 2003. Inactivation of BHD in sporadic renal tumors. *Cancer research*, 63(15), pp.4583–7.

Kim, D.-H. et al., 2002. mTOR interacts with raptor to form a nutrient-sensitive complex that signals to the cell growth machinery. *Cell*, 110(2), pp.163–75.

Kim, J. et al., 2011. AMPK and mTOR regulate autophagy through direct phosphorylation of Ulk1. *Nature cell biology*, 13(2), pp.132–41.

Kirisako, T. et al., 1999. Formation process of autophagosome is traced with

Apg8/Aut7p in yeast. *The Journal of cell biology*, 147(2), pp.435–46.

Klionsky, D.J. et al., 2011. A comprehensive glossary of autophagy-related molecules and processes (2nd edition). *Autophagy*, 7(11), pp.1273–94.

Klionsky, D.J., 2008. Autophagy revisited: A conversation with Christian de Duve. *Autophagy*, 4(6), pp.740–743.

Klionsky, D.J., 2005. The molecular machinery of autophagy: unanswered questions. *Journal of cell science*, 118(Pt 1), pp.7–18.

Kluger, N. et al., 2010. Birt-Hogg-Dubé syndrome: clinical and genetic studies of 10 French families. *The British journal of dermatology*, 162(3), pp.527–37.

Komatsu, M. et al., 2007. Homeostatic levels of p62 control cytoplasmic inclusion body formation in autophagy-deficient mice. *Cell*, 131(6), pp.1149–63.

Komori, K. et al., 2009. A novel protein, MAPO1, that functions in apoptosis triggered by O6-methylguanine mispair in DNA. *Oncogene*, 28(8), pp.1142–50.

Kraft, C. et al., 2012. Binding of the Atg1/ULK1 kinase to the ubiquitin-like protein Atg8 regulates autophagy. *The EMBO journal*, 31(18), pp.3691–703.

Kumasaka, T. et al., 2014. Characterization of pulmonary cysts in Birt-Hogg-Dubé syndrome: histopathological and morphometric analysis of 229 pulmonary cysts from 50 unrelated patients. *Histopathology*, 65(1), pp.100–10.

Kunogi Okura, M. et al., 2013. Pneumothorax developing for the first time in a 73-year-old woman diagnosed with Birt-Hogg-Dubé syndrome. *Internal medicine (Tokyo, Japan)*, 52(21), pp.2453–5.

Landau et al., 2009. Increased renal Akt/mTOR and MAPK signaling in type I

diabetes in the absence of IGF type 1 receptor activation. - PubMed - NCBI. Available at: http://www.ncbi.nlm.nih.gov/pubmed/19387875 [Accessed January 21, 2016].

Laviolette, L.A. et al., 2013. Human folliculin delays cell cycle progression through late S and G2/M-phases: effect of phosphorylation and tumor associated mutations. *PloS one*, 8(7), p.e66775.

Leter, E.M. et al., 2008. Birt-Hogg-Dubé syndrome: clinical and genetic studies of 20 families. *The Journal of investigative dermatology*, 128(1), pp.45–9.

Lim, T.H. et al., 2012. Activation of AMP-activated protein kinase by MAPO1 and FLCN induces apoptosis triggered by alkylated base mismatch in DNA. *DNA Repair*, 11(3), pp.259–266.

Lindor, N.M. et al., 2012. Birt-Hogg-Dube syndrome presenting as multiple oncocytic parotid tumors. *Hereditary cancer in clinical practice*, 10(1), p.13.

Lippai, M. & Lőw, P., 2014. The role of the selective adaptor p62 and ubiquitin-like proteins in autophagy. *BioMed research international*, 2014, p.832704.

Liu, V., Kwan, T. & Page, E.H., 2000. Parotid oncocytoma in the Birt-Hogg-Dubé syndrome. *Journal of the American Academy of Dermatology*, 43(6), pp.1120–2.

Liu, W. et al., 2013. Genetic characterization of the Drosophila birt-hogg-dubé syndrome gene. *PloS one*, 8(6), p.e65869.

Löffler, A.S. et al., 2011. Ulk1-mediated phosphorylation of AMPK constitutes a negative regulatory feedback loop. *Autophagy*, 7(7), pp.696–706.

Long, X. et al., 2005. Rheb binds and regulates the mTOR kinase. *Current biology :*

CB, 15(8), pp.702–13.

Luijten, M.N.H. et al., 2013. Birt-Hogg-Dube syndrome is a novel ciliopathy. *Human molecular genetics*, 22(21), pp.4383–97.

Maffé, A. et al., 2011. Constitutional FLCN mutations in patients with suspected Birt-Hogg-Dubé syndrome ascertained for non-cutaneous manifestations. *Clinical genetics*, 79(4), pp.345–54.

Martina, J. a et al., 2014. The nutrient-responsive transcription factor TFE3 promotes autophagy, lysosomal biogenesis, and clearance of cellular debris. *Science signaling*, 7(309), p.ra9.

Medvetz, D.A. et al., 2012. Folliculin, the product of the Birt-Hogg-Dube tumor suppressor gene, interacts with the adherens junction protein p0071 to regulate cell-cell adhesion. *PloS one*, 7(11), p.e47842.

Meley, D. et al., 2006. AMP-activated protein kinase and the regulation of autophagic proteolysis. *The Journal of biological chemistry*, 281(46), pp.34870–9.

Menko, F.H. et al., 2009. Birt-Hogg-Dubé syndrome: diagnosis and management. *The Lancet. Oncology*, 10(12), pp.1199–206.

Mercer, C.A., Kaliappan, A. & Dennis, P.B., 2009. A novel, human Atg13 binding protein, Atg101, interacts with ULK1 and is essential for macroautophagy. *Autophagy*, 5(5), pp.649–62.

Misago, N., Kimura, T. & Narisawa, Y., 2009. Fibrofolliculoma/trichodiscoma and fibrous papule (perifollicular fibroma/angiofibroma): a revaluation of the histopathological and immunohistochemical features. *Journal of cutaneous*

pathology, 36(9), pp.943–51.

Mizushima, N. & Komatsu, M., 2011. Autophagy: renovation of cells and tissues. *Cell*, 147(4), pp.728–41.

Mohr, A. et al., Dynamics and non-canonical aspects of JAK/STAT signalling. *European journal of cell biology*, 91(6-7), pp.524–32.

Moscat, J., Diaz-Meco, M.T. & Wooten, M.W., 2007. Signal integration and diversification through the p62 scaffold protein. *Trends in biochemical sciences*, 32(2), pp.95–100.

Mutizwa, M.M., Berk, D.R. & Anadkat, M.J., 2011. Treatment of facial angiofibromas with topical application of oral rapamycin solution (1mgmL(-1)) in two patients with tuberous sclerosis. *The British journal of dermatology*, 165(4), pp.922–3.

Nagase, T. et al., 1998. Prediction of the coding sequences of unidentified human genes. XI. The complete sequences of 100 new cDNA clones from brain which code for large proteins in vitro. *DNA research : an international journal for rapid publication of reports on genes and genomes*, 5(5), pp.277–286.

Nahorski, M.S. et al., 2011. Birt Hogg-Dubé Syndrome-associated FLCN mutations disrupt protein stability. *Human Mutation*, 32(8), pp.921–929.

Nahorski, M.S. et al., 2012. Folliculin interacts with p0071 (plakophilin-4) and deficiency is associated with disordered RhoA signalling, epithelial polarization and cytokinesis. *Human molecular genetics*, 21(24), pp.5268–79.

Nahorski, M.S. et al., 2010. Investigation of the Birt-Hogg-Dube tumour suppressor gene (FLCN) in familial and sporadic colorectal cancer. *Journal of medical*

genetics, 47(6), pp.385–90.

Nair, U. et al., 2012. A role for Atg8-PE deconjugation in autophagosome biogenesis. *Autophagy*, 8(5), pp.780–93.

Nickerson, M.L. et al., 2002. Mutations in a novel gene lead to kidney tumors, lung wall defects, and benign tumors of the hair follicle in patients with the Birt-Hogg-Dubé syndrome. *Cancer cell*, 2(2), pp.157–64.

Nishii, T. et al., 2013. Unique mutation, accelerated mTOR signaling and angiogenesis in the pulmonary cysts of Birt-Hogg-Dubé syndrome. *Pathology International*, 63(1), pp.45–55.

Noda, N.N. & Inagaki, F., 2015. Mechanisms of Autophagy. *Annual review of biophysics*, 44, pp.101–22.

Nookala, R.K. et al., 2012. Crystal structure of folliculin reveals a hidDENN function in genetically inherited renal cancer. *Open Biology*, 2(8), pp.120071–120071.

Orsi, A., Polson, H.E.J. & Tooze, S.A., 2010. Membrane trafficking events that partake in autophagy. *Current opinion in cell biology*, 22(2), pp.150–6.

Palmirotta, R. et al., 2008. Birt-Hogg-Dubé (BHD) syndrome: report of two novel germline mutations in the folliculin (FLCN) gene. *European journal of dermatology : EJD*, 18(4), pp.382–6.

Pampliega, O. et al., 2013. Functional interaction between autophagy and ciliogenesis. *Nature*, 502(7470), pp.194–200.

Pankiv, S. et al., 2007. p62/SQSTM1 binds directly to Atg8/LC3 to facilitate degradation of ubiquitinated protein aggregates by autophagy. *The Journal of*

biological chemistry, 282(33), pp.24131–45.

Papinski, D. et al., 2014. Early Steps in Autophagy Depend on Direct Phosphorylation of Atg9 by the Atg1 Kinase. *Molecular Cell*, 53(3), pp.471–483.

Park, H. et al., 2012. Disruption of Fnip1 Reveals a Metabolic Checkpoint Controlling B Lymphocyte Development. *Immunity*, 36(5), pp.769–781.

Park, H. et al., 2014. Metabolic regulator Fnip1 is crucial for iNKT lymphocyte development. *Proceedings of the National Academy of Sciences of the United States of America*, 111(19), pp.7066–71.

Pavlovich, C.P. et al., 2005. Evaluation and management of renal tumors in the Birt-Hogg-Dubé syndrome. *The Journal of urology*, 173(5), pp.1482–6.

Pavlovich, C.P. et al., 2002. Renal tumors in the Birt-Hogg-Dubé syndrome. *The American journal of surgical pathology*, 26(12), pp.1542–52.

Pemberton, T.J. et al., 2014. A mutation in the canine gene encoding folliculin-interacting protein 2 (FNIP2) associated with a unique disruption in spinal cord myelination. *Glia*, 62(1), pp.39–51.

Petit, C.S., Roczniak-Ferguson, A. & Ferguson, S.M., 2013. Recruitment of folliculin to lysosomes supports the amino acid-dependent activation of Rag GTPases. *The Journal of cell biology*, 202(7), pp.1107–22.

Piao, X. et al., 2009. Regulation of folliculin (the BHD gene product) phosphorylation by Tsc2-mTOR pathway. *Biochemical and Biophysical Research Communications*, 389(1), pp.16–21.

Pircs, K. et al., 2012. Advantages and limitations of different p62-based assays for

estimating autophagic activity in Drosophila. *PloS one*, 7(8), p.e44214.

Possik, E. et al., 2014. Folliculin regulates ampk-dependent autophagy and metabolic stress survival. *PLoS genetics*, 10(4), p.e1004273.

Pradella, L.M. et al., 2013. Where Birt-Hogg-Dubé meets Cowden syndrome: mirrored genetic defects in two cases of syndromic oncocytic tumours. *European journal of human genetics : EJHG*, 21(10), pp.1169–72.

Preston, R.S. et al., 2011. Absence of the Birt-Hogg-Dubé gene product is associated with increased hypoxia-inducible factor transcriptional activity and a loss of metabolic flexibility. *Oncogene*, 30(10), pp.1159–1173.

Ravikumar, B. et al., 2009. Mammalian macroautophagy at a glance. *Journal of cell science*, 122(Pt 11), pp.1707–11.

Reggiori, F. et al., 2004. The Atg1-Atg13 complex regulates Atg9 and Atg23 retrieval transport from the pre-autophagosomal structure. *Developmental cell*, 6(1), pp.79–90.

Reiman, A. et al., 2012. Gene expression and protein array studies of folliculin-regulated pathways. *Anticancer research*, 32(11), pp.4663–70.

Roberg, K.J. et al., 1997. Control of amino acid permease sorting in the late secretory pathway of Saccharomyces cerevisiae by SEC13, LST4, LST7 and LST8. *Genetics*, 147(4), pp.1569–84.

Russell, R.C. et al., 2013. ULK1 induces autophagy by phosphorylating Beclin-1 and activating VPS34 lipid kinase. *Nature cell biology*, 15(7), pp.741–50.

Sancak, Y. et al., 2010. Ragulator-Rag complex targets mTORC1 to the lysosomal

surface and is necessary for its activation by amino acids. *Cell*, 141(2), pp.290–303.

Sancak, Y. et al., 2008. The Rag GTPases bind raptor and mediate amino acid signaling to mTORC1. *Science (New York, N.Y.)*, 320(5882), pp.1496–501.

Sano, S. et al., 2013. Stabilization of MAPO1 by specific binding with folliculin and AMP-activated protein kinase in O^6-methylguanine-induced apoptosis. *Biochemical and biophysical research communications*, 430(2), pp.810–5.

Sarbassov, D.D., Ali, S.M. & Sabatini, D.M., 2005. Growing roles for the mTOR pathway. *Current opinion in cell biology*, 17(6), pp.596–603.

Schachtschabel, A.A., Küster, W. & Happle, R., 1996. [Perifollicular fibroma of the skin and colonic polyps: Hornstein-Knickenberg syndrome]. *Der Hautarzt; Zeitschrift für Dermatologie, Venerologie, und verwandte Gebiete*, 47(4), pp.304–6.

Schmidt, L.S. et al., 2005. Germline BHD-mutation spectrum and phenotype analysis of a large cohort of families with Birt-Hogg-Dubé syndrome. *American journal of human genetics*, 76(6), pp.1023–33.

Schulz, T. & Hartschuh, W., 1999. Birt-Hogg-Dubé syndrome and Hornstein-Knickenberg syndrome are the same. Different sectioning technique as the cause of different histology. *Journal of cutaneous pathology*, 26(1), pp.55–61.

Shpilka, T. et al., 2011. Atg8: an autophagy-related ubiquitin-like protein family. *Genome biology*, 12(7), p.226.

Shuch, B. et al., 2014. Defining early-onset kidney cancer: implications for germline

and somatic mutation testing and clinical management. *Journal of clinical oncology : official journal of the American Society of Clinical Oncology*, 32(5), pp.431–7.

Singh, S.R. et al., 2006. The Drosophila homolog of the human tumor suppressor gene BHD interacts with the JAK-STAT and Dpp signaling pathways in regulating male germline stem cell maintenance. *Oncogene*, 25(44), pp.5933–41.

Sirintrapun, S.J. et al., 2014. Oncocytoma-like renal tumor with transformation toward high-grade oncocytic carcinoma: a unique case with morphologic, immunohistochemical, and genomic characterization. *Medicine*, 93(15), p.e81.

Slobodkin, M.R. & Elazar, Z., 2013. The Atg8 family: multifunctional ubiquitin-like key regulators of autophagy. *Essays in biochemistry*, 55, pp.51–64.

Starink, T.M. et al., 2012. Familial multiple discoid fibromas: A look-alike of Birt-Hogg-Dub?? syndrome not linked to the FLCN locus. *Journal of the American Academy of Dermatology*, 66(2), pp.1–9.

Strømhaug, P.E. et al., 1998. Purification and characterization of autophagosomes from rat hepatocytes. *The Biochemical journal*, 335 (Pt 2, pp.217–24.

Suzuki, K. et al., 2007. Hierarchy of Atg proteins in pre-autophagosomal structure organization. *Genes to cells : devoted to molecular & cellular mechanisms*, 12(2), pp.209–18.

Takagi, Y. et al., 2008. Interaction of folliculin (Birt-Hogg-Dubé gene product) with a novel Fnip1-like (FnipL/Fnip2) protein. *Oncogene*, 27(40), pp.5339–5347.

Tanida, I., 2011. Autophagy basics. *Microbiology and Immunology*, 55(1), pp.1–11.

Tanida, I., Ueno, T. & Kominami, E., 2008. LC3 and Autophagy. *Methods in molecular biology (Clifton, N.J.)*, 445, pp.77–88.

Thoreen, C.C. et al., 2009. An ATP-competitive mammalian target of rapamycin inhibitor reveals rapamycin-resistant functions of mTORC1. *The Journal of biological chemistry*, 284(12), pp.8023–32.

Thoreen, C.C. & Sabatini, D.M., 2009. Rapamycin inhibits mTORC1, but not completely. *Autophagy*, 5(5), pp.725–6.

Tobino, K. et al., 2011. Characteristics of pulmonary cysts in Birt-Hogg-Dubé syndrome: thin-section CT findings of the chest in 12 patients. *European journal of radiology*, 77(3), pp.403–9.

Tobino, K. & Seyama, K., 2012. Birt-Hogg-Dubé syndrome with renal angiomyolipoma. *Internal medicine (Tokyo, Japan)*, 51(10), pp.1279–80.

Toro, J.R. et al., 2008. BHD mutations, clinical and molecular genetic investigations of Birt-Hogg-Dubé syndrome: a new series of 50 families and a review of published reports. *Journal of medical genetics*, 45(6), pp.321–31.

Toro, J.R. et al., 1999. Birt-Hogg-Dubé syndrome: a novel marker of kidney neoplasia. *Archives of dermatology*, 135(10), pp.1195–202.

Toro, J.R. et al., 2007. Lung cysts, spontaneous pneumothorax, and genetic associations in 89 families with Birt-Hogg-Dubé syndrome. *American journal of respiratory and critical care medicine*, 175(10), pp.1044–53.

Tossidou, I. & Schiffer, M., 2012. TGF-β/BMP pathways and the podocyte. *Seminars*

in nephrology, 32(4), pp.368–76.

Tsukada, M. & Ohsumi, Y., 1993. Isolation and characterization of autophagy-defective mutants of Saccharomyces cerevisiae. *FEBS letters*, 333(1-2), pp.169–74.

Tsun, Z.Y. et al., 2013. The folliculin tumor suppressor is a GAP for the RagC/D GTPases that signal amino acid levels to mTORC1. *Molecular Cell*, 52(4), pp.495–505.

van Steensel, M.A.M. et al., 2007. Novel mutations in the BHD gene and absence of loss of heterozygosity in fibrofolliculomas of Birt-Hogg-Dubé patients. *The Journal of investigative dermatology*, 127(3), pp.588–93.

van Zutphen, T. et al., 2010. Adaptation of Hansenula polymorpha to methanol: a transcriptome analysis. *BMC genomics*, 11, p.1.

Vander Haar, E. et al., 2007. Insulin signalling to mTOR mediated by the Akt/PKB substrate PRAS40. *Nature cell biology*, 9(3), pp.316–23.

Vernooij, M. et al., 2013. Birt-Hogg-Dubé syndrome and the skin. *Familial cancer*, 12(3), pp.381–5.

Vocke, C.D. et al., 2005. High frequency of somatic frameshift BHD gene mutations in Birt-Hogg-Dubé-associated renal tumors. *Journal of the National Cancer Institute*, 97(12), pp.931–5.

Wagle, N. et al., 2014. Response and acquired resistance to everolimus in anaplastic thyroid cancer. *The New England journal of medicine*, 371(15), pp.1426–33.

Wagner, S.A. et al., 2011. A proteome-wide, quantitative survey of in vivo ubiquitylation sites reveals widespread regulatory roles. *Molecular & cellular proteomics : MCP*, 10(10), p.M111.013284.

Wang, H. et al., 1999. GABA(A)-receptor-associated protein links GABA(A) receptors and the cytoskeleton. *Nature*, 397(6714), pp.69–72.

Wang, H. et al., 2015. GABARAPs regulate PI4P-dependent autophagosome:lysosome fusion. *Proceedings of the National Academy of Sciences of the United States of America*, 112(22), pp.7015–20.

Wang, L. et al., 2010. Serine 62 is a phosphorylation site in folliculin, the Birt-Hogg-Dubé gene product. *FEBS letters*, 584(1), pp.39–43.

Wang, Z. et al., 2001. Antagonistic controls of autophagy and glycogen accumulation by Snf1p, the yeast homolog of AMP-activated protein kinase, and the cyclin-dependent kinase Pho85p. *Molecular and cellular biology*, 21(17), pp.5742–52.

Wee, J.S. et al., 2013. Familial multiple discoid fibromas: Unique histological features and therapeutic response to topical rapamycin. *British Journal of Dermatology*, 169(1), pp.177–180.

Weidberg, H. et al., 2010. LC3 and GATE-16/GABARAP subfamilies are both essential yet act differently in autophagosome biogenesis. *Autophagy*, 6(6), pp.808–9.

Wullschleger, S., Loewith, R. & Hall, M.N., 2006. TOR signaling in growth and metabolism. *Cell*, 124(3), pp.471–84.

Yamada, Y. et al., 2015. Case of bilateral and multifocal renal cell carcinoma

associated with Birt-Hogg-Dubé syndrome. *International journal of urology : official journal of the Japanese Urological Association*, 22(2), pp.230–1.

Yan, M. et al., 2014. The tumor suppressor folliculin regulates AMPK-dependent metabolic transformation. *The Journal of clinical investigation*, 124(6), pp.2640–50.

Ying, Q.L. et al., 2003. BMP induction of Id proteins suppresses differentiation and sustains embryonic stem cell self-renewal in collaboration with STAT3. *Cell*, 115(3), pp.281–92.

Yu, Y. et al., 2011. Phosphoproteomic analysis identifies Grb10 as an mTORC1 substrate that negatively regulates insulin signaling. *Science (New York, N.Y.)*, 332(6035), pp.1322–6.

Zbar, B. et al., 2002. Risk of renal and colonic neoplasms and spontaneous pneumothorax in the Birt-Hogg-Dubé syndrome. *Cancer epidemiology, biomarkers & prevention : a publication of the American Association for Cancer Research, cosponsored by the American Society of Preventive Oncology*, 11(4), pp.393–400.

Zhang, D. et al., 2012. Discovery of Novel DENN Proteins: Implications for the Evolution of Eukaryotic Intracellular Membrane Structures and Human Disease. *Frontiers in genetics*, 3, p.283.

Zhang, Q. et al., 2013. Suppression of autophagy enhances preferential toxicity of paclitaxel to folliculin-deficient renal cancer cells. *Journal of experimental & clinical cancer research : CR*, 32, p.99.